PhD Program in Biomolecular Sciences

Department of Cellular, Computational and Integrative Biology – CIBIO

35th Cycle

"Telomeric localization of the TElomeric Repeat-containing RNA TERRA impairs telomerase activity in human cancer cells"

Tutor

Prof. Emilio CUSANELLI

Laboratory of Cell Biology and Molecular Genetics, Department CIBIO, UNITN

Ph.D. Thesis of

Nicole BETTIN

Laboratory of Cell Biology and Molecular Genetics, Department CIBIO, UNITN

Academic Year 2021-2022

DECLARATION

I, Nicole Bettin, confirm that this is my own work and the use of all material from other sources has been properly and fully acknowledged.

Grazie a chi mi ispira, anche senza farlo volutamente, tutti i giorni

INDEX

ABSTRACT

The telomeric repeat containing RNA TERRA represents a class of long non-coding RNAs transcribed from telomeres. TERRA has been shown to play key roles in telomere maintenance. During past years it has been reported that TERRA interacts with telomerase, suggesting it may act as regulator of telomerase. However, the role of TERRA in telomerase activity in human cells is still unknown and it needs to be further investigated.

Herein, we investigate the role of TERRA in telomerase activity in human cancer cells by exploiting different experimental conditions. By using single molecule RNA FISH (smiFISH) combined with confocal microscopy, we demonstrated that TERRA and the telomerase RNA subunit h*TR* colocalize in cancer cells. We observed that these events mainly occur in the nucleoplasm, while a fraction of TERRA transcripts colocalize with h*TR* molecules also at telomeres (Figure 1A). This result suggested us the possibility of a localization-dependent role of TERRA in the regulation of telomerase activity. Surprisingly, by studying TERRA and h*TR* interactions during telomere length homeostasis, we observed that fewer TERRA molecules localize at chromosome ends when telomeres are elongated by telomerase. Furthermore, the fraction of telomeric TERRA-h*TR* colocalizing foci markedly decreased during telomere elongation (Figure 1B and 1C). We observed that telomere shortening correlated with increased TERRA levels, in line with previously reported findings. Intriguingly, by quantifying the integrated density of the telomeric foci in smiFISH experiments combined with immunofluorescence (IF), we observed that TERRA transcripts preferentially localize to telomeres showing a brighter signal intensity as compared to the average telomeric signal of the cell, suggesting a preferential recruitment of TERRA to longer chromosome ends (Figure 1D).

These results suggest that TERRA transcripts may localize to telomeres *in trans* and that a displacement of TERRA from chromosome ends may be required for telomere elongation by telomerase. To gain insight into the role of TERRA in the regulation of telomerase, we used antisense oligonucleotides to deplete TERRA in cells. Interestingly, TERRA depletion resulted in increased telomerase localization to telomeres (Figure 1E). Altogether, our findings support a model in which telomeric TERRA transcripts act as negative regulators of telomerase activity at telomeres.

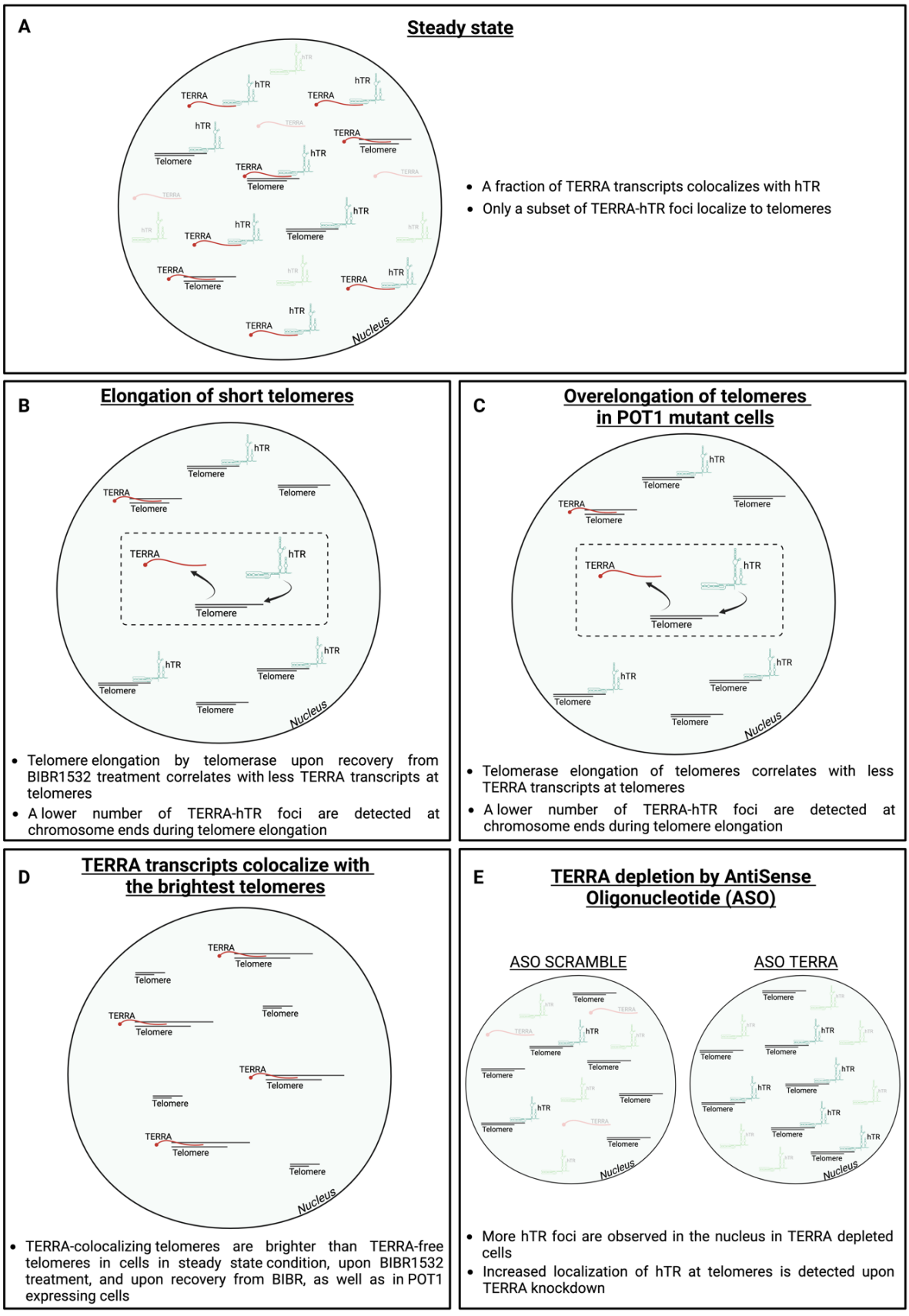

Figure 1. Graphical summary of the results reported in the thesis. Created with Biorender.com

INTRODUCTION

TELOMERES

Human chromosomes end with telomeres, complex protective structures involved in the maintenance of chromosome integrity. The natural end of linear chromosomes highly resembles damaged or broken DNA ends, also known as double strand breaks (DSBs), which are normally recognized by the DNA damage response (DDR) machinery and repaired through mechanisms of homology directed repair (HR) or nonhomologous end joining (NHEJ). These repair mechanisms, when activated at chromosome ends, induce the formation of deleterious recombination events and aberrant chromosomes fusion causing genomic instability. This phenomenon is called "end-protection problem" and is naturally avoided thanks to the presence of telomeres that cap the natural chromosome ends concealing them to avoiding their recognition as a site of DNA damage[1].

The structure of telomeres

Telomeres are nucleoprotein structures comprised of hundreds to thousands of hexameric double-stranded DNA repeats bound by several specialized proteins, terminating with a single-stranded guanine-rich (G-rich) overhang at their 3'-end[2]. In particular, the sequence of double-stranded (ds) tandem DNA repeats is conserved among many species: in vertebrates the telomeric sequence consists of 5'-TTAGGG-3' repeats whose number varies considerably not only between different species but also among different telomeres of the same individual[3-5]. In humans, telomere length ranges from approximately 5 to 15 kb while in *S. cerevisiae* and *S. pombe* telomeres are less than 1 kb long and *Mus musculus* presents telomeres of approximately 20 to 50 kb in length[2,6]. Telomeres do not present a blunt-ended termination at their 3' end but comprise a single-stranded (ss) protrusion of the G-rich strand of about 200 nucleotides (nt) in length in humans, known as G-overhang. The 3' overhang is able to fold on itself by invading the double-stranded telomeric sequence through the base-pairing with the C-rich strand thereby displacing the G-rich strand, and generating the displacement-loop, or D-loop[2,7,8]. This results in a higher-order lariat-like secondary structure called the telomeric-loop (or T-loop)[8]. T-loop function is to sequester the G-overhang from DDR pathways recognition thus avoiding inappropriate repair at chromosome ends[9] (Fig. 2).

Figure 2. Schematic representation of a telomere in T-loop configuration in mammals. The G-overhang invades the double stranded telomeric DNA by displacing the G-rich strand and forms a D-loops structure. Adapted from de Lange T., 2004[9]

The 3' overhang, thanks to its high guanine content, can also fold into G-quadruplexes structures where four guanine rings form planar square alignments which adopt a flat and cyclic configuration stabilized by hydrogen bonds (guanine tetrad)[10-13]. Assembly and dissolution of telomeric secondary structures influence the maintenance of telomeres and are indispensable for the proper telomere function; therefore, their assembly is strictly regulated during the cell cycle by proteins of the shelterin complex[12-15].

The shelterin complex

The shelterin multimeric complex is an important factor involved in telomere maintenance. In humans, this complex consists of six protein subunits, namely TRF1, TRF2, RAP1, TIN2, TPP1 and POT1[16,17]. TRF1 and TRF2 (Telomeric Repeat binding Factor 1 and 2) are directly recruited to the canonical double-stranded telomeric DNA to which they associate via Myb/SANT domains[18,19]; TPP1 (Telomere Protection Protein 1) and POT1 (Protection Of Telomeres 1) heterodimerize and bind the single-stranded G-rich telomeric tract [20,21]. TRF1 and TRF2, along with RAP1 (Repressor-Activator Protein 1) that regulates TRF2 association to telomeric repeats[22,23], are connected to the POT1-TPP1 heterodimer via the TIN2 (TRF1 Interacting Nuclear factor 2) protein bridge[24]. Additionally, TIN2 stabilizes the interaction between TRF1 and TRF2 proteins and the binding of TRF2 to telomeres[25] (Fig. 3).

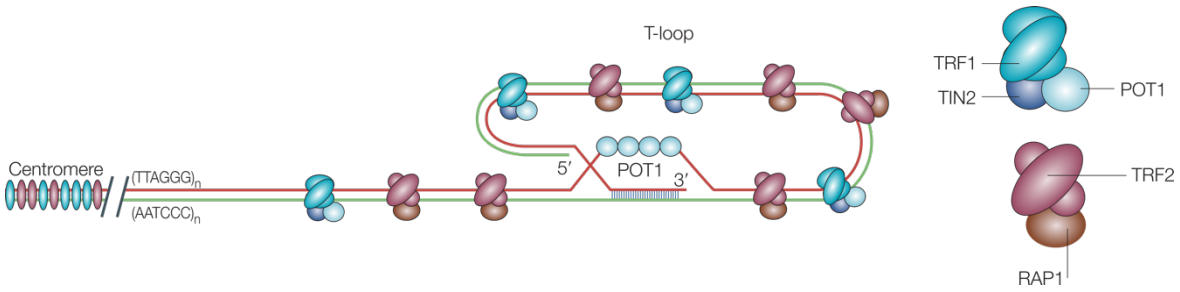

Figure 3. The human shelterin complex. Schematic representation of the multimeric shelterin complex at telomere. POT1 protein binds the single-stranded (ss) TTAGGG-repeat DNA, TRF1 and TRF2 instead form heterodimers which are associated with the duplex repeats. TIN2 and RAP1 stabilize TRF2-binding to the telomere. Adapted from de Lange T., 2004[9]

Overall, the shelterin complex mediates the proper formation of telomeric chromatin following DNA replication[16]. Its key function is to assist the T-loop formation, preserve the genome integrity by repressing the 5' end hyper-resection and avoid inappropriate activation of DDR pathways at chromosome ends[16]. Among the mechanisms averted by the shelterin complex, TRF2 specifically represses ATM (Ataxia Telangiectasia Mutated) kinase pathway by promoting the T-loop formation which sequesters the 3' overhang. Moreover, through the T-loop formation, TRF2 also represses NHEJ repair pathway and the consequent telomere fusion[17,26]. Instead, POT1-TPP1 heterodimer can prevent the activation of ATR (ATM- and Rad53- related) kinase pathway by displacing RPA (Replication Protein A) from its binding to the single-stranded telomeric DNA[27-29]. Additionally, the binding to double-stranded telomeric DNA of TRF2 hides the recognition site of PARP1 (poly (ADP-ribose) polymerase) positioned at the base of the T-loop, thus avoiding its cleavage[31]. Therefore, the telomeric DNA with its associated proteins guarantees the structural integrity of chromosome ends[2].

Telomere homeostasis

Besides the "end-protection problem", chromosome ends are characterized by their natural progressive shortening within each cell division due to the "end-replication problem". The conventional DNA replication machinery is unable to fully replicate the ends of linear DNA molecules[31,32]. As the two strands are synthetized in a 5'-3' direction, the leading strand will be synthetized continuously, in the same direction of the replication fork, while the replication of the lagging strand will be discontinuous and finally obtained through the joining of Okazaki fragments which are

the result of multiple priming events via RNA primers. In humans, it has been observed that the final lagging RNA primer is not in a terminal position but randomly positioned from 70 to 100 nt from the chromosome end[33] and its removal leads to the formation of an overhang of uncertain size. This process, combined with the fact that the newly synthesized leading telomere will be shorter than the lagging one (as its template 5' end strand is shorter than the 3' end), and with processing events occurring at telomeres to generate the G-overhang, leads to the gradual shortening of telomeric DNA[6,32]. As a consequence, telomeric repeats are lost and chromosome ends shorten of approximately 70-100 nt at each cell division[32,33] (Fig. 4).

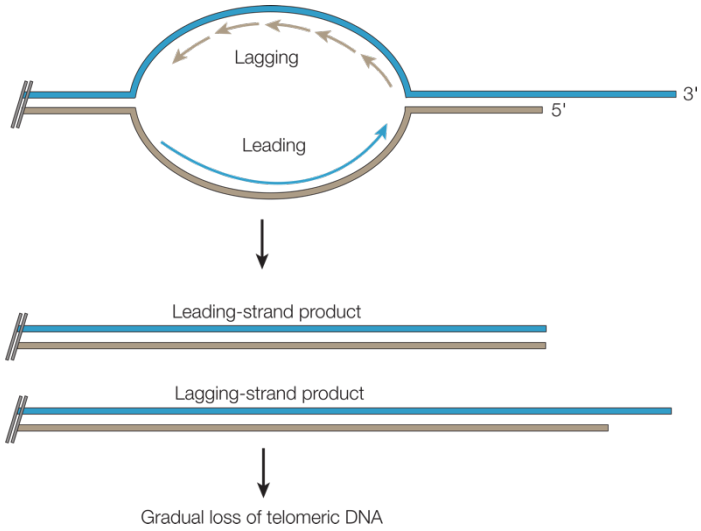

Figure 4. The end replication problem. Schematic representation of the gradual loss of telomeric DNA after replication of the telomeric lagging strand. Adapted from Verdun R.E., Karlseder J., 2007[32]

Telomeres, after a certain number of cell divisions, reach a critically short length, they become dysfunctional, and cause persistent activation of DDR pathways, which ultimately lead to replicative senescence[32,34,35]. For these reasons, the physiological shortening of telomeres acts as a powerful tumor-suppressor mechanism because it limits the proliferative capacity of cells, preventing them from entering mitosis[2,36]. In line with this scenario, the "end-replication problem" is also implicated in aging and in premature aging syndromes[37]. Additionally, continuously dividing cells, such as embryonic, germline and pluripotent cells, need to counteract this progressive telomere shortening. To maintain telomere length, the most frequent mechanism employed by proliferating cells exploits the expression of telomerase, a reverse transcriptase enzyme able to add telomeric repeats at the end of the 3' strand of chromosomes, conferring a potential unlimited proliferative capacity[38]. The proper

functionality of telomerase depends on the correct assembly of the ribonucleoprotein (RNP) catalytic core and on the correct interactions with its accessory proteins which are involved in its maturation, stability and trafficking[38,39]. The expression of telomerase is a key event not only in highly proliferative cells but also during tumorigenesis leading to replicative immortality of cancer cells[40]. Even though the expression of telomerase is the most used mechanisms for telomere length maintenance in eukaryotes, about 10-15% of cancer cells achieve replicative immortality through the Alternative Lengthening (ALT) pathway. In ALT cells, telomere length is maintained by homologous recombination (HR) through a mechanism in which, after the T-loop formation, the short telomere itself or a different telomere is used as a copy template[26,41].

TELOMERASE

Telomerase is a unique ribonucleoprotein (RNP) enzyme that counteracts the progressive shortening of telomeres by processively synthetizing new telomeric repeats at the 3' end of chromosomes[42]. The minimal catalytic core of the holoenzyme is composed of the specialized reverse transcriptase TERT, responsible for synthesizing telomeric repeats, and a RNA molecule known as *TR*, or *TERC*, that functions as a template for the telomeric DNA repeats synthesis, and as scaffold molecule to allow the formation of the holoenzyme through recruitment of associated proteins (see next paragraph)[24,43]. In physiological conditions, telomerase is expressed in both germline and somatic stem cells to allow their persisting cell division while it is inactivated in normal somatic cells through the silencing of the *TERT* gene[34,44]. Mutations in telomere- and telomerase-associated genes result in inherited stem cell-dysfunction diseases, also known as "telomeropathies", such as Dyskeratosis congenita, aplastic anemia and pulmonary fibrosis[24,45-47]. For these reasons, telomerase is considered a key determinant of human health, longevity and tumorigenesis[47-52].

The structure of telomerase

Telomerase is an RNA-dependent DNA polymerase containing a specialized reverse transcriptase, known as TERT, and the RNA *TR* subunit characterized by the presence of the template sequence 5'-CUAACCCUAAC-3' that directs telomeric repeats synthesis[53-55]. The proper biogenesis, maturation and localization of telomerase require the presence of five accessory proteins: Dyskerin, TCAB1, NOP10, NHP2 and GAR1, which interact with *TR*[38] (Fig. 5).

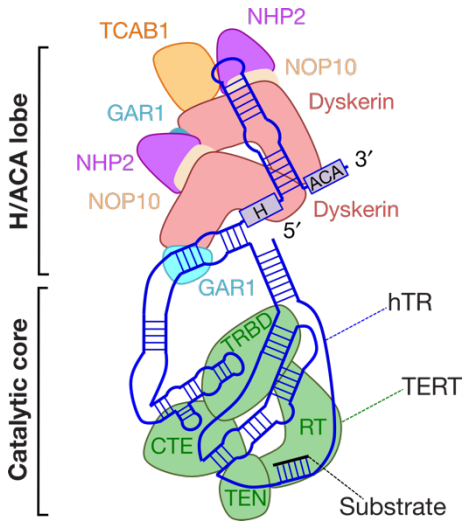

Figure 5. Cryo-EM based reconstruction of substrate-bound human telomerase holoenzyme. Schematic representation of the subunit arrangements of telomerase when bound to its substrate. The template region base pairs with the single-stranded telomeric DNA. Adapted from Nguyen *et al.*, 2018[55]

TR has been isolated from several species, including ciliates, yeast and mammals. Its length and sequence are not conserved throughout the evolution instead, the presence of functional domains has been found also in the other telomerase-presenting species[38,56]. In human cells, mature *TR* (h*TR*) is a 451 nt-long RNA comprising four key conserved structural domains: the pseudoknot/template (PK/t) domain, the conserved regions 4 and 5 (CR4/CR5), the H/ACA box and the CR7[55,57,58]. At its 5' end, h*TR* contains the P1 helix, followed by the pseudoknot and the CR4/5 motives forming the catalytic core domain that interacts with hTERT subunit. CR4/CR5 domains are characterized by a branched junction of RNA helices P5 and P6, and by the activity-critical stem-loop P6.1[55] (Fig. 6).

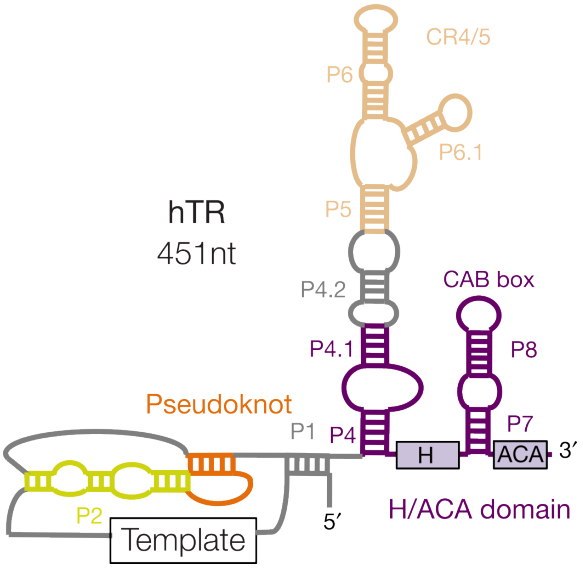

Figure 6. Reconstruction of the human telomerase RNA component. Schematic representation of h*TR* secondary structure. Pseudoknot and CR4/5 domains interact with hTERT. H/ACA domains harbors Dyskerin, NHP2, NOP10 and Gar1 accessory proteins. CAB domain interacts with TCAB1 accessory protein Adapted from Nguyen *et al.*, 2018[55]

Thanks to two recently reported cryo-EM structures of telomerase, it has been shown that one h*TR* molecule binds two sets of H/ACA heterotetrameric proteins (GAR1, NHP2, NOP10, Dyskerin)[55,57]: the first H/ACA set of proteins binds the hairpin P4 stem exclusively via Dyskerin while the second H/ACA set interacts more extensively with the 3' hairpin P7 stem- and CR7 stem-loops. The h*TR* P7 stem loop interacts

primarily with Dyskerin and CR7 permits the interactions with NOP10, NHP2 and one TCAB1 molecule[59].

The TERT subunit (127 kDa) contains four domains: a telomerase essential amino (N)-terminal (TEN) domain, a telomerase RNA-binding domain (RBD), a reverse transcriptase domain (RT, palm and fingers) and a carboxy-terminal element (CTE), also known as the thumb domain. Together, RBD, CTE and RT domains form a TERT ring structure while TEN domain is connected to RBD by a long linker[43] (Fig. 7).

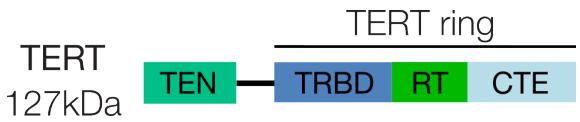

Figure 7. Reconstruction of the human telomerase reverse transcriptase component. Schematic representation of TERT domain architecture. TERT comprises four functional domains: TEN, TRBD, RT and CTE. Adapted from Nguyen *et al.*, 2018[55]

In the catalytic core of hTERT, the PK/t h*TR* domain encircles all domains of TERT forming extensive interactions, mostly through the RNA backbone. The telomeric DNA-h*TR* duplex is held in the active site of telomerase by interactions with conserved motifs of hTERT. The h*TR* template RNA is embedded within the reverse transcriptase domain and, although the telomeric DNA substrate can theoretically form up to 6 base pairs with h*TR*, it has been observed that only 4 base pairs occur at the AGGG-3' end of the substrate[57].

In human cells, the mature telomerase holoenzyme corresponds to a large complex of approximately 500 kDa[69,70] and its function *in vivo* requires the assembly with stably associated components (such as the dyskerin complex and TCAB1), and with transiently associated proteins as pontin, reptin and chaperones like HSP90 and TriC[60]. A fully assembled telomerase includes two dyskerin complexes that bind h*TR* on its two hairpins in the H/ACA domain. Dyskerin and NOP10 interact with h*TR*, GAR1 and NHP2 instead interact with dyskerin and NOP10 [55,71,72].

Biogenesis, assembly and trafficking within the cell

The regulation of telomerase activity occurs through both the control of TERT transcription and the post-transcriptional maturation of h*TR* 3' end[60]. The transcription from *TERT* promoter is highly regulated and surprisingly a core *TERT*-promoter

construct, which encompass the TSS, is active in telomerase-expressing human cancer cells but also in telomerase-negative fibroblasts suggesting a fine-tuned regulation which is mediated not only by the proximal promoter, but also involves distal regulatory elements and post-transcriptional regulatory mechanisms[60]. In general, *TERT* promoter contains native binding sites for ETS family transcription factors, and it is silenced by trimethylation of H3 Lys27 (H3K27me3) modification[60]. Furthermore, alternatively spliced variants of *TERT* mRNA have been reported[173]. h*TR* in vertebrates belongs to the family of small Cajal body RNAs (scaRNAs) and small nucleolar RNAs (snoRNAs). It is transcribed from a dedicated locus on its own promoter, differently from sca- and sno-RNAs that are normally encoded in introns, and transcribed by RNA Pol II[61,62]. In normal conditions, h*TR* transcripts are 451 nt long, however a small pool of h*TR* transcripts that displays a longer sequence has been observed. Indeed, h*TR* is initially transcribed as an extended molecule of around 461 nt presenting a short untemplated adenosine (A) tail, known as precursor, which is lately processed into the mature 451 nt-long RNA[60]. Additionally, even longer h*TR* precursors have been detected by RT qPCR and may represent either very early precursors or unproductive h*TR* transcripts targeted by the nuclear RNA surveillance for degradation[63,64]. Precursor forms of h*TR* are oligo-adenylated by the polyA polymerase PAPD5 and lately de-adenylated by the polyA ribonuclease PARN that preferentially removes untemplated A tails but can also trim the genomic extension of precursors in order to produce mature molecules of h*TR*[60]. However, the absence of both PARN and PAPD5 does not impair h*TR* transcript maturation indicating that 3'-5' exonucleases, in addition to PARN, are responsible for clipping h*TR* precursors into the mature form[65]. h*TR* precursors which are not processed into the mature form are subjected to degradation through the RNA exosome by the recruitment of NEXT and CBC complexes[66,67]. An additional step of h*TR* maturation includes the hypermethylation of its m7G monomethyl guanosine cap by TGS1. TGS1 mediated hypermethylation suppresses h*TR* accumulation and negatively regulates telomerase activity[68]. The telomerase subunit TCAB1 controls both the catalytic activity and the nuclear trafficking of telomerase and is stably bound to telomerase through an interaction with the CAB box of h*TR*. Dyskerin is bound by the NAF1 protein, which enables the stable association of dyskerin to telomerase, and the factor SHQ1 that facilitates telomerase assembly[73-76]. Additionally, pontin and reptin, which are both AAA+ ATPases, bind to TERT and dyskerin during the S phase, promoting the

assembly of telomerase into a stable complex[77]. HSP90 (chaperone heat shock protein 90) drives TERT binding to h*TR* and the chaperone TriC is required to assemble the TCAB1-telomerase complex[78-81]. TCAB1 targets h*TR* and its associated proteins to Cajal bodies (CBs), nuclear compartments enriched in splicing-related factors and other RNA-related processes, where they are retained for an extended time. h*TR* exit from CBs is mediated by the recruitment of hTERT and the consequent full assembly of the holoenzyme[82] (Fig. 8). In 2016, Collins' group demonstrated that a minimized human telomerase expressed in HCT116 cells lacking TCAB1 is able to maintain telomeres length[165]. Moreover, it has been recently demonstrated that only a small fraction of h*TR* molecules is targeted to CBs in a TCAB1-dependent manner, suggesting the activation of a backup pathway involved in telomerase assembly and telomeres maintenance[82]. During S phase, the mature and fully assembled enzyme is recruited to telomeres. This process will be discussed in the next section.

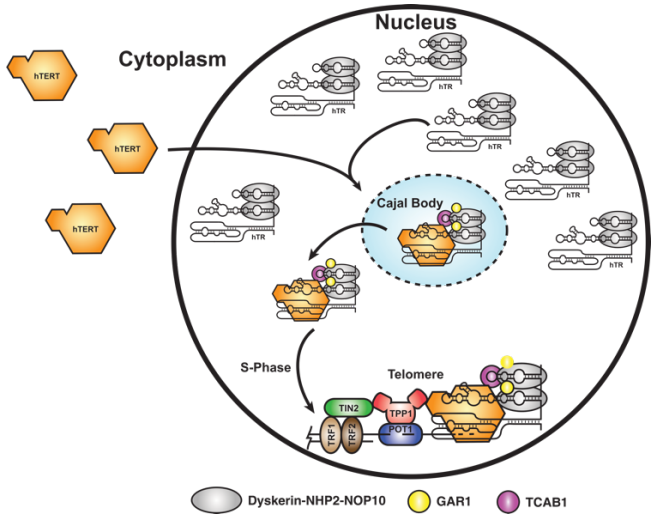

Figure 8. Human telomerase dynamics. hTERT is synthesized in the cytoplasm, h*TR* instead is found in the nucleus. The assembly of h*TR* and hTERT into the catalytically active telomerase enzyme occurs at the Cajal bodies (CBs). Telomerase RNA is recruited to CBs by its interaction with TCAB1 during G1. In S phase, telomerase is recruited to telomeres as active reverse transcriptase enzyme. Adapted from Schmidt and Cech, 2015[38]

Telomerase recruitment to telomeres and regulation of its activity

Telomere maintenance by telomerase plays a key role in several human pathologies and in cancer, thus a better understanding of its biology could lead to new therapeutical approaches[83]. *In vitro*, the human telomerase can processively

synthetize multiple telomeric repeats without dissociating from the telomeric DNA substrate. *In vivo*, human telomerase has been shown to add about 50-60 nt to most of the telomeres during a single processive step in cancer cells[84,85]. Interestingly, the nucleus of a cancer cell contains around 250 fully assembled telomerase holoenzyme molecules, a number that corresponds approximately to the number of telomeres once the DNA replication has occurred (250 telomerases/184 telomeres in late S phase)[86,87]. The shelterin subunit TPP1 is necessary for telomerase recruitment to telomeres[70,19,87]. POT1, that binds the single-stranded telomeric overhang, is also associated with TPP1 via its OB-fold domain and regulates telomerase activity[20,89]. Interestingly, the loss of TPP1 and TIN2 results in less telomerase recruitment to telomeres[90], while POT1 acts as repressor of telomere elongation[82]. Telomerase is recruited to chromosome ends during the S phase of the cell cycle by a direct interaction with the oligonucleotide/oligosaccharide-binding (OB)-fold domain of TPP1 shelterin protein and the TEN domain of TERT reverse transcriptase[91-94]. In particular, TERT-TPP1 interaction is driven by a specific patch of amino acids (TEL patch) present on the surface of the OB-fold domain of TPP1[70,90-93]. Mutations in TPP1 TEL patch cause telomere shortening and severe dyskeratosis congenita[95]. Interestingly, recent live cell imaging-based studies reported that telomerase molecules diffuse through the nucleus and form both transient and long-term interactions with telomeres favoring a model of “Recruitment-Retention” to explain telomere elongation in human cells[82,96]. According to this model, telomerase is firstly recruited to telomeres through an interaction with TPP1, leading to a series of short and highly diffusive telomere-telomerase associations. A fraction of telomerase molecules is retained at telomeres through base-pairing of the h*TR* template sequence with the single-stranded telomeric overhang resulting in long-lasting static telomerase-telomere interactions[82,97]. These telomeric h*TR* molecules present a longer time of residence and slow diffusive properties, and they are considered to be actively elongating the telomere[82,97]. Thus, while most telomeres have been described to be elongated by telomerase during each cell division in human cancer cells[84], in the same cellular setting only few telomeres (from 1-4) have been shown to stably associate with telomerase at any given time[82,96]. Interestingly, POT1 is involved in the regulation of telomerase activity at telomeres by competing with h*TR* for the binding of the single-stranded telomeric overhang[98]. In line with these findings, the

expression of an OB-fold mutated POT1 in HeLa cells resulted in enhanced telomerase retention and telomere overelongation[82,98] (Fig. 9).

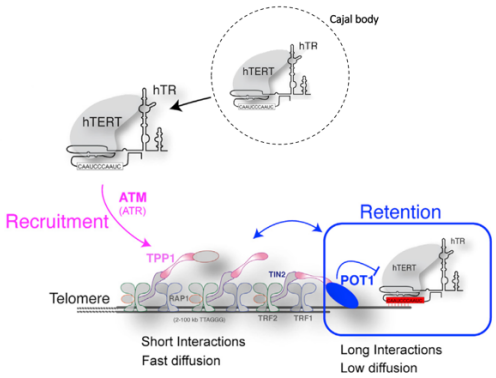

Figure 9. Proposed model for telomerase recruitment to telomeres. Telomerase is able to establish short and dynamic interactions with the telomeric repeat DNA. These interactions become stable at the single-stranded end if telomere elongation is needed. POT1 can act as inhibitor of the telomerase binding to the telomeres. Adapted from Laprade *et al.*, 2020[82]

In addition to POT1, other telomeric proteins inhibit telomerase activity at telomeres. In particular, the CST complex, a conserved trimeric complex comprising the subunits CTC1, STN1 and TEN1, is bound to the telomeric 3' overhang to assists the DNA replication at chromosome ends by stimulating the DNA polymerase α-primase[99-101]. Additionally, this complex restricts telomeres extension by limiting the access of telomerase to the telomere and inhibiting the TPP1-POT1-dependent telomerase stimulation[102,174]. Through this mechanism, the CST complex could facilitate the switch from telomerase-mediated elongation to fill-in synthesis of telomeres[60].

TERRA

Chromosome ends are characterized by the presence of heterochromatic features such as histone H3 trimethylated at lysine 9 (H3K9me3), histone H4 trimethylated at lysine 20 (H4K20me3), H3K27me3, methylated cytosines and by the presence of Heterochromatin Protein 1 α (HP1α)[103,104]. The heterochromatic state has been shown to be fundamental for telomeric integrity maintenance and to regulate both the ALT mechanism and telomerase activity[105]. This epigenetic signature combined with the gene-less structure of telomeres and their ability to silence transcription of experimentally inserted genes (a process known as Telomere Position Effect, TPE), supported for long time the idea that telomeres are transcriptionally silent[106]. However, in 1989 Rudenko and Van der Ploeg identified for the first time a heterogeneous population of RNAs containing telomeric repeats in *Trypanosoma brucei*[107]. In 2007, telomeric transcription was proven and characterized also in mammals. These studies demonstrated that telomeres are actively transcribed by RNA Polymerase II (RNA Pol II) into a family of long non-coding (lnc) RNA transcripts, known as TERRA[107,108].

The structure of TERRA transcripts

The expression of the Telomeric Repeat-Containing RNA (TERRA) has been observed in different organisms including yeast, zebrafish, mouse and human[108-111]. TERRA transcription is driven by RNA Pol II, that utilizes as transcription template the telomeric C-rich strand[113], starting from transcriptional start sites (TSSs) located in the subtelomeric regions of chromosomes and terminating within the region of telomeric repeats[114,115]. Therefore, each TERRA transcript is composed of a subtelomeric-specific sequence at its 5' end, that allows the discrimination of the different TERRA populations expressed by distinct telomeres, and a canonical telomeric tract of UUAGGG repeats at its 3' end which is shared among TERRA transcripts expressed from all telomeres[116]. Both during and after transcription, TERRA is subjected to co- and post-transcriptional modifications and the RNA processing mechanisms vary among TERRA transcripts resulting in biochemically different fractions of transcripts that have remarkably different biological functions[113]. As TERRA is transcribed by RNA Pol II, it presents a canonical 7-methylguanosine cap at its 5' end, like most coding RNA species, and only a small fraction (about 7%

in HeLa cells) contains a poly-A tail at its 3' end which affects its stability and affinity to chromatin[113,117,118] (Fig. 10). We have recently observed that TERRA polyadenylation occurs preferentially on transcripts expressed from specific telomeres and that the mechanisms of TERRA stability regulation are also telomere-specific[175]. A recent study indicates that TERRA transcripts are m6A-modified within subtelomeric sequences by METTL3 enzyme. This modification contributes to the stability of TERRA transcripts in ALT cancer cells[176]. Thus, the mechanisms coordinating TERRA stability are fine-tuned and regulated in a telomere specific manner. Importantly, the G-rich 3' end sequence of TERRA has been shown to form RNA G4 structures[147]; these structures are important for the regulation of TERRA functions and localization at telomeres, as discussed in the following paragraphs.

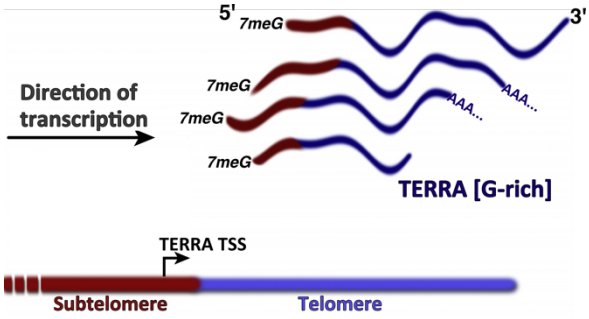

Figure 10. Schematic representation of human TERRA transcripts. TERRA transcription starts from the subtelomeric region and proceeds towards the chromosome end. The vast majority of TERRA molecules present a 5' 7-methylguanosine cap (7meG) and only a small fraction is polyadenylated in human cells. Adapted from Azzalin C.M., Lingner J., 2015[116]

Regulation of TERRA expression

TERRA transcription relies on promoters located within the subtelomeric region of chromosomes. In humans, a subset of TERRA promoters is positioned in proximity to the telomeric repeat tract and is characterized by the presence of both CpG islands and conserved repetitive regions known as "61-29-37 repeats"[114]. Moreover, a second class of promoters has been recently identified about 5 to 10 kb upstream of the telomeric tract of 10 distinct chromosome ends in HeLa cells[115,119]. Both groups of TERRA promoters show binding sites for CTCF (CCCTC-binding factor), a transcription regulator factor whose loss results in reduced TERRA levels due to a decreased recruitment of RNA Pol II at telomeres[120]. The presence of different promoters and the distinct distances of TSSs from the telomeric tract of chromosome

ends contribute to the heterogeneous length of TERRA molecules which vary in size from 100 nt to 9 kb in humans[108] and from 100 nt to 1.2 kb in *S. cerevisiae*. Additionally, while the 3' end of TERRA shows a rather constant length of the UUAGGG tract (as detected by modified protocols of RT-qPCR)[113], the length of TERRA was also demonstrated to positively correlate with the length of the telomeres, suggesting that the 3' end of TERRA can be heterogeneous[114,121]. Altogether, these data indicate a contribution of both 5' and 3' ends of TERRA in determining the heterogeneity in length of TERRA transcripts.

TERRA expression is further regulated by the heterochromatic state of telomeres and subtelomeres. In particular, TERRA levels are negatively affected by the presence of H3K9me3 and H4K20me3 at telomeric and subtelomeric regions, as well as by DNA methylation at CpG island-containing promoters[109,114]. In this regard, embryonic stem cells (ESCs) and induced pluripotent stem cells (iPSCs), which are characterized by lower methylation state of H3K9 and H4K20 compared to differentiated fibroblasts, show high levels of TERRA[122]. Additionally, histone acetylation and H3K4 methylation associate with increased TERRA levels in human cells[118,123]. Notably, a number of transcription factors has been observed to positively regulate TERRA expression, including Rb, p53 and the heat shock factor 1 (HSF1), and different studies have reported their involvement in the regulation of TERRA expression upon cellular stress[124-126]. Interestingly, TERRA expression is also regulated during the cell cycle as TERRA levels have been shown to peak during the G1 phase, then to progressively decrease during S phase until reaching the lowest expression during the transition from late S to G2 phase and to raise again during mitosis[113,127]. Notably, this cell cycle regulation of TERRA expression has been observed in both yeasts and human cells[113,127].

Subnuclear localization

In mammalian cells, TERRA transcripts are mostly found in the nucleus[128] while in yeast they were observed also in the cytoplasm, upon metabolic stress[129]. In mammalian cells, the non-polyadenylated TERRA pool can be found both in the nucleoplasm and chromatin-bound, while polyadenylated TERRA transcripts mainly localize in the nucleoplasm[108,113]. Interestingly, poly-A transcripts are more stable, displaying a longer half-life (8 hours) as compared to the non-poly-A TERRAs (around

3 hours)[113]. Recently, shorter fragments of TERRA molecules (around 400 nt in length) consisting principally in UUAGGG sequences have been reported in exosome fractions in the cytoplasm of human cells. These TERRA fragments are released in the extracellular environment and have been proposed to act as pro-inflammatory molecules in responsive cells[130,131]. A fraction of TERRA transcripts localizes at telomeres thanks to their direct interaction with TRF1 and TRF2 proteins of the shelterin complex as well as with several components of telomeric heterochromatin, including the histone methyltransferase SUV39H1, ORC1 (Origin of Replication 1) and PRC2 (Polycomb Repressive Complex 2)[118,132]. TERRA localization at telomeres is regulated by specific hnRNPs in mouse cells and components of the nonsense mRNA decay (NMD) pathway in human cells which can actively displace TERRA transcripts from chromosome ends[108,112]. Interestingly, TERRA is able to localize at telomeres not only through interaction with TRF1 and TRF2 but also by direct base-pairing with the C-rich strand of telomeric repeats, forming RNA:DNA hybrids, known as R-loops[133]. *In vitro*, the establishment of R-loops has been observed to be RAD51 DNA recombinase-dependent, as this enzyme can promote homology search and TERRA strand invasion. Interestingly, recent evidence indicates that BRCA2 (BReast CAncer type 2 susceptibility protein) facilitates TERRA-RAD51 association, while BRCA1 counteracts R-loops formation by resolving them in collaboration with SETX (Senataxin) and XRN2 (5'-3' RNA exonuclease 2)[134]. Chromosome ends are particularly prone to form RNA:DNA hybrids in ALT cells, due to the presence of higher levels of TERRA, as compared to telomerase positive cells. This feature underlines the importance of R-loops in facilitating HR-mediated telomere maintenance and in modulating the chromatin state in ALT cells[135,136]. On the other hand, R-loops can be a source of genomic instability at telomeres because they can represent an obstacle for the DNA replication machinery potentially leading to collapsed replication forks and activation of DDR pathway[137-149]. For this reason, R-loops formation and accumulation at telomeres are controlled by different mechanisms, such as BRCA1-mediated resolution or expression and activation of the RNase H1 enzyme[134,135,140]. As also subtelomeric regions present a high CG content in their sequence downstream of TERRA TSSs, R-loops can form not only at telomeres but also at subtelomeres through base-pairing of the 5' end of TERRA with its DNA template[141]. Thus, multiple mechanisms are involved in the regulation of TERRA expression and localization at telomeres, underlining the key role that these

transcripts, which are also highly conserved throughout the evolution, play in telomere biology.

TERRA roles

Several functions have been proposed for TERRA in different organisms, but the molecular mechanisms of its biological roles remain still largely elusive yet[116]. In mammals, TERRA RNA has been proposed to participate in heterochromatin formation at telomeres by acting as a scaffold molecule to mediate the recruitment of epigenetic factors to chromosome ends (Fig. 11C). In this regard, TERRA can interact with several heterochromatic marks, such as H3K9me3, HP1 protein and SUV39H1, and with chromatin remodeling factors including NoRC (Nuclear Remodeling complex)[142], MORF4L2 (component of the NuA histone acetyl transferase complex), and ARID1A (component of the BAF-type SWI/SNF nucleosome remodeling complex)[143]. It has been shown that TERRA depletion results in decreased association of H3K9me3, HP1 and SUV39H1 at telomeres, supporting the hypothesis of TERRA as one of the major contributors to heterochromatic factors recruitment at telomeres[115,121,144]. Moreover, TERRA has been found to associate with the histone methyl transferase PRC2 which is responsible for H3K27me3 deposition[145]. In the U2OS cell line, TERRA G-quadruplex structures can promote TERRA-PRC2 interactions leading to the deposition of H3K9me3, H4K20me3, H3K27me3 and HP1 protein to telomeres[145]. It has also been shown that TERRA G-quadruplexes are recognized as binding targets for other telomere-binding proteins, including the translocated in liposarcoma/fused in sarcoma (TLS/FUS) protein[146] and TRF2 shelterin subunit[144,147]. As TLS/FUS associates with the histone methyltransferase SUV4-20H2, TERRA-TLS/FUS interaction can boost heterochromatin establishment by promoting H4K20me3 at telomeres[146]. A tight regulation of TERRA levels and localization is fundamental to maintain telomere and chromosome stability (Fig. 11A), indeed both TERRA upregulation and downregulation lead to telomere-dysfunction induced foci (TIFs) formation as a consequence of the DDR pathways activation. Moreover, the unscheduled association of TERRA to telomeres results in TIFs formation and chromosome abnormalities[110,148]. Impairment of TERRA transcription by mutation in subtelomeric CTCF binding sites leads to increased sensitivity to replicative stress of the TERRA depleted telomere, resulting in sister-telomere loss, ultra-fine anaphase bridges and micronuclei[149]. On the other hand, a boost in TERRA

transcription results in an increased recruitment of LSD1 at telomeres that stimulates the activation of the NHEJ DNA repair pathway through the MRN complex (MRE11, RAD51, NBS1) and the consequent formation of telomere fusion events[150]. Additionally, when TERRA-interacting members of the hnRNP family or EST1A and UPF1 (components of NMD pathway) are silenced, an increased TERRA localization at telomeres can be observed in spite of TERRA levels remaining unaltered[108,151]. This condition also results in DDR pathways activation at telomeres and consequent loss of telomeric DNA integrity. Altogether, these findings underline the importance of a fine-tuned regulation of TERRA expression and localization in order to maintain telomere function and genome stability. Interestingly, several studies reported a key role for TERRA in telomere maintenance in ALT cancer cells (Fig. 11B). ALT cells are characterized by high TERRA expression levels and TERRA accumulation at telomeres throughout the cell cycle[152]. Telomeric R-loops are also detected at high levels in ALT cells, and they have been proposed to promote HR at telomeres, sustaining the ALT phenotype[135]. Indeed, inhibition of the RNase H1[135] or the ATPase/helicase FANC-M[153], which are known to disassemble R-loops at ALT telomeres, increased telomere instability and ALT activity; conversely, overexpression of RNase H1 or FANC-M has been shown to impair the ALT mechanism, pointing to R-loops as key regulators of ALT[135,139,153,154].

Importantly, TERRA has been shown to regulate telomerase activity. The interplay between TERRA and telomerase will be illustrated in the following paragraph.

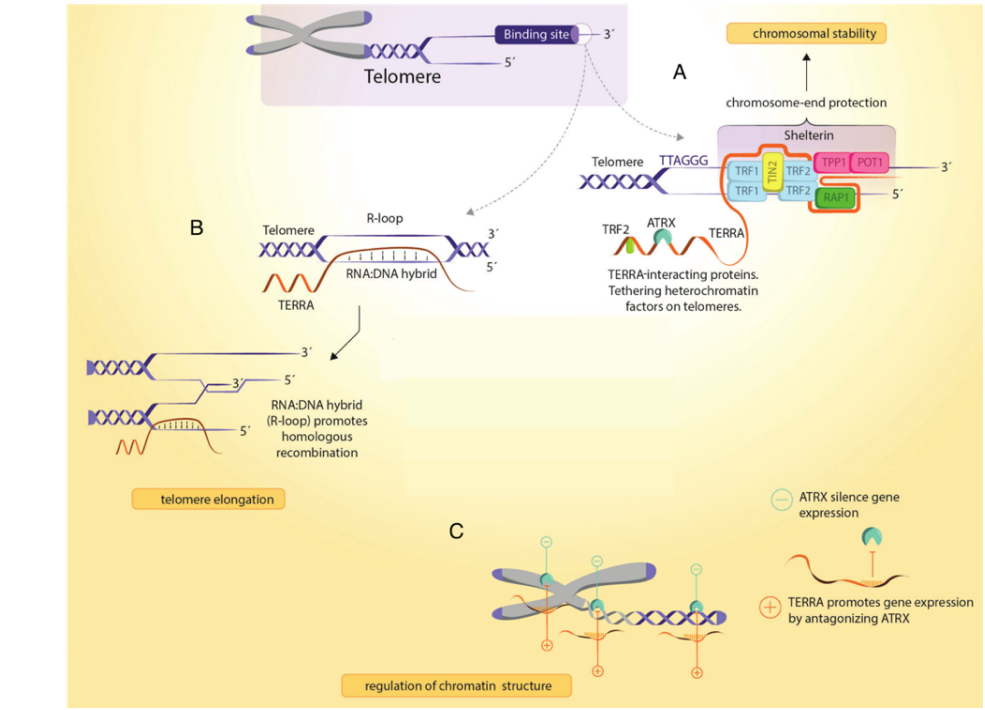

Figure 11. Proposed TERRA functions in mammals. A) TERRA together with the shelterin complex is implicated in chromosome ends protection by assembling secondary protective structures which include R-loops, T-loops and G-quadruplexes. B) In ALT^{+} cells, TERRA promotes telomere elongation by promoting homologous recombination. C) TERRA acts as remodeler of telomeric chromatin structure through an antagonistic interaction with ATRX. Adapted from Kroupa *et al.*, 2022[172]

TERRA as key regulator of telomerase activity: an open debate in the field

Telomerase activity and processivity regulation is essential in determining telomere length and therefore it is tightly regulated by several co-factors. One of the first biological functions proposed for the lncRNA TERRA was to act as a natural inhibitor of telomerase by blocking telomerase-telomere interaction thanks to its ability to base-pair with the template sequence of *TERC* (5'-CUAACCCUAAC-3' in mammals)[109,156](Figure 12A). In 2008, Schöftner and Blasco showed that short TERRA-like oligonucleotides are capable of inhibiting telomerase activity both in human and mouse cell extracts and that there is a correlation between high TERRA expression and short telomere length in various cell lines, supporting the idea of TERRA as negative regulator of telomerase[109]. A landmark study by Redon and colleagues showed that TERRA is associated with both h*TR* and hTERT by co-immunoprecipitation experiments performed in HeLa cells, suggesting that TERRA interacts with telomerase also *in vivo*[156]. Moreover, *in vitro* TERRA-h*TR* interaction is abolished when h*TR* sequence is mutated, further supporting the idea of TERRA as

negative regulator of telomerase activity[155]. Further studies in mouse embryonic stem cells obtained a co-purification of TERRA with *TERC* RNA and interestingly, the knockdown of TERRA resulted in increased telomerase activity and increased DNA damage at telomeres[148]. To validate the hypothesis of TERRA acting as negative regulator of telomerase, several studies overexpressed TERRA in isogenic cells in order to assess TERRA impact on telomere length and telomerase activity. Surprisingly, TERRA overexpression in mammalian cells did not inhibit telomere elongation by telomerase. Indeed, TERRA overexpression from a transcriptionally inducible telomere did not impact the elongation of this telomere[157]. On the other hand, the ectopic expression of inducible TERRA-like transcripts in human cancer cells resulted in telomerase activity inhibition by TRAP assay. Still, cells expressing TERRA-like transcripts did not showed reduced telomeres length[158]. Furthermore, cells lacking the DNA methyltransferase DNMT1 and DNMT3A/B present hypomethylation of CpG islands in subtelomeric promoters and consequent overexpression of TERRA[114,159]. Farnung *et al.* studied HCT116 cells lacking both DNMT1 and DNMT3B and observed a normal telomerase activity and an efficient elongation of telomeres[157]. These findings suggest that TERRA overexpression does not inhibit telomerase activity at telomeres. Similar results have also been obtained in fibroblasts from ICF (immunodeficiency, centromeric region stability and facial anomalies) syndrome type 1 patients. These patients present a loss-of-function mutations in the *DNMT3B* gene which leads to reduced methylation of CpG elements in subtelomeric promoters and increased TERRA transcription, and interestingly ICF-patient derived cells present abnormally short telomeres compared to fibroblast from healthy individuals[160]. Even if TERRA is overexpressed in this condition, the high TERRA levels do not prevent the reactivation of telomerase during iPSCs generation from ICF fibroblasts, and consequent telomere elongation. Altogether, these findings show that high TERRA levels are not sufficient to inhibit telomerase activity[155]. Intriguingly, in yeast TERRA has been proposed as a positive regulator of telomerase-mediated telomere elongation (Figure 12B). In budding yeast, TERRA expression is induced at short telomeres and TERRA transcripts act as scaffold to promote telomerase nucleation, favoring its recruitment to the TERRA telomere of origin for subsequent elongation[161]. A similar function for TERRA has been demonstrated also in fission yeast[162].

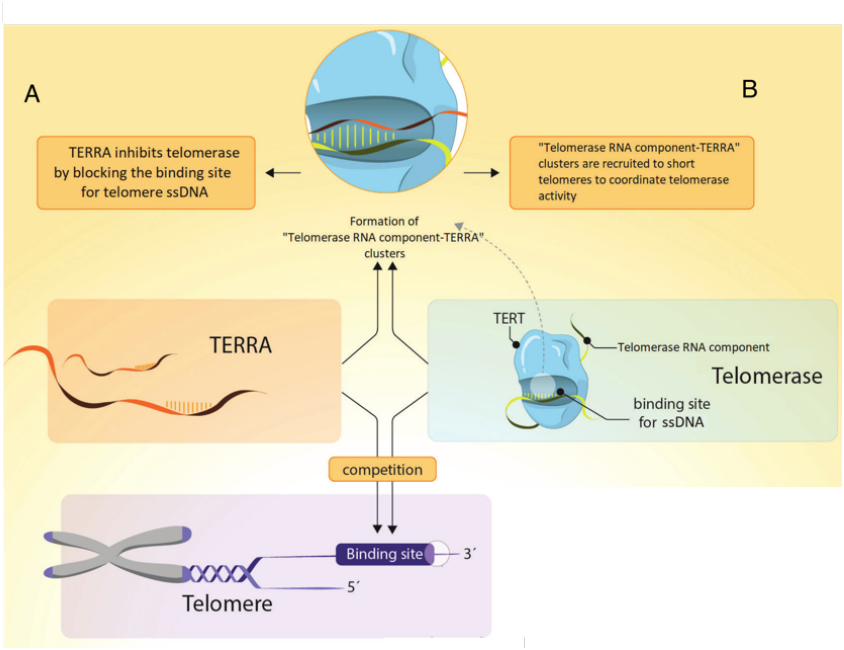

Figure 12. Proposed telomerase activity regulation by TERRA. TERRA can bind to h*TR* through base pairing and compete with the telomeric DNA for this binding. A) TERRA sequence is complementary to the template region of h*TR*. For this reason, TERRA is thought to inhibit telomerase activity by blocking its binding site for the telomeric ssDNA. However, conflicting evidence on the function of TERRA in telomerase regulation have been reported in human cells. B) In yeast, TERRA has been shown to cluster with h*TR* in order to recruit telomerase to short telomeres and promote telomere elongation. Adapted from Kroupa *et al.*, 2022[172]

Altogether, these findings indicate that TERRA interacts with telomerase in human cells. However, conflicting results are present in literature on the correlation between TERRA levels and telomerase activity. Indeed, while TERRA knockdown associates with increased telomerase activity, other studies have shown that overexpression of TERRA does not inhibit telomerase in different cellular setting. Perhaps, to confound even more this scenario is also the function of TERRA as positive regulator of telomerase observed in yeast.

To reconcile these results, we hypothesized that the role of TERRA in telomerase regulation may be dependent not only on TERRA levels but also, and perhaps even more importantly, on the localization of TERRA transcripts. However, direct visualization of both TERRA and telomerase in human cells has not yet been achieved. For this reason, it remains unclear whether TERRA-telomerase interaction occurs at Cajal bodies, where h*TR* maturation is presumed to occur, in the

nucleoplasm, or at telomeres. Each of these scenarios would underline distinct mechanisms of TERRA-mediated telomerase regulation.

In order to gain insight into the function of TERRA in telomerase activity, I thus set out to study TERRA and telomerase localization in human cancer cells in different cellular settings.

AIMS OF THE THESIS

TERRA has been shown to interact with telomerase, however conflicting evidence on its role in the regulation of telomerase in human cells are reported in literature. Therefore, the influence of TERRA on telomerase activity in humans remains elusive.

The main aim of this PhD project is to gain insights into the function of TERRA transcripts in the regulation of telomerase. I hypothesized that a fine-tuned control of TERRA localization may be the key for this function. Thus, I set out to visualize both TERRA and the telomerase RNA h*TR* using single molecule inexpensive RNA FISH (smiFISH) and confocal microscopy.

I applied different approaches to study TERRA and h*TR* localization during telomere length homeostasis and used antisense oligonucleotides targeting TERRA molecules to investigate their function in the regulation of telomerase.

The findings here reported suggest that telomeric TERRA transcripts act as negative regulators of telomerase activity in humans. Displacement of TERRA from telomeres may represent a mechanism for telomerase regulation. These results will enable to reconcile conflicting evidence on TERRA expression levels and telomerase activity in human cells.

Furthermore, given the crucial role of telomerase in tumorigenesis, this information may unveil novel avenues for cancer treatment.

A manuscript with the results presented in this thesis is in preparation and will be submitted soon.

MATERIALS AND METHODS

Cell culture

HeLa (ATCC CCL-2), HCT116 (ATCC CCL-247) and Phoenix cell lines were cultured in DMEM (Gibco) supplemented with 10% fetal bovine serum (Gibco), 2 mM L-Glutamine (Gibco), 100 IU/mL penicillin, and 100 μL streptomycin solution (Gibco). Cells were passaged every 48-72 hours, incubated at 37°C with 5% CO_2 and regularly tested for mycoplasma contamination.

Telomere shortening

To induce progressive telomere shortening, cells were treated with 10 μM BIBR1532 (Cayman chemical) compound for more than 120 population doublings (PDs). Medium was freshly added to cells every 48-72 hours. To the untreated controls solvent (DMSO) only was administered.

In vitro knock-down of TERRA and TCAB1

For TERRA depletion, cells were grown at a 50% confluence on 6-wells plates and transfected with 200 nM Antisense Oligonucleotides (ASO) LNA Gapmers (Qiagen) specifically designed to target TERRA (Validated by Chu *et al.*[148]) using Oligofectamine transfection reagent (Thermo Fisher Scientific) for 48 hours following the manufacturer's instructions. A Scrambled LNA was used as negative control (Qiagen). After transfection, RNA extraction or cell fixation were performed as described later. Transfection efficiency was previously assessed by transfecting an oligonucleotide labelled with FAM fluorophore and observed at 24 and 48 hours post transfection by fluorescence microscopy. For TCBA1 knock-down, cells were grown at a 50% confluence on 6-well plates or 10 cm Petri dishes and transfected with 50 nM siRNA against TCAB1 or control siRNA (SMART pool, Dharmacon) for 48 hours using JetPRIME (Polyplus) transfection reagent according to the manufacturer's instructions. After transfection, proteins extraction or cell fixation were carried out as reported in cell lysis and immunoblotting section.

Oligonucleotides and siRNAs	Sequence (5'-3')
LNA Gapmer TERRA (ASO TERRA)	TAACCCTAACCCTAAC
LNA Gapmer SCRAMBLED (ASO SCR)	AACACGTCTATACGC
LNA MS2-FAM	/56FAM/ACATGGGTGATCCTCAT GT/iFluorT/TTCT/36FAM/
WRAP53 (TCAB1) siRNA SMART pool	GCAGAAGAAGCAAACGGGA CUGAUAACAUCUUGCGAAU AGAAGAAGCGAACGGGCCA UUUGGAGACUCAACCGUUA
Non-Targeting siRNA #1 (siCTR)	UGGUUUACAUGUCGACUAA

Table 1: List of oligonucleotides used.

Generation of retroviral particles and cell transduction

Retroviral particles were produced in Phoenix cells. Cells were seeded in antibiotic-free medium and co-transfected with pCMV-VSV-G (a gift from Pascal Chartrand, Addgene plasmid #8454) and the required plasmid (pLPC myc hPOT1, Addgene plasmid #12387; pLPC myc hPOT1 ΔOB, Addgene plasmid #13241) using calcium phosphate[177]. 24 hours after transfection, cells were grown for maximum 8 hours in medium enriched with 10 mM Sodium Butyrate (Sigma). Supernatants were harvested 48 hours after transfection, filtered using 0.22 μm Primo Syringe Filters (Euroclone) and precipitated overnight in PEG-8000 (Sigma). The following day, the viral particles were centrifuged at 2000 xg for 15 minutes and, after carefully removing the supernatant, resuspended in medium without serum. Aliquots of viral particles were stored at -80°C. Cells between 50% and 70% of confluence were transduced with frozen stocks of viral particles in medium enriched with 8 μg/mL Polybrene. The virus-containing medium was replaced with fresh one 24 hours after transduction and cells were grown in an antibiotic-containing medium for 7 days. The proper concentration of antibiotic was previously assessed by setting up a toxicity curve per each cell line.

Immunofluorescence microscopy

Cells were seeded on 22x22 mm glass coverslips (Prestige), previously stripped with 1 M HCl, sterilized and stored in 100% Ethanol, and fixed directly fixed in 4% PFA (Electron Microscopy Science) in 1X PBS for 20 minutes at room temperature. After fixation, cells were washed twice in 1X PBS and kept at +4°C for maximum 1 month or directly permeabilized in 0.5% Triton X-100 1X PBS for 5 minutes at room temperature. After two rinses in 1X PBS, permeabilized cells were blocked with 2% BSA in 0.1% Triton X-100 1X PBS for 3 hours and then stained for 1 hour at room temperature with the appropriate primary antibody diluted in blocking solution (Novus Biological, mouse antiTERF2-IP, 1:500). Cells were washed six times for 5 minutes with 0.1% Triton X-100 1X PBS and incubated with the appropriate species-specific fluorescent secondary antibody (Thermo Scientific, goat anti mouse AF488, 1:1500) for 1 hour. After incubation, cells were washed again for six times for 5 minutes with 0.1% Triton X-100 1X PBS and stained with 1ng/μL DAPI in 1X PBS for 8 minutes. After washing cells twice with 1X PBS, coverslips were mounted in ProLong Diamond Antifade Reagent (Invitrogen) on precleaned glass slides.

smiFISH microscopy

The smiFISH protocol is divided in the following steps:

Probe preparation

As described by Querido *et al*.[163], smiFISH technique requires the hybridization between primary probes, which recognize the RNA of interest, and fluorescently labelled secondary "FLAP" probes. The h*TR* smiFISH probeset is prepared as a 20 μM equimolar mixture (1.33 μM each) of 15 different h*TR*-specific probes (Table 2) in milliQ water. For TERRA smiFISH probeset instead, a single 20 μM primary probe (Table 2) in milliQ water was used. smiFISH probesets consist of 40 pmol of specific primary probe mixed together with 50 pmol of FLAP probe and 1X NEB3 solution (100 mM NaCl, 50 mM Tris-HCl pH 8, 10 mM $MgCl_2$) in a final volume of 10 μL. Primary probesets were annealed with FLAP oligos in a PCR thermocycler (85°C for 3 minutes, 65°C for 3 minutes, 25°C for 5 minutes). Dual-color smiFISH was performed

by annealing each specific probeset with its FLAP probe in a separate tube and once annealed mix together in the hybridization buffer.

Probe name	Sequence
hTR Probe 1	GCATGTGTGAGCCGAGTCCTGGGTGCTTACACTCGGACCTCGTCG ACATGCATT
hTR Probe 2	CGCGCGGGGACTCGCTCCGTTCCTTACACTCGGACCTCGTCGACA TGCATT
hTR Probe 3	TTCCTGCGGCCTGAAAGGCCTGAACTTACACTCGGACCTCGTCGA CATGCATT
hTR Probe 4	GGGCCAGCAGCTGACATTTTTTGTTTGCTTTACACTCGGACCTCG TCGACATGCATT
hTR Probe 5	GGCTTTTCCGCCCGCTGAAAGTCAGCTTACACTCGGACCTCGTCG ACATGCATT
hTR Probe 6	GTCCCACAGCTCAGGGAATCGCGCTTACACTCGGACCTCGTCGAC ATGCATT
hTR Probe 7	GCCCAACTCTTCGCGGTGGCAGTGTTACACTCGGACCTCGTCGAC ATGCATT
hTR Probe 8	GCGGCCTCCAGGCGGGGTTCGGGTTACACTCGGACCTCGTCGAC ATGCATT
hTR Probe 9	CCGCAGGTCCCCGGGAGGGGCGATTACACTCGGACCTCGTCGAC ATGCATT
hTR Probe 10	AGAATGAACGGTGGAAGGCGGCAGGCCTTACACTCGGACCTCGT CGACATGCATT
hTR Probe 11	CGCCTACGCCCTTCTCAGTTAGGGTTTTACACTCGGACCTCGTCG ACATGCATT
hTR Probe 12	CCCCGAGAGACCCGCGGCTGACATTACACTCGGACCTCGTCGAC ATGCATT
hTR Probe 13	CCTCCGGAGAAGCCCCGGGCCGATTACACTCGGACCTCGTCGAC ATGCATT
hTR Probe 14	GAAAAACAGCGCGCGGGGAGCAAAAGCACTTACACTCGGACCTC GTCGACATGCATT
hTR Probe 15	ACAAAAAATGGCCACCACCCCTCCCTTACACTCGGACCTCGTCGA CATGCATT
TERRA probe	TAACCCTAACCCTAACCCTAACCCTAACCCTTACACTCGGACCTC GTCGACATGCATT
FLAP Y- AF647	/5AF647/AATGCATGTCGACGAGGTCCGAGTGTAA/3AF647Sp/
FLAP Y-AF555	/5AF555/AATGCATGTCGACGAGGTCCGAGTGTAA/3AF555Sp/

Table 2: List of primary and secondary "FLAP" probes used for smiFISH experiments. To detect TERRA 1 specific probe named "TERRA probe" was used, whereas for h*TR* detection a mix of 15 different specific probes (h*TR* probe 1-15) was used. TERRA probe was annealed with the secondary probe FLAP Y-AF647, the h*TR* pool of primary probes was annealed with the secondary probe FLAP Y-AF555.

Cells fixation and probe hybridization

The smiFISH protocol was adapted from Querido *et al.*[163] Cells were grown on 22x22 mm glass coverslips and fixed in 4% PFA (Electron Microscopy Science) for 20 minutes at room temperature. After washing two times with 1X PBS, cells were kept at +4°C for maximum 1 month or directly permeabilized in 0.5% Triton X-100 1X PBS for 5 minutes at room temperature. Control samples were treated with 300 U/mL RNase T1 (Macherey-Nagel) and 200 U/mL PureLink RNase A (Invitrogen) for at least 2 hours at 37°C. Once permeabilized, samples were incubated at room temperature with 1X SSC 15% Formamide for 40 minutes (at least 15 minutes of incubation are required) and placed cell-side down on a 50 μL drop of hybridization buffer (1X SSC, 15% Formamide, 4.5 mg/mL BSA, 10.6% Dextran Sulphate, 2 mM VRC, 0.4 mg/mL yeast tRNA, 1 μL annealed probeset) in an air-tight hybridization chamber protected from light overnight at 37°C. The following day, coverslips were placed cell-side up in a clean 6-well plate and washed twice with 1X SSC 15% formamide for 30 minutes at 37°C. After two rinses with 1X PBS, cells were stained for 8 minutes with 1 ng/μL DAPI in 1X PBS, washed again with 1X PBS and finally mounted with ProLong Diamond Antifade Mountant on precleaned glass slides.

smiFISH combined with Immunofluorescence microscopy

The combination of smiFISH and IF techniques imply to perform smiFISH (as described above) as first step. After washing twice in pre-warmed 1X SSC 15% formamide, cells were washed twice in 1X PBS before proceeding with the IF protocol, as described above.

smiFISH-IF image acquisition and quantification

All images were acquired as a 0.30 μm Z-stack using a confocal laser scanning Leica TCS SP8 inverted microscope (Leica Camera AG) with a plan apochromatic 63X/1.40 oil immersion objective and 2X zoom. Normal photomultipliers (PMTs) were used to detect telomeres and DAPI signals while a Hybrid Detector (HyD) was used to image both TERRA and h*TR*-derived smiFISH signals. Optimal acquisition parameters such as nm range of excitation, gain, offset and laser power were

optimized for the visualization of each fluorophore at the beginning of the acquisition and maintained throughout each experiment. Images were acquired with a 2048x2048 resolution using Leica Application Suite X (LAS X) imaging software. Post-processing of acquired images, including background subtraction and image editing, was performed by Fiji software (version 2.3.0/1.53o), a distribution of ImageJ software. For the quantification of h*TR* and TERRA single molecule signals, analysis of the image stacks in 3D was performed taking advantage of 3D ImageJ Suite plugin created by Thomas Boudier[182]. To quantify the colocalizations between two populations of signals an object-based method was used. As first, an initial segmentation of fluorescent signals is required to identify objects (TERRA, h*TR* and telomeric foci and clusters) and to subsequently proceed with the analyses of their spatial distribution through distance analysis algorithm by using DiAna plugin[183]. Briefly, after determining the optimized threshold and background subtraction for all the signals, DiAna segmented and labelled each object of two different images at a time and evaluated the overlaps between them. Threshold and size parameters used for the object segmentation were kept constant for all the images. Two objects (A and B) are considered overlapping by DiAna when at least 1 voxel of object A colocalizes with 1 voxel of object B. DiAna output reports not only the number of colocalization events but also their xyz position and signal-specific integrated density. A semi-automated pipeline was designed by Dr. Michela Roccuzzo (CIBIO imaging facility) and optimized by Irene Gialdini, a former lab member.

DNA-FISH combined with IF

DNA-FISH protocol was adapted from Rossiello, Fumagalli and d'Adda di Fagagna 2013[178]. Cells seeded on 22x22 mm glass coverslips, previously stripped with 1 M HCl and sterilized with 100% Ethanol, were fixed for 20 minutes at RT with 4% PFA in 1X PBS after reaching the required density and permeabilized with 0.2% Triton X-100 in 1X PBS for 10 minutes. Subsequently, cells were blocked with 1X PBG (0.2% Fish Gelatin, 0.5% BSA, 1X PBS) for 1-6 hours, incubated with a primary antibody against RAP1 diluted 1:500 in 1X PBG for 1 hour, washed 3 times with 1X PBG and incubated for 1 hour with the proper secondary antibody diluted 1:1500 in 1X PBG. After washing two times in 1X PBG and in 1X PBS, cells were post-fixed and simultaneously permeabilized in 4% PFA 0.1% Triton X-100 for 10 minutes. At this point, cells were incubated for 30 minutes at room temperature with glycine 10 mM

diluted in milliQ water and washed 3 times for 5 minutes with 1X PBS. Coverslips were then inverted cell-side down on a 40 μL drop of hybridization mixture (70% Formamide, 1X Blocking reagent Roche, 10 mM Tris-HCl pH 7.4, 0.5 μM Telomeric PNA FAM probe) spotted on a precleaned glass slide, placed on a heat-block for 5 minutes at 80°C and let hybridize in a humified chamber for 2 hours at room temperature protected from light. Following hybridization, coverslips were placed cell-side up on a clean 6-well plate and washed two times for 15 minutes with Wash Solution I (70% Formamide, 0.1% BSA, 10 mM Tris-HCl pH 7.4) and 3 times with Wash Solution II (100 mM Tris-HCl pH 7.4, 150 mM NaCl, 0.07% Tween 20). After a quick rinse with 1X PBS, cells were stained for 8 minutes with 1 ng/μL DAPI in 1X PBS, washed again with 1X PBS and finally mounted with ProLong Diamond Antifade Mountant on precleaned glass slides. All images were acquired as a Z-stack on a spinning disk Eclipse Ti2 inverted microscope (Nikon Instruments Inc), equipped with Lumencor Spectra X Illuminator as LED light source, an X-Light V2 Confocal Imager and an Andor Zyla 4.2 PLUS sCMOS monochromatic camera using a plan apochromatic 100x/1.45 oil immersion objective. Images were analyzed and assembled with Fiji, an ImageJ software.

Cell lysis and immunoblotting

Cells were harvested by scraping in 1X ice-cold PBS and lysed for 20 minutes on ice in 150 mM NaCl, 1% IGEPAL, 0.5% Sodium deoxycholate, 0.1% SDS, 25 mM Tris pH 7.4, 1 mM PMSF, one tablet/10 mL Pierce Protease Inhibitors Mini Tablets, 1 mM EDTA (RIPA buffer). Protein concentration was determined by Bradford (Invitrogen) assay using a spectrophotometer. For immunoblotting analysis, equal amounts of proteins were resolved on 8-10% polyacrylamide self-made gels and electroblotted on Polyvinylidene Difluoride (PVDF) membranes (Bio-Rad) using a wet transfer. 5% non-fat skim milk (Sigma) in TBS-Tween 0.1% was used as blocking solution. Membranes were incubated overnight at 4°C with primary antibodies diluted in TBS-Tween (20 mM Tris base pH 7.4, 150 mM NaCl, 1% Tween 20) and then incubated with Horseradish peroxidase (HRP)-conjugated secondary antibody (Abcam) for 1 hour at room temperature. Immunoreactive bands were detected by SuperSignal West Pico PLUS Chemiluminescent substrate ECL (Invitrogen) using a Chemidoc XRS$^+$ Biorad.

RNA isolation

Total RNA was isolated from cells using TRIzol reagent (Thermo Scientific) according to manufacture instructions. Briefly, cells cultivated on 10 cm Petri dishes were lysed with 1 mL of TRIzol Reagent, scraped and collected in sterile tubes. After 10 minutes incubation at room temperature, 200 μL of Chloroform were added to the lysates, the samples were mixed by vortexing and incubated for 15 minutes at room temperature. After centrifuged at 4°C, the upper aqueous phase was collected, 500 μL of Isopropanol were added to the tubes and mixed by inversion. After a 10 minutes incubation, samples were centrifuged at 4°C. The pellet was washed 2 times with 70% EtOH and finally resuspended in the appropriate volume of nuclease and RNAse-free water. If needed, RNA samples were precipitated adding 1/10 of total volume of 3 M NaAc pH 5.2 and 2 volumes of 100% EtOH. RNA concentration and purity were assessed using Nanodrop 1000 Spectrophotometer and integrity checked on a 1% Agarose 1X MOPS pH 7 (20 mM MOPS, 2 mM Sodium Acetate, 1 mM EDTA) gel.

RT-qPCR

Total RNA was treated with DNase I (Thermo Scientific) for 1 hour at 37°C. The integrity of DNase I treated RNAs was confirmed by loading them on a 1% Agarose 1X MOPS gel. Afterwards, RNAs were reverse transcribed with either TERRA RT, h*TR* RT or random hexamers primers using the Superscript III RT enzyme (Thermo Scientific), following manufacturer's protocol. TERRA and hTR expression levels at different human subtelomeres were monitored via quantitative PCR using KAPA SYBR FAST qPCR Mastermix (KAPA Biosystems) by running 50 ng of RT reaction in triplicates in a CFX Touch Real-Time PCR Detection System (Bio-Rad) or a QuantStudio5 PCR machine (ThermoFisher). Ct values were extracted using a Bio-Rad CFX Manager Software or QuantStudio Design and Analysis (ThermoFisher), expression values were normalized to the geometric mean of U6 or GAPDH housekeeping genes and the relative quantification presented as linearized Ct values ($2^{-\Delta\Delta Ct}$), normalized to the wild-type untreated reference values. All primers used in this thesis were purchased from Metabion and Eurofins Genomics and are listed in Table 3.

Name	Sequence 5'-3'	Reference
TERRA 2q FOR	GCCTTGCCTTGGGAGAATCT	Deng et al., 2012
TERRA 2q REV	AAAGCGGGAAACGAAAAGC	Deng et al., 2012
TERRA 9p FOR	GAGATTCTCCCAAGGCAAGG	Feretzaki and Ligner, 2017
TERRA 9p REV	ACATGAGGAATGTGGGTGTTAT	Feretzaki and Ligner, 2017
TERRA 15q FOR	CAGCGAGATTCTCCCAAGCTAAG	Porro et al., 2010
TERRA 15q REV	AACCCTAACCACATGAGCAACG	Porro et al., 2010
TERRA 17p FOR	CTTATCCACTTCTGTCCCAAGG	Feretzaki and Ligner, 2017
TERRA 17p REV	CCCAAAGTACACAAAGCAATCC	Feretzaki and Ligner, 2017
TERRA 17q FOR	GTCCATGCATTCTCCATTGATAAG	Deng et al., 2012
TERRA 17q REV	AGCTACCTCTCTCAACACCAAGAAG	Deng et al., 2012
TERRA XpYp FOR	AAGAACGAAGCTTCCACAGTAT	Porro et al., 2010
TERRA XpYp REV	GGTGGGAGCAGATTAGAGAATAAA	Porro et al., 2010
TERRA XqYq FOR	GAAAGCAAAAGCCCCTCTGA	Deng et al., 2012
TERRA XqYq REV	CCCCTTGCCTTGGGAGAA	Deng et al., 2012
GAPDH FOR	ACATCGCTCAGACACCAT	Costello et al., 2017
GAPDH REV	TGTAGTTGAGGTCAATGAAGG	Kaneko et al., 2013
U6 FOR	GTGCTCGCTTCGGCAGCACA	Zhang et al., 2014
U6 REV	GGAACGCTTCACGAATTTGCGTGTCAT	Zhang et al., 2014
TERRA RT	CCCTAACCCTAACCCTAACCCTAACC CTAA	Avogaro et al., 2018
Random Hexamers	-	Metabion
hTR RT	CATGTGTGAGCCGAGTCCTG	This study
hTR Mature FOR	GCGAAGAGTTGGGCTCTGTCA	Tseng et al., 2015
hTR Mature REV	TTCCTCTTCCTGCGGCCTGAAA	Tseng et al., 2015
hTR Precursor FOR	GGGTGTGGGAGAACAGTCAT	Chen et al., 2020
hTR Precursor REV	ACCTCTGGCATAAACCGATG	Chen et al. 2020

Table 3: List of primers for RT-qPCR used for TERRA and h*TR* expression levels analysis.

Northern Blotting and probe preparation

Total RNA was extracted from cells using TRIzol reagent as previously reported. 20 μg of total RNA were treated with 2.5 μL of DNase I enzyme for 1 hour at 37°C. 0.5 μL of RiboLock RNase inhibitor (Thermo Scientific) were added to the mix together with DNase I enzyme. As a negative control, 20 μg of the same RNA were incubated with 2 mg/mL PureLink RNase A (Invitrogen) for 1 hour at 37°C and subsequently treated with 2.5 μL of DNase I enzyme as above. DNase I treated RNAs integrity was checked on a 1% Agarose 1X MOPS gel. All RNAs were denatured for 5 minutes at 65°C after adding to them 2X RNA Loading Dye and subsequently loaded on a 1.2% Agarose 1X MOPS 2% Formaldehyde gel with 1:20000 Atlas ClearSight (Bioatlas) intercalating dye. The gel run for 2 hours at 125V and the RNA was blotted on an Amersham Hybond H+ membrane (GE Healthcare) by capillarity. The gel was washed three times for 10 minutes in water and two times in 10X SSC for at least 15 minutes on a rocking platform. RNA samples were transferred overnight at room temperature through capillarity on a membrane activated in 10X SSC (3 M NaCl, 0.3 M Sodium Citrate). Then, RNAs were crosslinked to the membrane with UV light (365 nm) for 1 minute at 120mJ/cm^2 on the UVP CL-1000L Longwave (Fisher Scientific), pre-hybridized for at least 1 hour at 42°C with pre-heated CHURCH hybridization buffer (1% BSA, 1 mM EDTA, 0.5 M phosphate buffer, 7% SDS) and hybridized overnight at 45°C with a TERRA-γ^{32}P labeled probe previously denatured at 95°C for 5 minutes and then diluted in CHURCH hybridization buffer. The following day, the membrane was washed with 2X SSC 0.1% SDS for 5 and 15 minutes at room temperature. Then, two washes with 0.5X SSC 0.1% SDS for 5 minutes were performed and the membrane was subsequently washed twice for 15 minutes at 42°C with pre-heated 0.5X SSC 0.1% SDS. After rinsing it quickly in 2X SSC, the membrane was wrapped in saran wrap and maintained in an exposure cassette for up to 4 days. Detection of the radioactive signal was performed using a Typhoon. TERRA-γ^{32}P probe was generated using T4 Polynucleotide Kinase (PNK) to label TERRA RT primer with 50 μCi of γ^{32}P-ATP. The labeled probe was subsequently purified on G-50 column (GE Healthcare) and diluted in CHURCH hybridization buffer.

Genomic DNA extraction

Genomic DNA was isolated from cells using Phenol/Chloroform/Isoamyl alcohol (25:24:1, Fisher Scientific) according to manufacturer's instructions. Briefly, cells were collected by scraping in ice-cold 1X PBS and the pellet resulting after centrifugation was resuspended in Lysis Buffer (10 mM Tris-HCl pH 7.4, 10 mM EDTA, 0.5% SDS, 10 mM NaCl, 1:750 RNase A 20mg/mL) and incubated at 37°C. After 1 hour, 0.2% Proteinase K (Invitrogen) was added to lysates, mixed by inversion, placed at 50°C for 3 hours and incubated overnight at 37°C. The following day, the samples were heated at 50°C again for 3 hours. At this point, Phenol/Chloroform/Isoamyl alcohol (Fisher Scientific) was added in a ratio 1:1 to the samples. The tubes were shaken vigorously to obtain a milky emulsion and centrifuged at 15000 xg for 15 minutes at room temperature. The upper aqueous phase was collected in a new tube and as before Phenol/Chloroform/Isoamyl alcohol was added, samples shaken and centrifuged. After collecting the aqueous upper phase into a new tube, Chloroform in a ratio 1:1 was added. Samples were shaken, centrifuged and the resulting upper phase was harvested and precipitated using 1/10 of total volume of NaAc 3 M pH 5.2 and 2 volumes of 100% EtOH. DNAs were placed at -20°C overnight and after one wash with 70% EtOH, pellets were resuspended in an appropriate volume with nuclease free water. Concentration and purity were assessed using Nanodrop 1000 Spectrophotometer and DNA integrity checked on a 1% Agarose 0.5X TBE gel.

Telomere Restriction Fragment (TRF) Southern blotting

10 μg of genomic DNA were mixed in an 80 μL reaction with 1 μL of *RsaI* enzyme (Thermo Scientific) and 1 μL of *HinfI* enzyme (NEB) and incubated at 37°C. After at least two hours, 1.5 μL of both *RsaI* and *HinfI* enzymes were added and the digestion reactions left at 37°C overnight. The following day, 500 ng of digested samples were checked on a 1% agarose 0.5X TBE gel run at 100 V for 1 hour. At this point, samples were precipitated with 1/10 of total volume of NaAc 3 M pH 5.2 plus 2 volumes of 100% EtOH for at least 2 hours at -20°C. After a wash with 70% EtOH, pellets were resuspended in the appropriate volume of nuclease-free water. After adding 6X DNA Loading dye (Thermo Scientific), samples were loaded on a 0.8% Agarose in 0.5X TBE gel (no intercalating dye in the gel) and run at 25 V for 18 hours. The day after, the gel was stained in Atlas ClearSight dye (25 μL/100 mL) in 0.5X TBE for at least

30 minutes by gently agitation, quickly rinsed with 0.5X TBE and deionized water, and subsequently denatured for 1h at room temperature in Denaturing Solution (0.5 M NaOH,1.5 M NaCl) by gently rocking on a platform. After a wash with deionized water, the gel was socked two times for 30 minutes in Neutralizing Solution (0.5 M Tris-HCl pH 7.5, 1.5 M NaCl) on a rocking platform and equilibrated for 10 minutes in 10X SSC. The DNA was blotted on an Amersham Hybond H+ membrane (GE Healthcare) overnight at room temperature through capillarity on a membrane activated in 10X SSC. The following day, DNAs were crosslinked to the membrane with UV light (365 nm) for 1 min at 120 mJ/cm^2 on the UVP CL-1000L Longwave (Fisher Scientific), pre-hybridized for at least 1 hour at 50°C with pre-heated hybridization buffer (5X SSC, 0.1% Sarcosyl, 0.04% SDS) and hybridized overnight at 50°C with 40 ng/mL Telo DIG-NICK probe previously denatured at 95°C for 5 minutes and then diluted in hybridization buffer. The next day, the membrane was washed with 2X SSC 0.1% SDS for 5 and 15 minutes at room temperature, twice with 0.5X SSC 0.1% SDS for 5 minutes. Subsequently, two washes of 15 minutes at 42°C with pre-heated 0.5X SSC 0.1% SDS were performed. After rinsing it quickly in 2X SSC, the membrane was blocked for 1 hour in blocking solution (1% Blocking reagent Roche, 1X MAB) and incubated with anti-DIG-AP antibody (1:10000) diluted in blocking solution for at least 2 hours. Before detecting the chemiluminescent signal, the membrane was washed two times with WASH BUFFER 2 (15 minutes each), equilibrated for 2 minutes in AP buffer and incubated with CDP-Star Chemiluminescence Substrate (Roche) for 5 minutes. The membrane was exposed to UV light for 2 hours using a ChemiDoc XRS$^+$ (Biorad).

TRF probe preparation

Telo DIG-NICK probe was generated starting from the psXNeo-1.6-T2AG3 plasmid and labelled through DIG-Nick Translation Mix for in situ probes (Roche) according to the manufacturer's instructions. Briefly, psXNeo-1.6-T2AG3 plasmid was amplified in bacteria at 30°C, purified using MINI PREPs kit (Machelerey Nagel) and digested with *BglI* and *SmaI* restriction enzymes. The band corresponding to the 1.6 kb T2AG3 insert was extracted from the gel using Wizard SV Gel and PCR Clean-Up System (Promega) and precipitated in 1/10 of total volume of NaAc 3 M pH 5.2 and 2 volumes of 100% EtOH for at least 2 hours at -20°C. After one wash with 70% EtOH, the pellet

was resuspended in 10-15μL of nuclease-free water. 1 μg of extracted DNA was then diluted to 500 ng/μL, mixed with 4 μL of DIG-Nick Translation Mix (Roche) and incubated at 15°C for 2 hours and 10 minutes. Afterwards, the reaction was chilled on ice and stopped by boiling it at 65°C for 10 minutes after the addition of 1 μL of 0.5 M EDTA pH 8.

TRF signal quantification

The average length of telomeres was assessed by using Image Lab 6.1 software (BioRad). The image was divided into lanes (one for each sample) using the “Lanes and bands” tool. Subsequently, for each sample both the start and the end of the corresponding telomeric smear was defined using the “Lanes and bands” command which resulted in a table reporting the values of relative front detected for each smear. The relative front parameter indicates the relative movement of the analyzed band from the top to the bottom. The correlation between relative front value and kilobase (kb) was calculated by assessing the relative front of the molecular weight marker.

DNA content analysis by flow cytometry

Cells were harvested by trypsinization, washed with 1X PBS and fixed with ice-cold 70% EtOH in 1X PBS for at least 20 minutes at -20°C. Fixed cells were centrifuged for 3 min at 1000g, washed two times with 1X PBS and stained with 10 μg/mL propidium iodide (Invitrogen) for 30 minutes at 37°C in the presence of 100 μg/mL PureLink RNase A (Invitrogen). Cells were analyzed in a flow cytometer (FACSCanto, BD Bioscience). Data analysis and figure preparation were performed using FlowJow software (FlowJo, LLC).

Statistical analysis

Statistical significance of colocalization events is given by DiAna plugin through its shuffle function which results in a cumulative distribution graph of counted objects from two images. GraphPad Prism 9 (license: GPS-1810727-TFRO-F3E3C) was used to produce graphs and statistical analyses. Data are represented either as bar chart or dot blot (mean +/- SD), unless differently specified in the corresponding figure legend. Normality of datasets was determined by Shapiro-Wilk test. Details about the

statistical test performed for each experiment are provided in the figure legends. P-values are indicated as follows: *: $p < 0.05$, **: $p<0.01$, ***: $p<0.001$, ****: $p<0.0001$, ns: not significant

RESULTS

TERRA and telomerase colocalize at telomeres

Analysis of TERRA localization at telomeres

We previously used a live cell imaging approach based on the MS2-GFP system to study the spatiotemporal dynamics of TERRA transcripts in a human cancer cell line engineered to express MS2-tagged TERRA molecules from a single telomere (telomere 15q)[164,179]. These analyses revealed that telomere 15q-derived MS2-TERRA transcripts only transiently localize at telomeres, with MS2-TERRA-telomeres colocalizations detected in 44% of the cells. These findings indicated that TERRA transcripts are not stable constituents of telomeres[164]. To gain further insights into this matter and broaden our analyses to TERRA transcripts expressed from multiple telomeres, we employed a version of single molecule FISH, called single molecule inexpensive FISH (smiFISH), adapted from Querido *et al.*[163], to visualize TERRA transcripts in fixed HeLa cells. This approach relies on the use of a primary probe designed to target the UUAGGG telomeric sequence which is shared by TERRA transcripts expressed from all telomeres. This probe contains a tail sequence at its 3' end (FLAP sequence) that does not base pair with TERRA transcripts. The use of a fluorescent secondary probe targeting the FLAP sequence enables the detection of TERRA molecules (Figure 13).

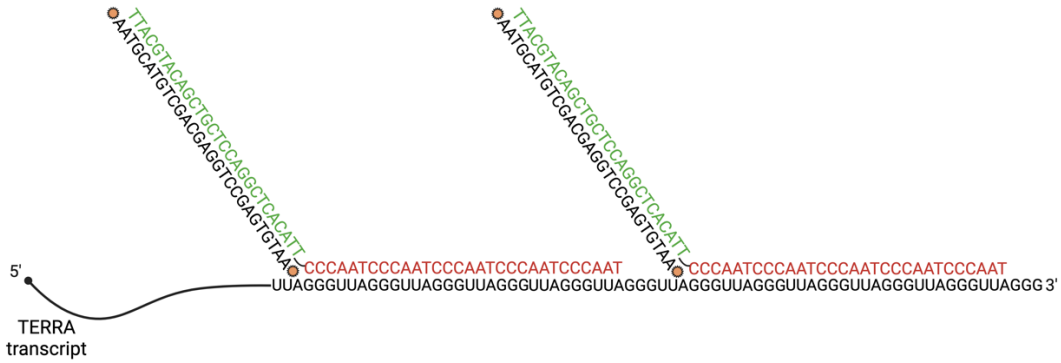

Figure 13: Schematic of smiFISH TERRA-specific probe binding to a TERRA transcript. Each primary probe comprises a gene-specific region (in red) and a FLAP sequence at its 3' end (in green). Each secondary probe consists in a FLAP-specific sequence (in black) labeled at both 5' and 3' ends with an AF647-fluorophore (orange dots). Primary and secondary probes are pre-hybridized *in vitro* resulting in the smiFISH TERRA-specific probes that carry two fluorophores and recognize several

times the 3' end sequence of TERRA RNA. The *in vivo* hybridization of several specific probes to the repetitive telomeric sequence of TERRA allows the signal amplification leading to a better visualization of individual molecules. Based on Tsanov *et al.*, 2016[181]. Created with Biorender.com

We used this approach for the visualization of TERRA transcripts in HeLa cells. Using confocal microscopy, we observed the formation of discrete TERRA foci predominantly localizing within the nucleus (Figure 14A). TERRA signal was sensitive to RNase treatment confirming the specificity of the signal (Figure 14A). Quantification analyses confirmed the detection of 13 TERRA foci on average per cell (Figure 14B), consistent with previous findings[175].

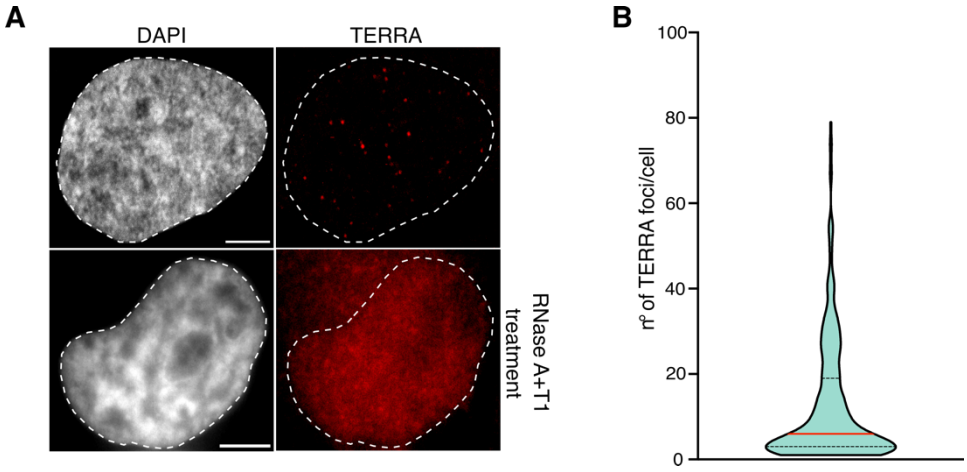

Figure 14: Visualization of TERRA transcripts by smiFISH in HeLa cells. A) Detection of TERRA in fixed HeLa cells by smiFISH. Control experiment after treatment with RNase A and RNase T1 was performed showing no TERRA-specific signal. DAPI is used to stain nuclei. Scale bar: 5 μm. Images were obtained by using a confocal laser scanning Leica TCS SP8 inverted microscope (Leica Camera AG) with a plan apochromatic 63X/1.40 oil immersion objective and 2X zoom. B) Quantification of TERRA foci number detected per nucleus in HeLa cells. Median ± SD is shown. N= 400 cells, n= 5 biological replicates.

To investigate TERRA localization at telomeres, we combined TERRA smiFISH with immunofluorescence (IF) for RAP1, a protein of the shelterin complex, which is frequently used for the visualization of telomeres[164] and will be used throughout this thesis to mark telomeres in fixed cells. As expected, RAP1 IF enabled the detection of discrete nuclear foci (Figure 15A). Quantification analyses confirmed the presence of about 62 RAP1 foci per cell (Figure 15B).

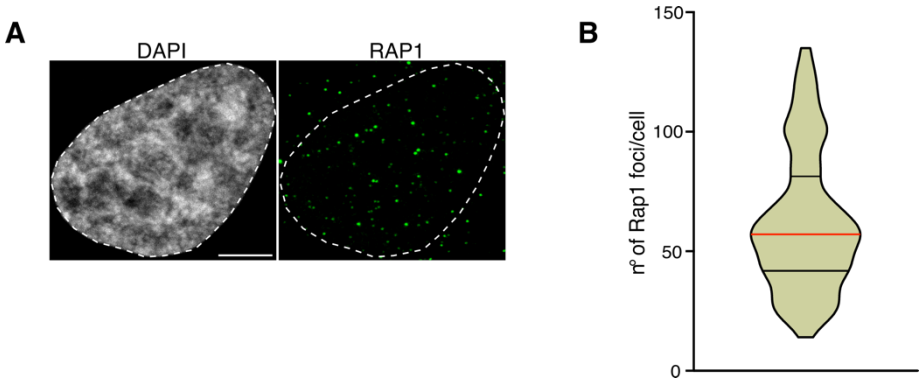

Figure 15: Telomere visualization by RAP1 IF in HeLa cells. A) Detection of telomeric signal by using RAP1-specific antibody in immunofluorescence (IF) experiments performed in HeLa cells. DAPI is used to stain nuclei. Scale bar: 5 μm. Images were obtained by using a confocal laser scanning Leica TCS SP8 inverted microscope (Leica Camera AG) with a plan apochromatic 63X/1.40 oil immersion objective and 2X zoom. B) Quantification of the number of RAP1 foci per nucleus in HeLa cells. Median ± SD is shown. N= 150 cells, n= 3 biological replicates

By analyzing the presence of colocalization events between TERRA and RAP1 foci in smiFISH/IF experiments, we observed that on average 77% of cells present TERRA-RAP1 colocalizing foci (Figure 16A). As it can be observed in panel B of Figure 16, analysis of the distribution of TERRA-RAP1 colocalizations revealed that about half (58%) of the HeLa cells displaying TERRA-RAP1 colocalizations presents maximum 4 telomeres colocalizing with TERRA; the other half of the analyzed cells can be divided into two groups: 19% displaying from 5 to 10 telomeres colocalizing with TERRA and 23% showing more than 10 TERRA-RAP1 colocalization events. Thus, only a subset of telomeres colocalize with TERRA molecules at any given time in HeLa cells. These results are in agreement with previous results indicating that TERRA molecules are not stable components of the telomeric architecture. Furthermore, these results indicate that the smiFISH technique can be used for TERRA detection and analyses of TERRA localization at telomeres in fixed cells, in combination with RAP1 IF.

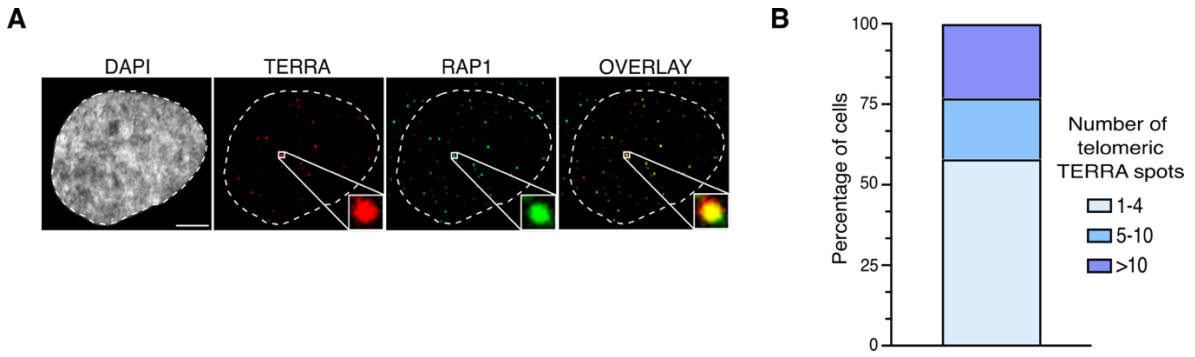

Figure 16: Quantification of the number of TERRA foci at telomeres by smiFISH/IF. A) Detection of TERRA and telomeres in fixed HeLa cells by smiFISH coupled with RAP1 IF. An example of a colocalization between TERRA and RAP1 is highlighted in the enlargement. DAPI is used to stain nuclei. Scale bar: 5 μm. B) Quantification of telomeric TERRA foci per nucleus: colocalization events have been divided into three groups and are represented as percentage of cells displaying 1-4, 5-10 or >10 telomeres colocalizing with TERRA. N= 110 cells, n= 3 biological replicates.

Analysis of TERRA and hTR interaction

The role of TERRA as telomerase regulator in human cells is still debated in the field. It has been previously shown *in vitro* that TERRA interacts with telomerase through base-pairing with the template region of h*TR*, inhibiting telomerase activity[109]. However, as discussed in the introduction section, increased TERRA levels do not necessarily correlate with inhibition of telomerase. Convinced that a direct visualization of TERRA and h*TR* at single-cell resolution may provide key understanding of their functional interplay *in vivo*, we set out to detect both TERRA and h*TR* by smiFISH, an approach recently used for h*TR* detection by the Chartrand lab[163]. To this aim, we used primary probes base pairing with either TERRA or h*TR* transcripts and fluorescent secondary probes enabling the simultaneous detection of both RNAs (TERRA-recognizing secondary probes would emit at 647 nm, while fluorescence of h*TR* secondary probes is emitted at a wavelength of 555 nm). Using this approach, TERRA and h*TR* were observed as discrete nuclear foci (Figure 17C). RNase treatment of the samples before probes hybridization confirmed the specificity of the signal (data not shown). Quantification analyses revealed the detection of approximately 94 h*TR* foci per nucleus (Figure 17A), which is in line with previous findings[82]. The number of TERRA foci per cell detected was also in line with the results obtained in TERRA smiFISH experiments, confirming that the combination of h*TR* and TERRA probes did not influence the detection of TERRA. Interestingly, TERRA-h*TR* colocalization events were detected in 43% of cells (Figure 17C).

Analyses of the distribution of the number of TERRA-h*TR* colocalizations per cell showed that 82% of cells displays 1 – 4 TERRA-h*TR* colocalizing foci, hereafter TERRA-h*TR* particles, while a small fraction of HeLa cells presents more than 5 TERRA foci colocalizing with h*TR* (Figure 17B). These findings suggest that while TERRA can base pair with h*TR in vitro*, TERRA-h*TR* interaction is tightly regulated *in vivo*. We reasoned that providing further information into the nuclear localization of the TERRA-h*TR* particles may provide key clues on the impact of these colocalizing events in telomerase activity.

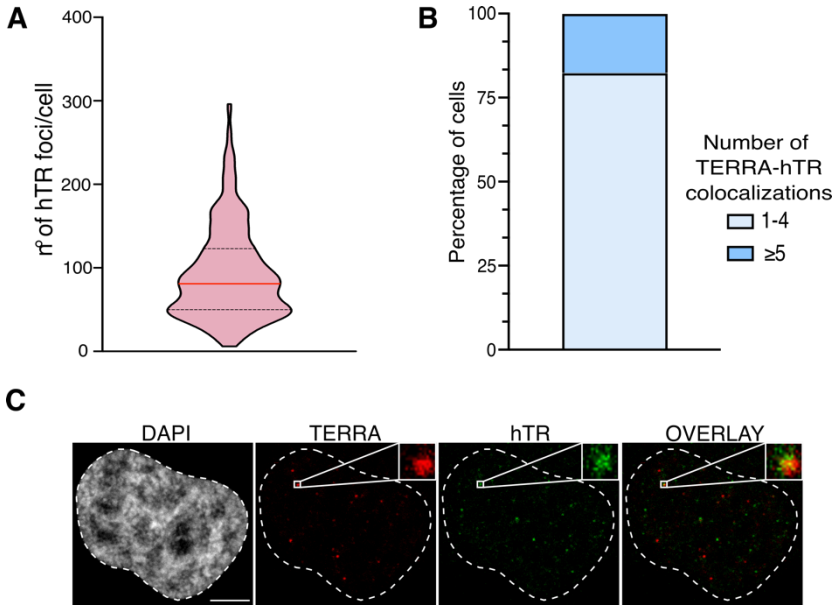

Figure 17: A fraction of TERRA and h*TR* foci colocalize in the nucleus. A) Quantification of h*TR* foci detected per nucleus by confocal microscopy in HeLa cells. Median ± SD is shown. B) Quantification of the number of TERRA and h*TR* colocalizing foci (TERRA-h*TR* particles) per nucleus: colocalization events have been divided in two groups and are represented as percentage of cells presenting 1-4 or ≥ 5 TERRA foci colocalizing with h*TR*. C) Detection of TERRA and h*TR* by smiFISH in fixed HeLa cells. An example of a colocalization event between TERRA and h*TR* is highlighted in the magnification. DAPI is used to stain nuclei. Scale bar: 5 μm. N= 244 cells, n= 3 biological replicates.

Investigating TERRA-hTR particles localization at telomeres

We asked whether TERRA-h*TR* colocalizations occur at telomeres. To address this question, we coupled smiFISH for TERRA and h*TR* with immunofluorescence against RAP1 (smiFISH/IF) (Figure 18A). This analysis revealed that approximately 41,5% of cells display TERRA-h*TR*-RAP1 colocalizations, suggesting that TERRA-h*TR* particles localize only transiently at telomeres. Moreover, by analyzing the distribution of TERRA-h*TR* colocalizing foci, we observed that the majority of analyzed cells

(70%) show maximum 2 TERRA-h*TR* particles localized to telomeres (Figure 18B), supporting a view of their transient telomeric localization. Shed light on the mechanisms that promote TERRA-h*TR* particles localization to telomeres may be critical to understand TERRA function in the regulation of telomerase.

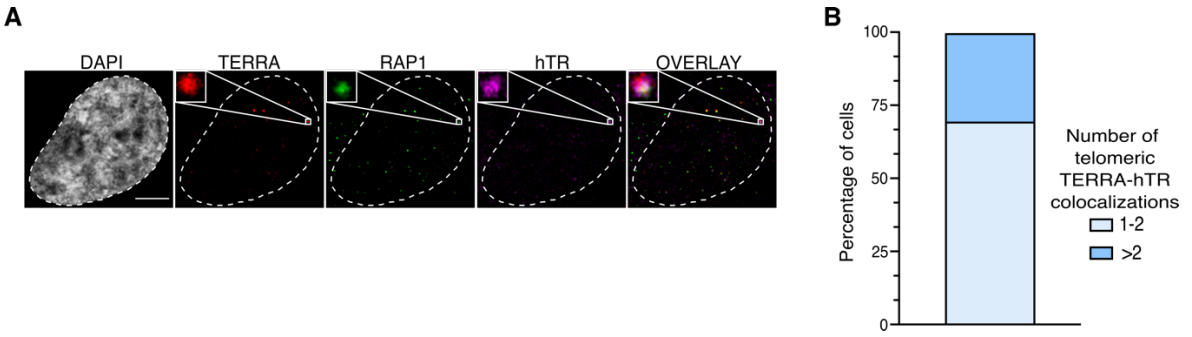

Figure 18: A fraction of TERRA-h*TR* particles localize to telomeres. A) Detection of TERRA, h*TR* and telomeres by smiFISH coupled with RAP1 IF in fixed HeLa cells. An example of triple colocalization between TERRA, h*TR* and RAP1 is shown in the image insets. DAPI is used to stain nuclei. Scale bar: 5 μm. B) Quantification of TERRA-hTR-RAP1 colocalizing events represented as percentage of cells showing from 1 to 2 (mean 69.55% and SD ± 7.4%) or more than 2 TERRA-h*TR* particles (mean 30.45% and SD ± 7.4%) localizing at telomeres. N= 102 cells, n= 2 biological replicates.

Depletion of TCAB1 does not impair telomeric TERRA localization

Telomerase is known to be subjected to a complex trafficking which leads to the formation of the mature form of the holoenzyme[38]. The telomerase accessory protein TCAB1 is essential for the regulation of telomerase nuclear trafficking. Depletion or knockout of TCAB1 impairs telomerase recruitment to telomeres[184,185]. Since a fraction of telomeric TERRA foci colocalize with h*TR*, we decided to investigate whether telomeric localization of TERRA may be promoted by the mechanisms involved in telomerase recruitment to chromosome ends. To address this question, we depleted TCAB1 by siRNAs in HeLa cells (Figure 19A) and analyzed TERRA localization at telomeres by smiFISH/IF (Figure 19B). At these analyses, we observed no changes in the number of telomeric TERRA foci in TCAB1 depleted cells, as compared to control cells (Figure 19C). As it can be observed in panel D of Figure 19, this result is further confirmed when we analyze the distribution of the telomeric TERRA foci. Thus, TERRA localization at telomeres is not influenced by TCAB1 depletion. While a fraction of TERRA and h*TR* colocalize at telomeres, the mechanisms that promote telomerase recruitment and activity at chromosome ends are not involved in the telomeric localization of TERRA. These findings suggest that TERRA and TERRA-h*TR* particles localization at telomeres does not correlate with telomerase activity at these chromosome ends. We next attempted to gain insights on this matter.

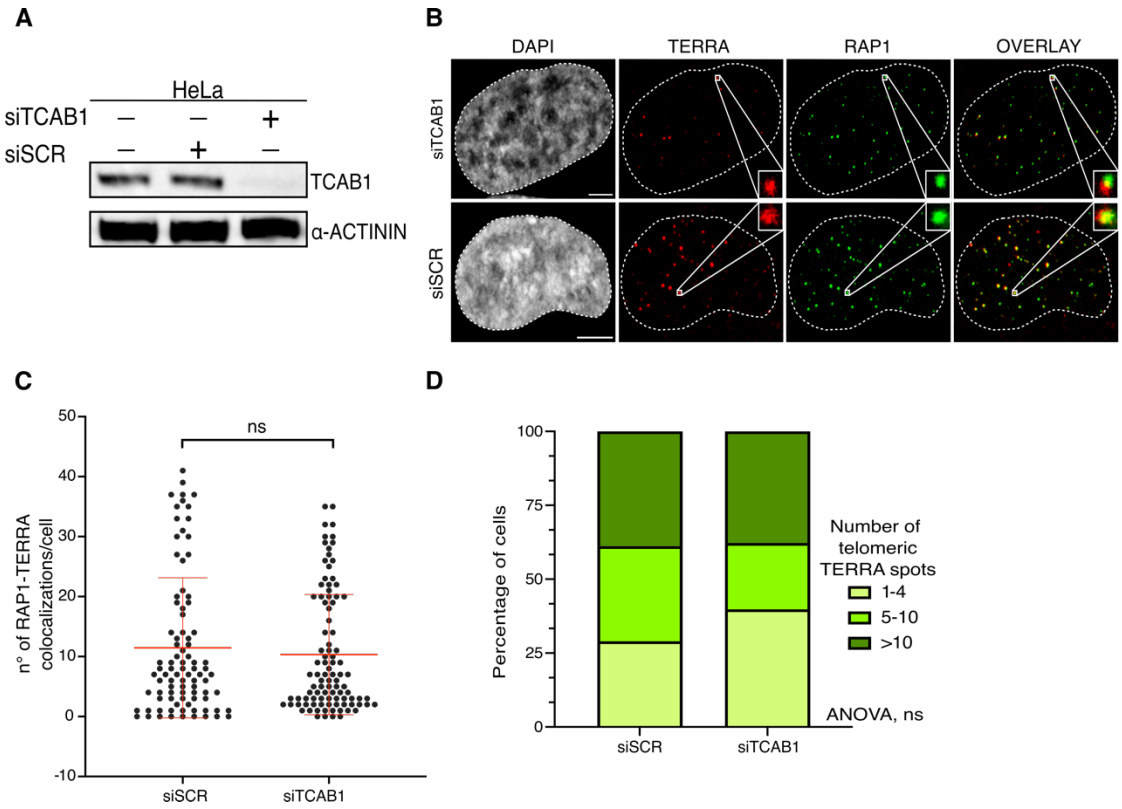

Figure 19: TERRA localization at telomeres is not impaired upon TCAB1 knockdown. A) Western blot analysis of TCAB1 from total protein lysates of HeLa cells untransfected, transfected with control scrambled siRNA (siSCR) or transfected with TCAB1-targeting siRNAs (siTCAB1). TCAB1 is detected as a 65 kDa protein, while the housekeeping protein α-ACTININ is detected at around the 100 kDa. B) Detection of TERRA and telomeres by smiFISH coupled with RAP1 IF in fixed HeLa cells transfected with siSCR or siTCAB1. An example of a telomeric TERRA focus is shown in the enlargement. DAPI is used to stain nuclei. Scale bar: 5 μm. C-D) Quantification of telomeric TERRA foci detected per nucleus in siSCR and siTCAB1 transfected cells: in C colocalizing events are represented as n° of RAP1/TERRA colocalizations per cell (each dot represents a nucleus), in D the percentage of cells presenting 1-4, 5-10 or >10 TERRA foci at telomeres is reported. In C, mean ± SD is shown and unpaired non-parametric Mann-Whitney test was used for statistical analysis. In D, TWO-WAY ANOVA test coupled with a post hoc Sidak's multiple comparison test was used for statistical analysis. p-value: ns: non-significative. N= 97 cells for siTCAB1, 89 cells for siSCR. n= 2 biological replicates.

TERRA-h*TR* particles localization at telomeres is impaired during telomerase-dependent telomeres elongation

A setting to study TERRA localization during telomere elongation

Since a fraction of TERRA-h*TR* particles resides at telomeres, we hypothesized that the telomeric localization of TERRA may impact telomerase activity. To study this hypothesis and provide information into the role of TERRA in telomerase regulation, we decided to attempt investigations of TERRA transcripts localization during telomere elongation. The reasoning was the following: if TERRA acts as positive regulator of telomerase, its localization to telomeres would positively correlate with telomerase activity at chromosome ends. This scenario has been observed in budding yeast, where TERRA molecules localize at short telomeres during telomere elongation[161]. Yet, the fact that TCAB1 depletion does not influence TERRA localization at telomeres would argue against this hypothesis. Conversely, if telomeric TERRA transcripts impair telomere elongation, the telomeric localization of TERRA would inversely correlate with telomerase activity at chromosome ends. If the telomeric localization of TERRA is not influenced by telomere elongation, TERRA function in the regulation of telomerase may not be exerted at telomeres, allowing us to reject our hypotheses. Indeed, in principle, TERRA may also influence h*TR* maturation in Cajal bodies, or its trafficking in the nucleoplasm.

To study the telomeric localization of TERRA we needed to confront with two main challenges: first, it is not possible to visualize a telomere that is actively elongated by telomerase in fixed cells; second, as mentioned in the introduction section, live imaging analyses indicate that only few telomeres display stable localization of TERT or h*TR* particles at any given time, suggesting that only a subset of telomeres are elongated by telomerase during the time of the experiments (seconds or minutes)[82,96]. Forcing telomerase activity at chromosome ends by exogenous expression of TERT would be one possible approach to face these issues[82]. However, this condition may influence the localization of TERRA which interacts with both TERT and h*TR*[156]. Thus, in order to promote telomerase activity at telomeres without altering the levels of the endogenous enzyme, we decided to induce telomere shortening in cells, and then allow telomere re-lengthening by the endogenous telomerase. We reasoned that the

presence of short telomeres could attract telomerase for telomere elongation. To this aim, I cultivated HeLa cells in the presence of BIBR1532, a well-known inhibitor of telomerase, to promote telomere shortening. BIBR1532 is a non-nucleosidic small molecule which acts as a competitive inhibitor for the binding of dNTPs in the catalytic active site of telomerase. Thus, BIBR1532 treatment inhibits telomerase by interfering with the processivity of the holoenzyme[166,167]. Telomere restriction fragment analyses (TRF) confirmed a progressive decrease in telomere length during the treatment for up to 123 population doublings (PDs) (Figure 20A). At this time point, the cells showed an average telomere length of 2 kb, which is much shorter than the telomere length observed in control cells (averaging 4 kb in length) (Figure 20B). Removal of BIBR1532 after 123 PDs of treatment enabled telomere re-elongation by the endogenous telomerase (rescue time points) (Figure 20A). Notably, as shown in Figure 20A and Figure 20B, cells cultured for 7 PDs after BIBR1532 removal (7 PDs rescue time point) displayed a marked increase in telomere length as compared to BIBR1532 123 PDs, with an average telomere length of 2.75 kb, from the 2kb average telomere length of the 123 PDs BIBR1532 cells, suggesting an elongation rate of 100 bp per PD. In addition, inspection of the telomeric signal on the TRF membrane showed an increase in size of both the shortest and the longest telomeres detected, corresponding to the lower and upper signal of the telomeric smear (Figure 20A). Quantification of the telomeric signal from each sample compared to the molecular weight marker confirmed that telomere length ranged from 2 to 4 kb in 7 PDs rescue cells, as compared to 1 to 3.5 kb detected in the BIBR1532 123 PDs sample (Figure 20B). Notably, the average telomere length increased much more subtly from rescue 7 PDs to rescue 24 PDs time points, moving from 2.75 kb to about 3 kb in length on average, respectively, suggesting an elongation rate of 14 bp per PD. Furthermore, inspection of the TRF membrane and the telomeric signal quantification indicated that mainly the shortest telomeres became elongated from 7 PDs to 24 PDs rescue time points. A telomere elongation rate similar to the 24 PDs rescue (14 bp/PD) was also observed at the 45 PDs rescue time point. This rate of telomere elongation is much smaller than the estimated elongation rate at 7 PDs rescue (100 bp/PDs). These findings suggest that while at 7 PDs rescue telomerase elongates both long and short telomeres, at 24 PDs and 45 PDs rescue time points, when telomeres are longer, telomerase elongates a lower number of telomeres per PD, and appears less

processive, adding a lower number of telomeric repeats at chromosome ends during each cell division.

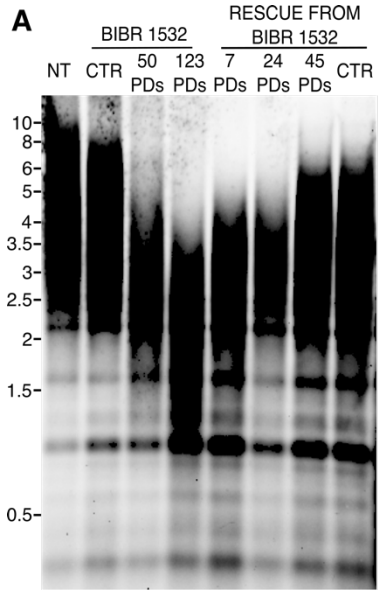

B

HeLa NT	Start Kb	End Kb	Average Kb
Telomeric smear	10	2.5	4
BIBR CTR			
Telomeric smear	8	2	3.5
BIBR 50PDs			
Telomeric smear	3.5	2	2.75
BIBR 123PDs			
Telomeric smear	3.5	1	2
RESCUE 7PDs			
Telomeric smear	4	2	2.75
RESCUE 24PDs			
Telomeric smear	4	2.5	3
RESCUE 45PDs			
Telomeric smear	6	2	3.25
RESCUE CTR			
Telomeric smear	6	2	3.25

Figure 20: Telomere shortening and consequent re-lengthening upon BIBR1532 treatment and its subsequent removal from culturing medium. A) Measurement of telomere length by Southern blot analysis of terminal restriction fragment lengths. Genomic DNA extracted from the indicated samples were transferred on a positively charged membrane after *RsaI-HinfI* restriction enzymes digestion and detected by hybridization with a digoxigenin-labeled telomeric repeats-specific probe. B) Determination of the average length of telomeres in the indicated samples. The TRF signal was calculated using Image Lab 6 (BioRad) by assessing the relative front of the telomeric smear considering the one of the molecular weight marker (for details please refer to materials and methods section). The experiment was performed two independent times showing similar results.

Thus, the different time points of these experiment provide a useful experimental setting to evaluate TERRA localization at telomeres when telomerase is actively elongating chromosome ends and telomeres are promptly elongated (7 PDs rescue time point), as compared to control cells (cells not treated with BIBR1532) or to a condition with a less pronounced ongoing telomerase activity and telomere elongation (24 PDs rescue time point).

Telomeric localization of TERRA inversely correlates with telomerase activity

I performed smiFISH/IF experiments to study TERRA localization at telomeres in control, 7 PDs rescue, and 24 PDs rescue time points of the experiments described in the previous paragraph. These analyses revealed a decrease in the number of

telomeric TERRA foci at the 7 PDs rescue time point, as compared to control and 24 PDs rescue cells (Figure 21A and B). The distribution of the number of telomeric TERRA foci per cells showed a clear and significant difference among the samples analyzed, with the 7 PDs rescue sample displaying a higher number of cells with 1 – 4 telomeric TERRA foci and a lower number of cells showing 5 – 10 and >10 telomeric TERRA foci than control and 24 PDs rescue samples (Figure 21C). Notably, these differences were detected despite the total number of TERRA foci increased at 7 PDs (Figure 21D). Furthermore, Northern blot analyses revealed no changes in the total TERRA levels between control and the 7 PDs rescue time point (Figure 21E). Importantly, no changes in the cell cycle profile were detectable between the different samples (Figure 21F). Altogether, these results indicate that a lower number of TERRA foci is detectable at telomeres at the 7 PDs rescue time point, when more pronounced telomere elongation occurs, as compared to control and the 24 PDs rescue time points. These findings suggest that in our experimental conditions TERRA localization at telomeres inversely correlates with telomerase activity. This effect is not due to altered TERRA levels or impaired cell cycle profile in these cells suggesting that it may be determined by the relocation of TERRA molecules from chromosome ends.

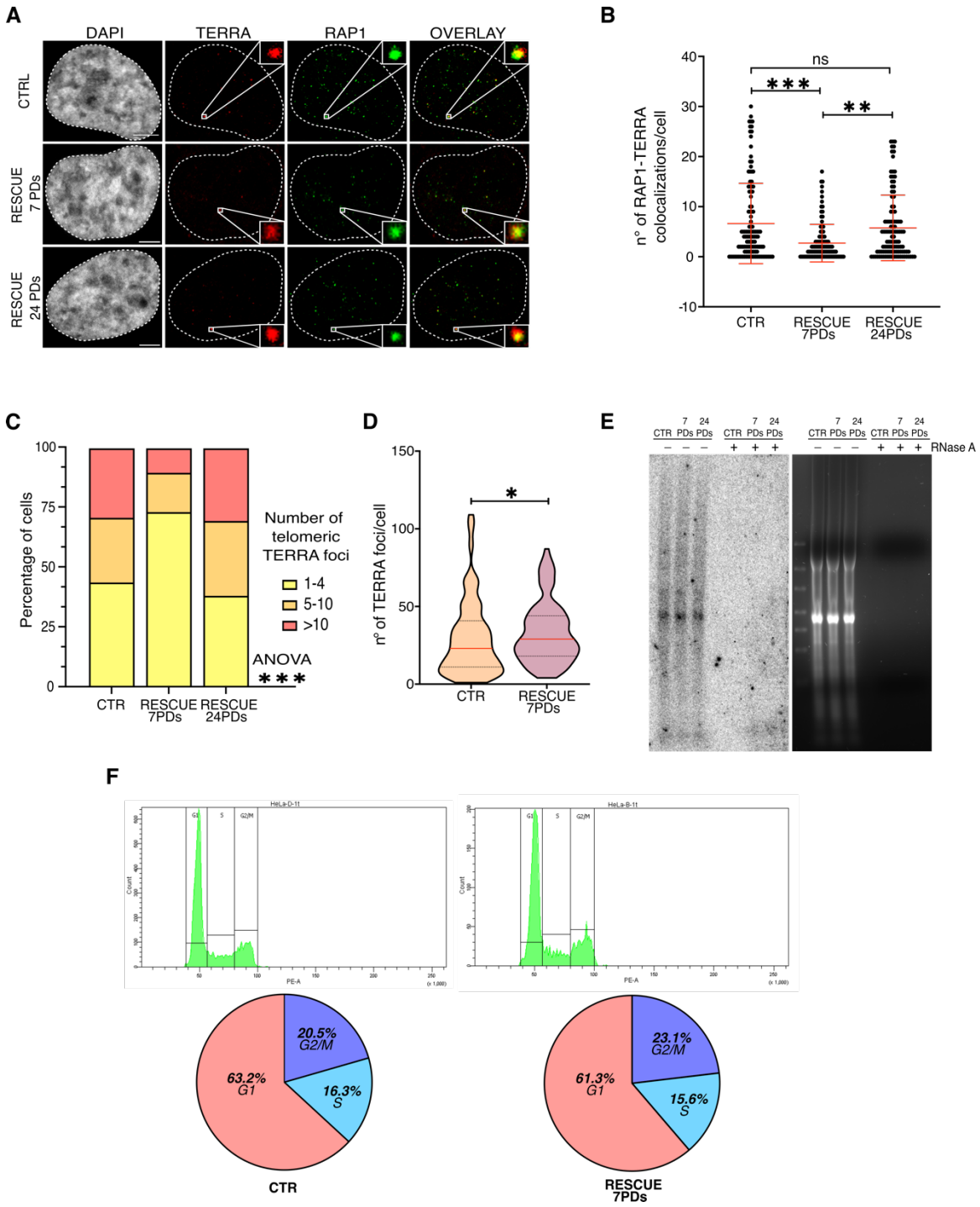

Figure 21: Less TERRA localizes to telomeres during telomere elongation. A) Detection of TERRA and telomeres by smiFISH/IF in HeLa cells fixed 7 or 24 PDs after removing BIBR1532 from the medium and in control (CTR) cells. An example of telomeric TERRA focus is shown in the magnifications. DAPI is used to stain nuclei. Scale bar: 5 μm. B-C) Quantification of telomeric TERRA foci per nucleus in the indicated samples: in B colocalizing events are represented as n° of RAP1/TERRA colocalizations per cell (each dot represents a nucleus); in C the percentage of cells presenting 1-4, 5-10 or >10 TERRA foci at telomeres are presented. In B, mean ± SD is shown and unpaired non-parametric Kruskal-Wallis test coupled with a post hoc Dunn's multiple comparison test was used for statistical analysis. In C, TWO-WAY ANOVA test confirms significant difference among

samples considering all groups of each sample: p-value: ***< 0.001. TWO-WAY ANOVA test coupled with a post hoc Tukey's multiple comparison test provides the following significances among groups and samples: group 1-4 telomeric TERRA foci: CTR vs 7 PDs, p-value 0.011; 7 PDs vs 24 PDs, p-value 0.0066; CTR vs 24 PDs, p-value >0.99. D) Quantification of the number of TERRA foci detected by smiFISH in control cells and 7PDs rescue cells. Median ± SD is shown and unpaired non-parametric Mann-Whitney test was used for statistical analysis. *, p-value <0.05. E) Northern blot analysis of TERRA levels in the indicated samples. On the right, total RNA run on 1.2% MOPS-Formaldehyde denaturing gel; on the left, TERRA transcripts transferred on a positively charged nylon membrane are detected by hybridization with a probe recognizing the telomeric repeated tract of TERRA. The probe used is γ^{32}P-labelled. RNA treated with RNase A was included as control for the specificity of the signal. F) FACS analyses of cell cycle profiles of control cells and 7 PDs rescue cells. These analyses revealed no changes in cell cycle profile among the samples. For B, C and D: N= 124 cells for CTR, 111 cells for RESCUE 7 PDs, 112 cells for RESCUE 24 PDs; n= 2 biological replicates. p-values: ns: non-significative; *, < 0.05; **, <0.01, ***<0.001.

The number of telomeric TERRA-hTR particles declines during telomere elongation

Next, we decided to investigate the telomeric localization of TERRA-h*TR* particles in control, 7 PDs rescue and 24 PDs rescue cells. We did so by combining smiFISH for TERRA and h*TR* with RAP1 IF and analyzing cells for triple colocalizations by confocal microscopy. Interestingly, these experiments revealed a significant difference in the number of telomeric TERRA-h*TR* foci detected between the different samples, with the fraction of TERRA-h*TR* foci at telomeres decreasing from 16% or 20% detected in control cells and 24 PDs rescue cells, respectively, to 8% detected in 7 PDs rescue cells (Figures 22A and 22B). Furthermore, while up to 5 telomeric TERRA-h*TR* particles per cell were detected in control and 24 PDs rescue cells, no more than 3 telomeric TERRA-h*TR* foci were observed at the 7 PDs rescue time point (Figure 22C). Notably, the number of telomeric h*TR* foci remained stable (Figure 22D) while the total number of TERRA-h*TR* colocalizations per cell even increased in 7 PDs cells, as compared to control cells (Figure 22E). These findings indicate that a lower number of TERRA-h*TR* particles are detected at telomeres at the 7 PDs rescue time point, when marked telomere elongation occurs, as compared to control and the 24 PDs rescue time points. This effect is most likely due to the impaired telomeric localization of TERRA during this time point. Given these results, it is intriguing to speculate that TERRA transcripts may be relocated from chromosome ends as a mechanism to facilitate telomere elongation by telomerase.

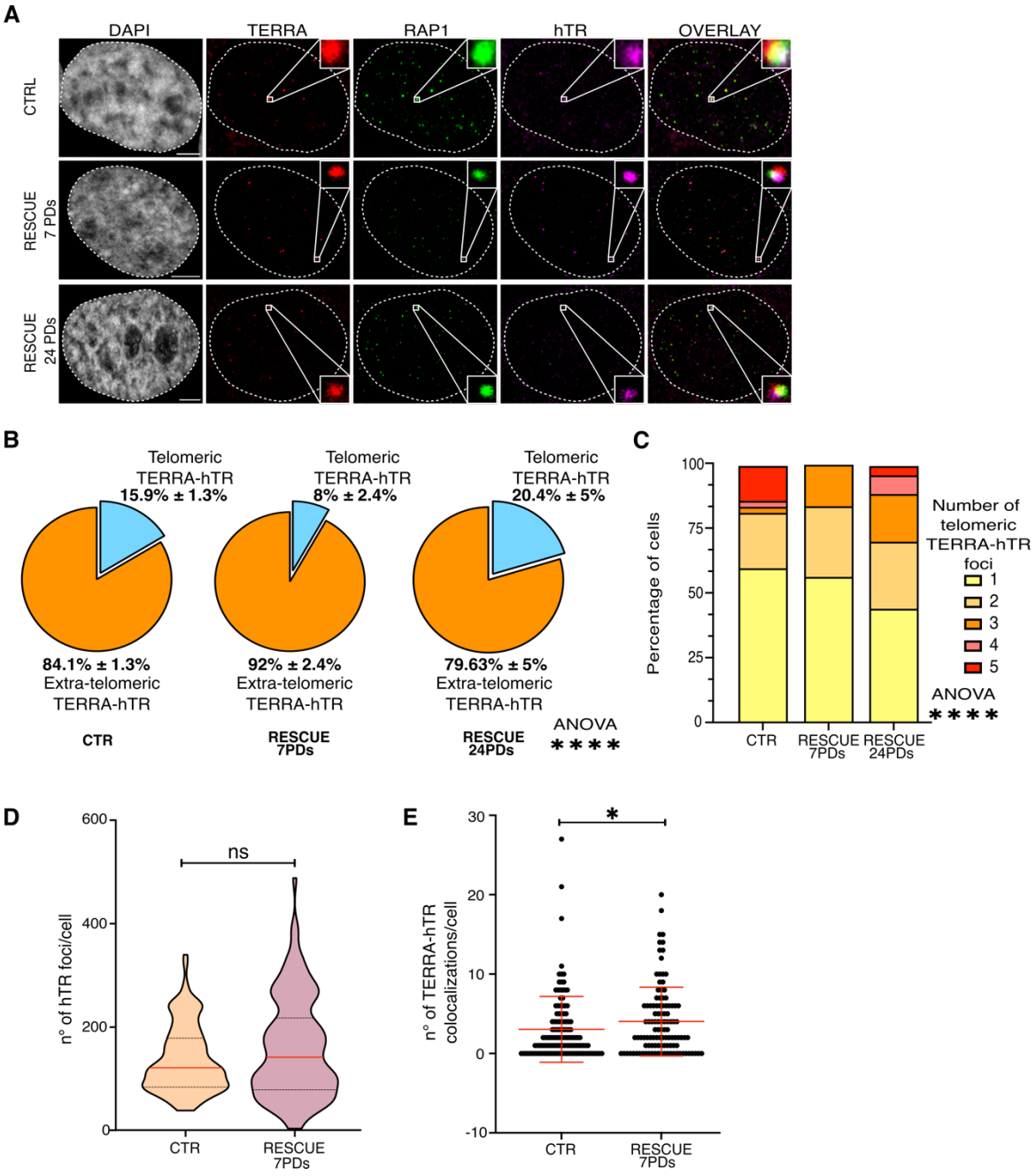

Figure 22: The number of telomeric TERRA-h*TR* particles declines during telomere elongation. A) Detection of TERRA, h*TR* and telomeres by smiFISH/IF in HeLa cells fixed at 7 or 24 PDs rescue time points and in control (CTR) cells. Examples of triple colocalizations between TERRA, h*TR* and RAP1 are shown in the enlargements. DAPI is used to stain nuclei. Scale bar: 5 μm. B-C) Quantification of the number of telomeric TERRA-h*TR* particles in the indicated samples. In B, pie charts report the percentage of TERRA-h*TR* particles at telomeres versus the non-telomeric ones. In C the percentage of cells showing 1 to 5 TERRA-h*TR* particles at telomeres per nucleus are reported. In both B and C, TWO-WAY ANOVA test confirms significant difference among samples considering all groups of each sample: p-value: ****< 0.0001. D) Quantification of h*TR* foci detected by smiFISH in control and 7 PDs rescue cells. Median ± SD is shown and unpaired non-parametric Mann-Whitney test was used for statistical analysis. E) Quantification of TERRA-h*TR* colocalizing foci detected per nucleus in control

cells and cells 7 PDs rescue cells. Mean ± SD is shown and unpaired non-parametric Mann-Whitney test was used for statistical analysis. N= 124 cells for CTR, 111 cells for RESCUE 7 PDs, 112 cells for RESCUE 24 PDs; n= 2 biological replicates. p-values: ****, <0.0001.

Telomeric localization of TERRA-h*TR* particles inversely correlates with telomerase activity in POT1 ΔOB-expressing cells

In order to confirm the abovementioned results, we decided to use a different experimental setting to study TERRA localization at telomeres during telomere elongation by telomerase. To this aim, we generated HeLa cells expressing a mutant form of POT1 (POT1-ΔOB), a key component of the shelterin complex that negatively regulates telomerase activity. POT1-ΔOB contains a truncation of one of the two POT1 OB-fold DNA binding domains, allowing POT1 to localize to telomeres but eliminating its ability to bind single-stranded telomeric DNA[82,180]. Therefore, POT1-ΔOB expression leads to unrestrained telomerase activity at telomeres and consequent chromosome ends over-elongation, as compared to HeLa cells and POT1-WT expressing cells. We reasoned that this system would represent a useful tool to study the localization of TERRA at telomeres during telomere elongation. We generated POT1-ΔOB expressing cells by transducing HeLa cells with POT1 ΔOB-, or POT1 WT-coding retroviral vectors. We collected genomic DNA at 10 PDs and 60 PDs from transduced cells and analyzed telomere length through TRF southern blotting. At these analyses, POT1-ΔOB expressing cells displayed longer telomeres (average length above 10 kb) compared to POT1-WT (circa 6 kb) at both time points analyzed (Figure 23), as expected given the unrestrained activity of telomerase in POT1-ΔOB expressing cells.

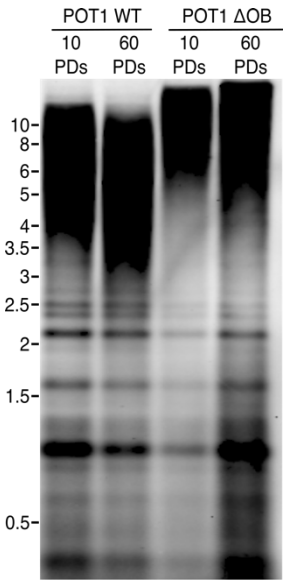

Figure 23: POT1-ΔOB expressing cells are characterized by over-elongated telomeres. Measurement of telomere length by Southern blot analysis of terminal restriction fragment lengths. Genomic DNA extracted from HeLa cells overexpressing POT1-WT or POT1-ΔOB proteins was transferred on a positively charged membrane after *RsaI-HinfI* restriction enzymes digestion and hybridized with a telomeric repeats-specific probe to detect telomeres. The probe used is digoxigenin-labelled.

smiFISH experiments revealed fewer TERRA foci in POT1-ΔOB cells than in POT1-WT control cells (Figure 24A). Furthermore, signal quantification analyses showed that TERRA foci detected in POT1-ΔOB cells are less bright than the ones detected in POT1 WT cells, suggesting that TERRA transcripts form less clusters in this cellular setting (Figure 24B). These findings are in line with previous evidence indicating that cells with over-elongated telomeres express lower TERRA levels although longer TERRA transcripts than cells with short telomeres[121].

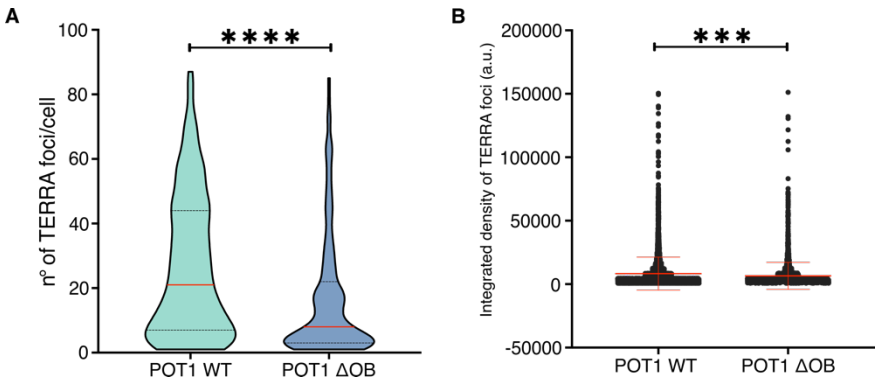

Figure 24: POT1-ΔOB cells present less TERRA transcripts than POT1-WT cells. A) Quantification of the number of TERRA detected foci per nucleus in POT1-WT and POT1-ΔOB expressing cells.

Median ± SD is shown and unpaired non-parametric Mann-Whitney test was used for statistical analysis. B) Quantification of TERRA foci integrated density in POT1-WT versus POT1-ΔOB expressing cells. Integrated density was measured with Fiji plug-in DiAna. Each dot represents a single TERRA focus. Mean ± SD is shown and unpaired non-parametric Mann-Whitney test was used for statistical analysis. p-value: ***, <0.001; ****, <0.0001. a.u.=arbitrary units. N= 151 cells for POT1 WT, 148 cells for POT1 ΔOB. n= 3 biological replicates.

Conversely, an increased number of RAP1 IF foci were detected in POT1-ΔOB cells, compared to POT1-WT cells (Figure 25A); integrated density quantification revealed that these foci are brighter than the ones detected in POT1-WT cells (Figure 25B). These findings are consistent with the presence of longer telomeres in POT1-ΔOB cells.

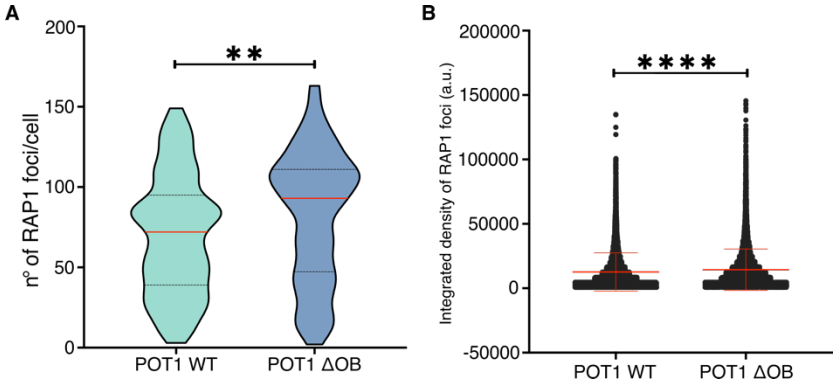

Figure 25: The number of RAP1 foci per cell and the intensity of the RAP1 signals are higher in POT1-ΔOB cells compared to POT1-WT. A) Quantification of the number of RAP1 foci per nucleus detected by IF in cells expressing POT1-WT or POT1-ΔOB protein. Median ± SD is shown and unpaired non-parametric Mann-Whitney test was used for statistical analysis. B) Quantification of RAP1 foci integrated density in POT1-WT versus POT1-ΔOB expressing cells. Integrated density was measured with Fiji plug-in DiAna. Each dot represents a single RAP1 focus. Mean ± SD is shown and unpaired non-parametric Mann-Whitney test was used for statistical analysis. p-value: **, <0.01; ****, <0.0001. a.u.=arbitrary units. N= 151 cells for POT1 WT, 148 cells for POT1 ΔOB. n= 3 biological replicates.

Interestingly, TERRA-RAP1 colocalization analyses by smiFISH/IF revealed a significantly lower number of telomeric TERRA foci in POT1-ΔOB cells (Figures 26A and 26B), confirming that also in this cellular context, telomerase activity at telomeres inversely correlates with the telomeric localization of TERRA. By analyzing TERRA and h*TR* by smiFISH, we observed a lower number of TERRA-h*TR* particles in POT1-

ΔOB cells (Figure 26C), even if the number of h*TR* foci per cell is increased as compared to POT1-WT cells (Figure 26D).

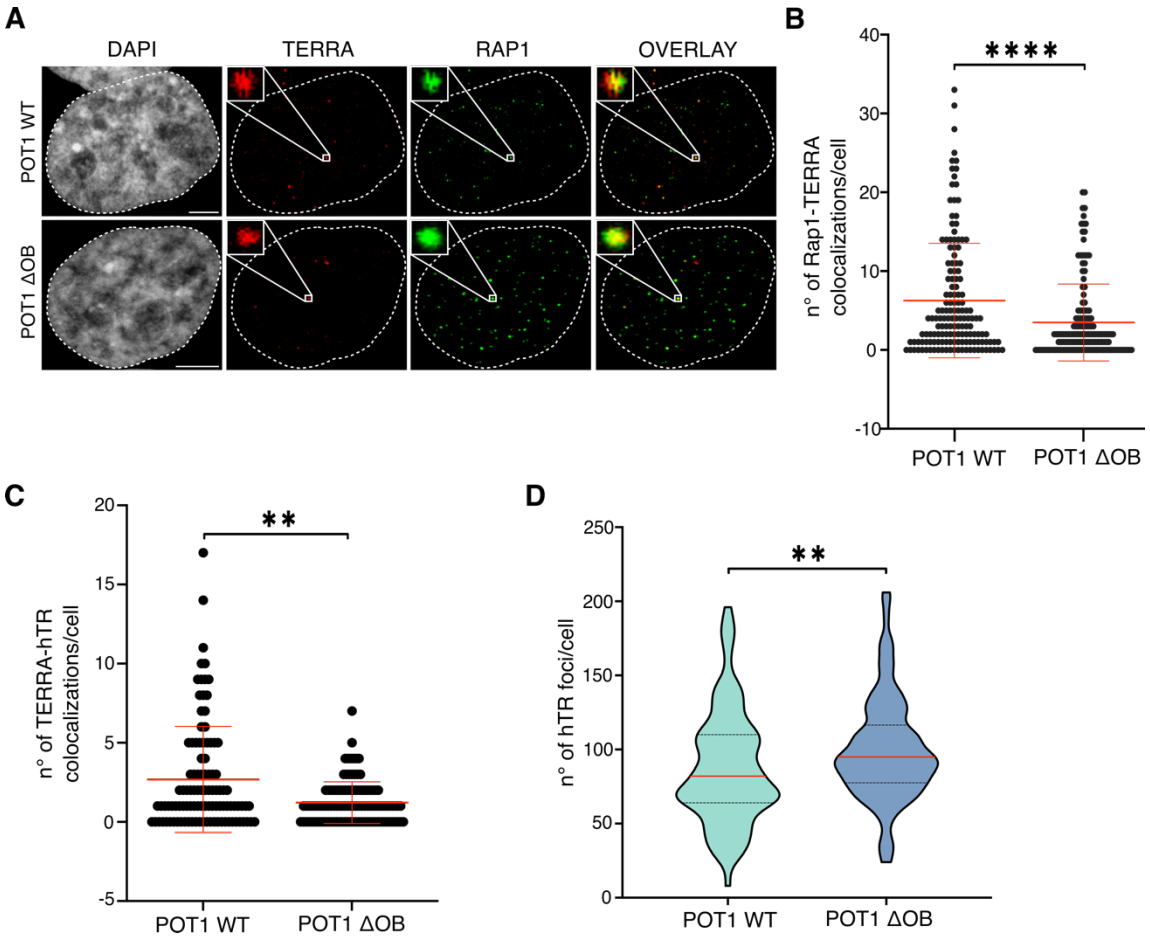

Figure 26: A lower number of telomeric TERRA foci is detectable in POT1-ΔOB displaying over-elongated telomeres, as compared to POT1-WT cells. A) Detection of TERRA and telomeres by smiFISH/IF in fixed HeLa cells overexpressing POT1-WT or POT1-ΔOB proteins. Examples of colocalization events between TERRA and RAP1 are shown in the magnifications. DAPI is used to stain nuclei. Scale bar: 5 μm. B) Quantification of the number of telomeric TERRA foci detected per nucleus in POT1-WT and POT1-ΔOB expressing cells: colocalizing events are represented as n° of RAP1/TERRA colocalizations per cell where each dot represents a nucleus. Mean ± SD is shown and unpaired non-parametric Mann-Whitney test was used for statistical analysis. N= 151 cells for POT1 WT, 148 cells for POT1 ΔOB. n= 3 biological replicates. C) Quantification of TERRA and h*TR* colocalizing foci per nucleus in POT1-WT and POT1-ΔOB expressing cells: colocalizing events are represented as n° of h*TR*/TERRA colocalizations per cell where each dot represents a nucleus. Mean ± SD is shown and unpaired non-parametric Mann-Whitney test was used for statistical analysis. D) Quantification of h*TR* detected foci per nucleus in cells expressing POT1-WT or -ΔOB protein. Median ± SD is shown and unpaired non-parametric Mann-Whitney test was used for statistical analysis. N= 100 cells for POT1 WT, 105 cells for POT1 ΔOB. n= 2 biological replicates. p-values: **, <0.01; ****, 0.0001.

Interestingly, smiFISH/IF experiments revealed less telomeric TERRA-h*TR* particles in POT1-ΔOB cells which displayed no more than 2 telomeric TERRA-h*TR* colocalizations per cell, with 85.5% of POT1-ΔOB cells displaying only 1 triple colocalization, as compared with POT1-WT cells, where up to 6 telomeric TERRA-h*TR* particles per cell were detected (Figures 27A and 27B). No changes in the number of h*TR* colocalizations at telomeres were observed, with most cells displaying 1 to 4 h*TR*-Rap1 colocalizing foci (Figure 27C). Furthermore, no changes in the cell cycle profile were detected between POT1-WT ad POT1-ΔOB cells (Figure 27D).

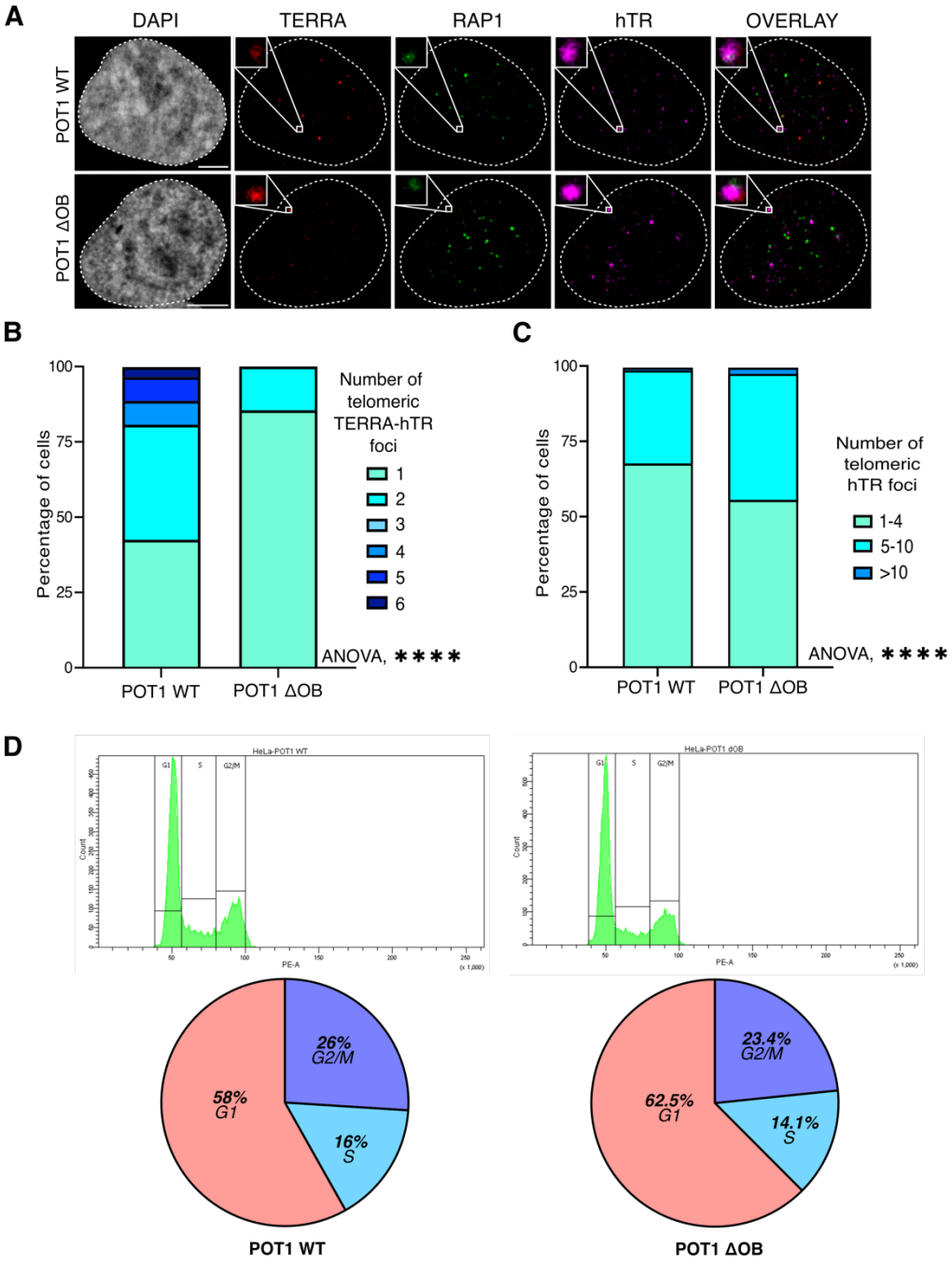
A
DAPI
TERRA
RAP1
hTR
OVERLAY
POT1 WT
POT1 ΔOB
B
Percentage of cells
Number of telomeric TERRA-hTR foci
1
2
3
4
5
6
ANOVA, ****
POT1 WT
POT1 ΔOB
C
Percentage of cells
Number of telomeric hTR foci
1-4
5-10
>10
ANOVA, ****
POT1 WT
POT1 ΔOB
D
HeLa-POT1 WT
HeLa-POT1 dOB
26% G2/M
58% G1
16% S
POT1 WT
23.4% G2/M
62.5% G1
14.1% S
POT1 ΔOB
E
n° of RAP1-hTR "TERRA-free" colocalizations/cell
*
POT1 WT
POT1 ΔOB

Figure 27: POT1-ΔOB expressing cells show less telomeric TERRA-h*TR* particles and more "TERRA-free" telomeric h*TR* foci. A) Detection of TERRA, h*TR* and telomeres by smiFISH/IF in fixed HeLa cells expressing POT1-WT or POT1-ΔOB. Examples of triple colocalizations between TERRA, h*TR* and RAP1 are shown in the image insets. DAPI is used to stain nuclei. Scale bar: 5 μm. B) Quantification of the number of telomeric TERRA-h*TR* complexes in the indicated cells. The percentage of cells presenting from 1 to 6 TERRA-h*TR* particles at telomeres are shown. TWO-WAY ANOVA test confirms significant difference in the number of telomeric TERRA-h*TR* foci among samples considering all groups of each sample: p-value: ****< 0,0001. TWO-WAY ANOVA test coupled with a post hoc Sidak's multiple comparison test confirms significance between the samples POT1 WT and POT1 ΔOB considering the group of 1 telomeric TERRA-h*TR* particle per nucleus: p-value= 0.0017. C) Quantification of the number of telomeric h*TR* foci observed per nucleus in the indicated cells. Percentage of cells showing 1-4, 5-10 or >10 telomeric h*TR* foci is shown. TWO-WAY ANOVA test confirms significant difference among samples considering all groups of each sample: p-value: ****< 0.0001. D) FACS analyses of cell cycle profiles of POT1-WT and POT1-ΔOB expressing cells. These analyses revealed no changes in cell cycle profile among the samples. E) Quantification of the number of telomeric h*TR* foci not colocalizing with TERRA foci ("TERRA-free" telomeric h*TR*) detected per nucleus. Data are shown as n° of h*TR*/RAP1 colocalization events per nucleus. Mean ± SD is shown and unpaired non-parametric Mann-Whitney test was used for statistical analysis. p-values: *, <0.05; ****, 0.0001. N= 100 cells for POT1-WT, 105 cells for POT1-ΔOB. n= 2 biological replicates.

Notably, for all colocalization analyses performed in this study, the DiAna plug-in of Fiji was used to confirm significance of the results. This approach revealed to be particularly important for analyses of samples in which the overall number of the foci of interest differ, such as TERRA-RAP1 colocalization analyses in POT1-WT versus POT1-ΔOB cells displaying differences in total number of TERRA and RAP1 foci (Details of colocalization analyses are indicated in Materials and Methods section).

Overall, these findings indicate that TERRA localization to telomeres is impaired in POT1-ΔOB expressing cells, where telomerase activity is unrestrained, and telomeres are over-elongated. Furthermore, telomere elongation in POT1-ΔOB cells correlates with fewer TERRA-h*TR* colocalizations at chromosome ends and increased number of telomeres displaying "TERRA-free" telomerase molecules Figure 27E). Importantly, these findings also indicate that this effect is not dependent on the length of telomeres because POT1-ΔOB cells display much longer telomeres than the 7 PDs rescue cells. These findings further support our hypothesis that TERRA transcripts relocate from chromosome ends in order to facilitate telomerase activity. Thus, telomeric TERRA transcripts may act as inhibitors of telomerase.

TERRA expression levels and its localization to telomeres increase upon telomere shortening

Previous evidence indicates that human cells with short telomeres express higher levels of TERRA than cells with over-elongated telomeres[121]. This would be in apparent contradiction with our findings indicating that telomeric TERRA transcripts may act as negative regulators of telomerase. Indeed, if so, increased transcription of TERRA from short telomeres would prevent their elongation. Thus, we decided to gain more insight into this matter and we used our experimental systems to better understand the interplay between telomere shortening and TERRA expression and localization.

Firstly, we performed Northern blot analysis on RNA extracted from cells cultivated in BIBR1532 for 123 PDs and from control cells treated with DMSO (CTR). As shown in panel A (Figure 28) a mild increase in TERRA expression in the BIBR-treated sample can be appreciated. To further investigate this increase in TERRA expression levels, RT-qPCR analyses on the same samples were performed. In the graph reported in Figure 28B, an increase in TERRA expression from the indicated subtelomeres was observed. These results are in line with previous findings reported in literature using other cell lines[121]. Additionally, BIBR1532-treated cells showed a higher number of TERRA foci, compared to control cells, as detected by smiFISH, consistent with the increased TERRA levels in these cells (Figure 28C).

Taken together, these results suggest that TERRA expression levels are upregulated in HeLa cells with short telomeres as consequence of BIBR1532 treatment.

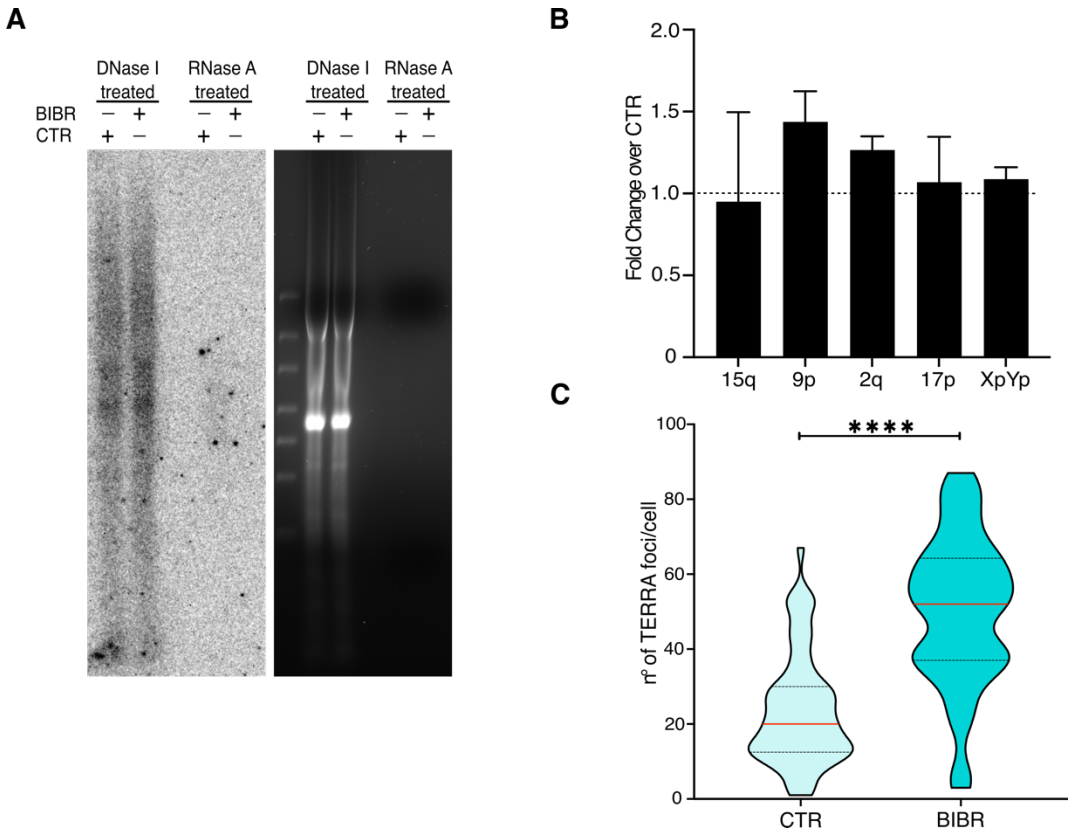

Figure 28: TERRA expression levels mildly increase in cells with short telomeres. A) Northern blot analysis of TERRA levels in HeLa cells treated for 123 PDs with BIBR1532 or DMSO (CTR). On the right, total RNA run on 1.2% MOPS-Formaldehyde denaturing gel; on the left, TERRA transcripts transferred on a positively charged nylon membrane and detected by hybridizing a probe specifically recognizing telomeric repeated tract of TERRA. The probe used is γ^{32}P-labelled. RNA treated with RNase A was included to test the RNase sensitivity of the signal. B) RT-qPCR analyses were performed to assess TERRA levels derived from the indicated telomeres. The experiment was performed from total RNA extracted from HeLa cells with short telomeres (BIBR1532 123 PDs). Data are normalized on the housekeeping GAPDH gene and are shown as fold change over control (CTR) cells (dashed line) with mean and SD derived from two biological replicates (each experiment performed in technical triplicates). Data shown represent the mean between biological replicates. C) Quantification of the number of TERRA foci detected per nucleus in both BIBR1532- treated (BIBR) and control (CTR) cells. Median ± SD is shown and unpaired non-parametric Mann-Whitney test was used for statistical analysis. p-value: ****, <0.0001. N= 67 cells for BIBR, 64 cells for CTR; n= 2 biological replicates.

Next, we investigated TERRA localization at telomeres in these cells by smiFISH/IF. Interestingly, we observed no major changes in the number of TERRA-RAP1 colocalizations per cell, compared to CTR sample (Figure 29A), although the percentage of BIBR-treated cells presenting more than 10 telomeric TERRA foci was found higher compared to CTR cells (Figure 29B). This last result is in agreement

with the increased telomeric localization of TERRA reported in HeLa clones with short telomeres, compared to clones with long telomeres recently shown by the Lingner's lab in 2019[168]. Altogether, these findings indicate that cells with short telomeres express higher TERRA levels than cells with normal length telomeres. Cells with short telomeres display an increased number of telomeric TERRA foci per cell. In the attempt to reconcile these results with our hypothesized model of telomeric TERRA transcripts acting as inhibitors of telomerase, we decided to obtain more information into the state of the telomeres interacting with TERRA.

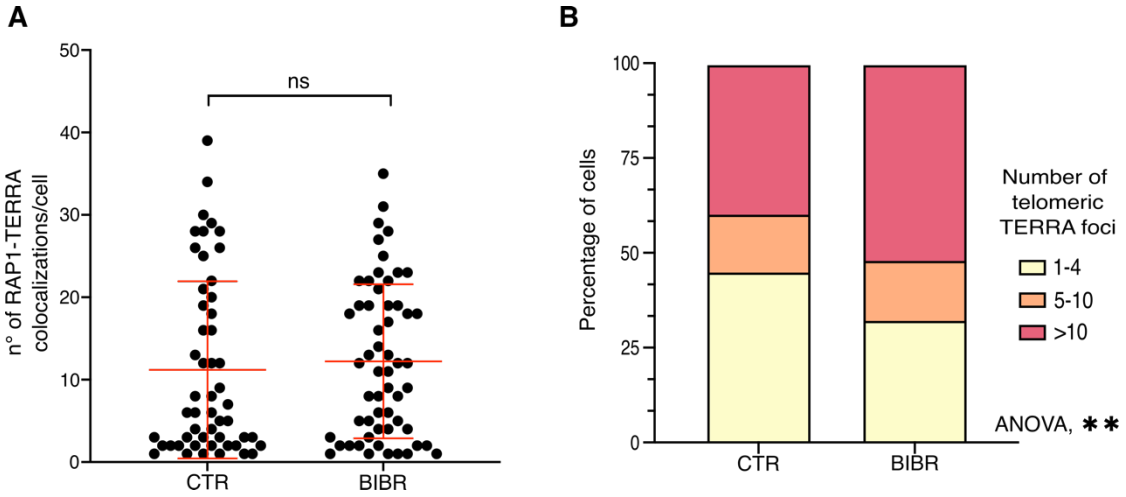

Figure 29: TERRA localization to telomeres slightly changes upon telomere shortening. A-B) Quantification of telomeric TERRA foci observed per nucleus in BIBR1532-treated cells and CTR cells: in A colocalizing events are represented as n° of RAP1/TERRA colocalizations per cell where each dot represents a nucleus. Mean ± SD is shown and unpaired non-parametric Mann-Whitney test was used for statistical analysis. In B the percentage of cells presenting 1-4, 5-10 or >10 TERRA foci at telomeres is shown. TWO-WAY ANOVA test confirms significant difference among samples considering all groups of each sample: p-value: **, < 0.01. p-values: ns: non-significative; **, <0.01. N= 67 cells for BIBR, 64 cells for CTR; n= 2 biological replicates.

TERRA transcripts preferentially localize to long telomeres in human cells

In *S. cerevisiae*, TERRA transcripts localize preferentially to short telomeres to promote the recruitment of telomerase to these chromosome ends. Our data envisage an opposite scenario in human cells, where telomeric TERRA transcripts inversely correlate with telomerase activity, suggesting that they may interfere with telomere elongation by telomerase. Since we also observed that TERRA expression levels and localization at chromosome ends increase upon telomere shortening, we decided to shed lights into the state of the telomeres interacting with TERRA and we investigated whether TERRA molecules localize to short or long telomeres.

Previous evidence in our lab indicates that the integrated density quantification of RAP1 IF signal can be used to discriminate long versus short telomeres compared to the average telomere length of the cell. These experiments were performed by Marta Andolfato (a master student who worked under my supervision) combining RAP1 IF with telomeric DNA FISH signals. The results from these experiments are shown in Supplementary Figure S1.

Upon image acquisition, the integrated density parameter calculates the sum of the values of each pixel (i.e., pixel brightness) that composes the examined object resulting in an indication of the intensity of the signal. These analyses can be done using Fiji software. We performed integrated density quantification of RAP1 IF signals obtained in smiFISH/IF experiments carried out in BIBR1532-treated cells (123 PDs time point), 7 PDs rescue time point, BIBR1532 control cells, POT1-WT, POT1-ΔOB and HeLa WT cells. In these analyses we compared integrated density quantification of RAP1 IF signal colocalizing, and not colocalizing, with TERRA foci. Strikingly, in all the conditions tested the RAP1 IF signals colocalizing with TERRA showed significantly higher integrated densities than the RAP1 signals not colocalizing with TERRA (Figure 30). These results were not dependent on the average telomere length of the cells, since they were reproduced in HeLa WT cells and also in both BIBR1532 treatments, displaying very short telomeres, and POT1-ΔOB cells with over-elongated telomeres. Furthermore, these findings were not dependent on the activity of telomerase, which is inactivated in BIBR1532-treated cells and unrestrained in POT1-ΔOB cells. This strongly suggests that TERRA transcripts

preferentially localize to the longest telomeres in a cell. Thus, while TERRA expression may rise upon telomere shortening, TERRA transcripts are expected to relocate from short telomeres to the longer ones. This mechanism may contribute to regulating telomerase activity, repressing it at longer chromosome ends. Experimental data in support of the localization of TERRA molecules *in trans*, relocating from their telomere of origin to other chromosome ends, have been obtained by a master student in the lab, Elena Goretti, using the MS2-GFP system to track single-telomere TERRA molecules in living cells. These data are presented in Figure 33 and Figure 34 and discussed in the discussion section of this thesis.

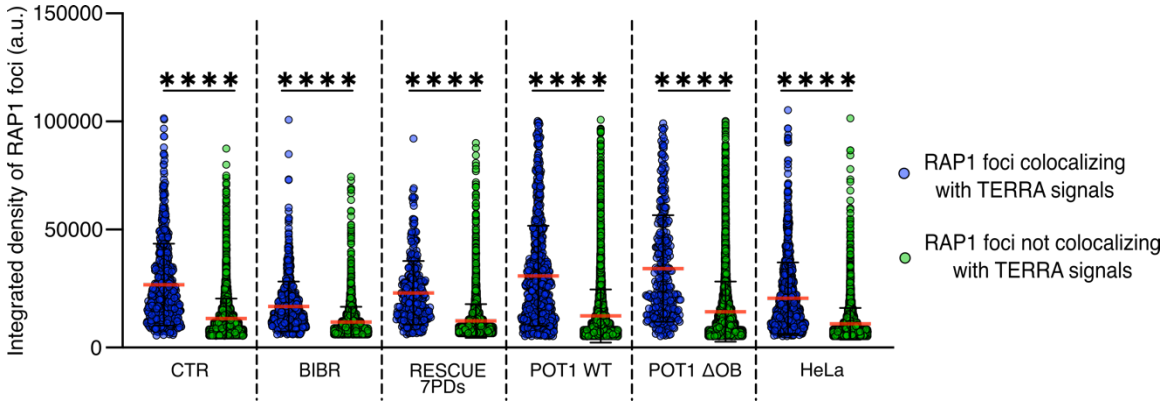

Figure 30: Telomeres colocalizing with TERRA foci display higher intensity than telomeres not colocalizing with a TERRA signal. Comparison of RAP1 foci integrated density between telomeres colocalizing and not colocalizing with TERRA transcripts in different experimental conditions. Integrated density was measured with Fiji plug-in DiAna. Each dot represents a single RAP1 focus. Mean ± SD is shown and unpaired non-parametric Mann-Whitney test was used for statistical analysis. p-value: ****, <0.0001. a.u.=arbitrary units.

TERRA depletion results in increased telomerase RNA localization at telomeres

Our results are supportive of a scenario in which TERRA molecules can be transcribed from short chromosome ends to localize to the longer telomeres. Furthermore, the localization of TERRA at telomeres inversely correlates with telomerase activity during telomere elongation in BIBR1532-treated cells and in a cell system where telomerase activity is unrestrained (POT1-ΔOB expression). These findings suggest that the telomeric localization of TERRA transcripts may impair telomerase activity and/or its recruitment at telomeres.

To provide insight into this process, we decided to investigate whether TERRA depletion influences the recruitment of telomerase to telomeres. To this aim, I used antisense oligonucleotides targeting the telomeric repeat tract of TERRA (TERRA-ASO) to downregulate TERRA molecules in cells. This approach has been extensively used in literature to deplete TERRA in cells[148,169,191]. TERRA-ASO consists of locked nucleic acids (LNA) containing oligonucleotides with a phosphorothioate backbone which upon base pairing with the target RNA promote its degradation by the endogenous RNase H enzyme. RT-qPCR experiments confirmed depletion of TERRA from multiple telomeres upon 48h transfection of TERRA-ASO (Figure 31A). Transfection of a scrambled ASO was performed as negative control. Interestingly, smiFISH experiments revealed that decreased TERRA levels resulted in increased number of h*TR* foci (Figure 31B). In light of these results, we used RT-qPCR to analyze the expression levels of h*TR*, both its mature and precursor forms. Surprisingly, no differences in h*TR* levels were detected between TERRA-ASO and scrambled ASO transfected cells (Figure 31C). These results suggest that TERRA depletion correlates with increased telomerase RNA clustering.

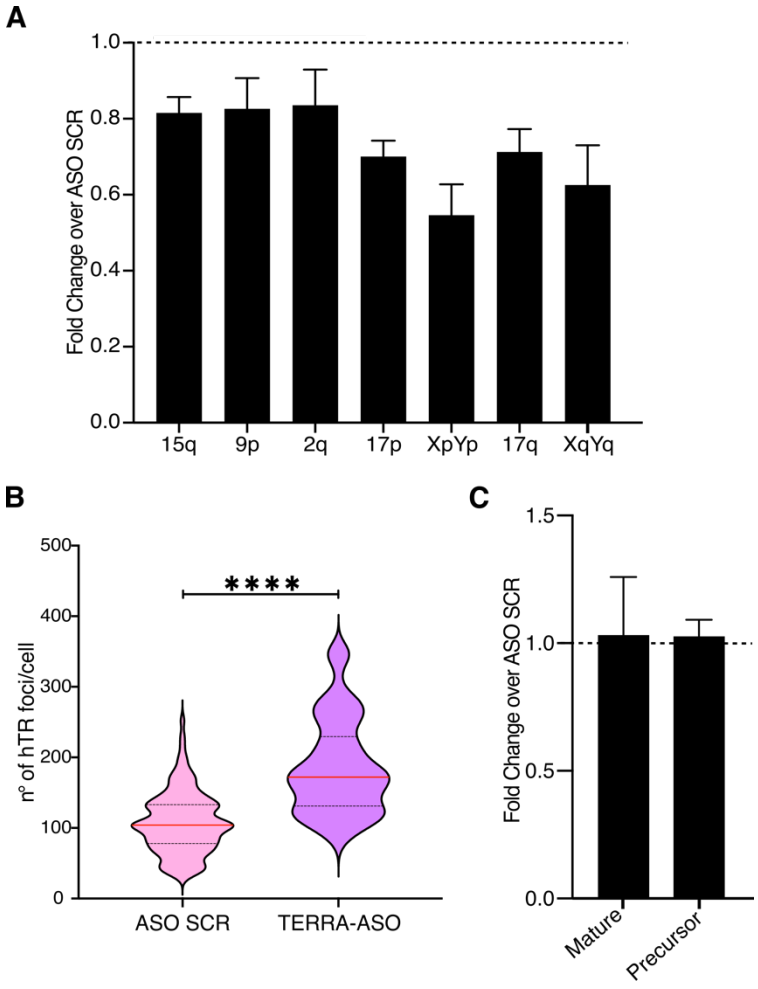

Figure 31: TERRA knockdown results in increased h*TR* foci number without affecting its expression levels. A) RT-qPCR analyses to assess TERRA levels derived from the indicated telomeres performed from total RNA extracted from HeLa cells transfected with scrambled ASO (ASO SCR) or TERRA-ASO. Data are normalized on the housekeeping U6 gene and are shown as fold change over control (ASO SCR) cells (dashed line) with mean and SD derived from technical triplicates. Data shown represent one biological replicate. B) Quantification of h*TR* foci detected per nucleus in both TERRA-ASO and ASO SCR transfected cells. Median ± SD is shown and unpaired non-parametric Mann-Whitney test was used for statistical analysis. p-value: ****, <0.0001. N= 131 cells for ASO SCR, 122 cells for TERRA-ASO; n= 2 biological replicates. C) RT-qPCR to assess h*TR* levels, as precursor (from +772 to +896 nt coordinates of the h*TR* gene locus) or mature transcripts (451 nt in length), performed from total RNA extracted from HeLa cells transfected with ASO SCR or TERRA-ASO. Data are normalized on the housekeeping U6 gene and are shown as fold change over control (ASO SCR) cells (dashed line) with mean and SD derived from technical triplicates. Data shown represent one biological replicate.

Next, I analyzed h*TR* localization at telomeres by smiFISH/IF. Intriguingly, these experiments revealed a significant increase in the number of telomeric h*TR* foci in TERRA-depleted cells as compared to control cells (Figure 32A). Notably, the percentage of cells displaying more than 10 telomeric h*TR* per nucleus increased from 1.6% in ASO SCR transfected cells to 8% in TERRA-ASO transfected cells (Figure 32B). These findings indicate that TERRA molecules may impede h*TR* clustering and its localization to chromosome ends. These results are consistent with the role of TERRA in impairing telomerase activity in human cancer cells.

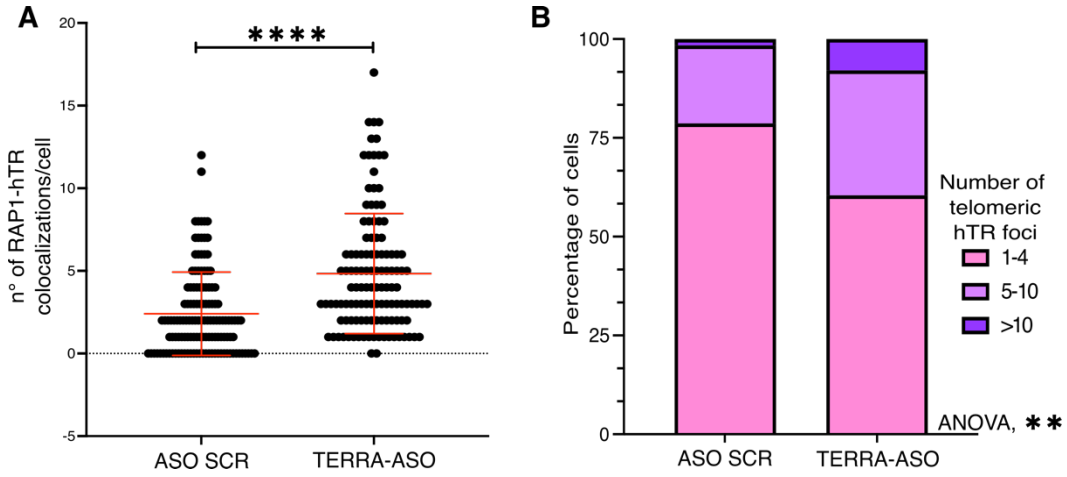

Figure 32: TERRA knockdown leads to increased number of h*TR* foci at telomeres. A-B) Quantification of the number of telomeric h*TR* foci observed per nucleus in the indicated samples: in A, colocalizing events are represented as n° of RAP1/h*TR* colocalizations per cell (each dot represents a nucleus). Mean ± SD is shown and unpaired non-parametric Mann-Whitney test was used for statistical analysis. In B, the percentage of cells presenting 1-4, 5-10 or >10 h*TR* foci at telomeres is shown. TWO-WAY ANOVA test confirms significant differences among samples considering all groups of each sample: p-value: **< 0.01. p-values: ns: non-significative; **, <0.01; ****, <0.0001. N= 131 cells for ASO SCR, 122 cells for TERRA-ASO; n= 2 biological replicates.

DISCUSSION

The length of chromosome ends is a key determinant of cellular replicative senescence as it determines the number of cell divisions a cell can undergo throughout its life. The physiological telomere shortening acts as a powerful tumor-suppressor mechanism by limiting the proliferative capacity of a cell. The activity of telomerase confers replicative immortality to most cancer cells and extends the lifespan of stem cells and progenitor cells, by adding telomeric repeats to the 3' end of chromosomes.

In 2008 it has been shown by Schöftner and Blasco[109] that short TERRA-like oligonucleotides are able to inhibit telomerase activity both in mouse and human cellular extracts, most likely by base pairing with the template region of h*TR*. Subsequently, the association of TERRA with both h*TR* and hTERT was reported by co-immunoprecipitation experiments[156] supporting a probable TERRA inhibitory role in telomerase activity regulation. Despite these findings, it remains unclear why increased levels of TERRA do not result in telomerase inhibition in different cellular contexts (iPSCs, stem cells, ICF derived cells)[160] and perhaps even more surprisingly, why inducible over-expression of TERRA from an engineered telomere does not impair the elongation of this chromosome[157]. Here, using a single molecule approach combined with confocal microscopy I obtained data supporting a model in which the localization of TERRA transcripts at telomeres may be critical for the function of TERRA in the regulation of telomerase. While the mechanism of TERRA-mediated telomerase regulation still needs to be dissected, this model will enable to reconcile the conflicting evidence in the field. Indeed, increased TERRA expression does not necessarily correlate with telomeric localization of TERRA transcripts due to the presence of several pathways involved in the active displacement of TERRA from chromosome ends[108,151].

In support of this model, I found that TERRA and the RNA subunit of telomerase (h*TR*) colocalize in HeLa cells. These results indicate that only a minority of TERRA and h*TR* molecules are involved in the formation of TERRA-h*TR* particles, since 82% of cells displays only 1 to 4 TERRA-h*TR* colocalizing foci (average number of TERRA and h*TR* foci detected per cell is 13 and 94, respectively), suggesting that the TERRA-

h*TR* interaction is a highly regulated process. Interestingly, also the telomeric localization of TERRA-h*TR* particles is tightly regulated, since only about 41% of cells shows TERRA-h*TR* particles at chromosome ends. In this regard, I report that the localization of TERRA and TERRA-h*TR* particles at telomeres inversely correlates with telomerase activity. This observation comes from two different model systems: a model in which short telomeres are re-elongated by telomerase, and a second approach involving HeLa cells expressing a mutant form of POT1 that enables unrestrained elongation of telomeres by telomerase. Notably, both models do not exogenously alter the levels of telomerase. Furthermore, the two models involve cells with different telomere length, indicating that these observations are not dependent on the length of telomeres. Remarkably, the opposite scenario has been observed in budding yeast, in which TERRA transcripts expressed from a single telomere colocalize with the telomerase RNA *TLC1* at short chromosome ends to promote telomerase activity[161]. The evidence presented here suggests that the presence of TERRA transcripts at human telomeres may instead impair telomerase activity. While the molecular details of this process will need to be elucidated, we hypothesize that TERRA-h*TR* base pairing at chromosome ends will affect the recruitment and/or the retention of telomerase to telomeres. Indeed, it has been observed that the base pairing between the single-stranded telomeric DNA and the h*TR* template sequence is essential to stabilize telomerase recruitment to chromosome ends[82,97]. The presence of TERRA to telomeres may interfere with such pairing by competing with the G-rich single-stranded telomeric DNA for h*TR* binding. This process is expected to impact telomerase recruitment and/or its retention to telomeres. In support of this hypothesis, the experiments of TERRA knock-down using antisense oligonucleotides have shown increased number of hTR molecules to chromosome ends upon TERRA depletion. In these experiments I observed a mild decrease in TERRA levels from telomeres upon TERRA ASO transfection, as detected by RT-qPCR. In future studies, TERRA downregulation should be assessed by Northern Blot in order to quantify the effect of the TERRA ASO transfection on the total levels of TERRA. Despite this mild decrease in TERRA levels, our experiments also revealed increased formation of h*TR* foci upon TERRA depletion, even if the h*TR* expression levels remained unchanged. Importantly, a similar effect was previously observed in mouse embryonic stem cells (mESCs), where TERRA downregulation by TERRA ASO transfection resulted in increased number of h*TR* foci[148]; however, in that case, an increase in h*TR* levels

was also detected. These findings suggest that TERRA-h*TR* interaction could impact h*TR* clustering in human cells. While the biological relevance of this effect remains to be defined, it has been observed that it is a cluster of telomerase molecules to stably associate with telomeres to promote telomere elongation[82,97]. In this respect, by preventing telomerase clustering, TERRA molecules may thus also negatively impact telomerase recruitment to chromosome ends. Notably, also in this case, the opposite scenario has been observed in budding yeast, where TERRA positively regulates telomerase activity. Indeed, in this model system, TERRA transcripts were observed to promote telomerase RNA clustering and its subsequent recruitment to short chromosome ends as a cluster containing both TERRA and telomerase RNA molecules[161]. Recently it has been developed an approach to tag and visualize h*TR* molecules in living human cells[82]. It would be interesting to use this approach to study the effect of TERRA downregulation on h*TR* clustering by live cell imaging. By these experiments it will be possible to study the clustering as well as the residence time of h*TR* to telomeres. The use of fluorescence recovery after photobleaching (FRAP) will also give information on the dynamics of h*TR* clusters.

In addition to the inverse correlation between the telomeric localization of TERRA and telomerase activity, I observed that downregulation of the essential component of telomerase TCAB1 does not influence the telomeric localization of TERRA. As TCAB1 has been observed to be essential to telomerase stability at telomeres and telomere elongation[184,185], these findings are in agreement with a model in which, differently from the condition in yeasts, TERRA is not recruited at human telomeres while interacting with telomerase.

In this regard, TERRA has been observed to interact with both TRF1 and TRF2[118,132], and with components of the telomeric chromatin, such as HP1 and H3K9me3[115,121,144]. In addition, TERRA transcripts can form R-loop structures by base pairing with their C-rich DNA template strand[135,136]. Thus, different mechanisms may promote TERRA recruitment to telomeres in a telomerase independent way. In line with previous evidence, I observed that telomere shortening upon BIBR1532 treatment of HeLa cells results in increased TERRA levels[121]. Why would TERRA levels increase from short telomeres if one of TERRA functions is to repress telomere elongation? We have not yet an answer to this question, although we can hypothesize that short telomeres have a less compact chromatic state that enables increased

transcription of TERRA[121]. Furthermore, eroded telomeres may retain a lower number of TERRA repressors, and TRF2 has been shown to inhibit TERRA expression[115]. Shorter telomeres would result in a lower number of TRF2 binding sites and less TRF2 bound to repress TERRA transcription. Further studies are needed in order to define the mechanism of TERRA expression from short telomeres. Nevertheless, the observations presented here suggest that even if TERRA levels increase when telomeres shorten, TERRA transcripts preferentially localize to the longest telomeres, thus to the chromosome ends with lowest priority to be elongated. This conclusion was based on the quantification of the integrated density of RAP1 IF signal colocalizing or not with TERRA foci. The results were surprising as the signal of TERRA-colocalizing RAP1 foci was found to be much more intense than the signal of telomeres not colocalizing with TERRA. Remarkably, this effect was observed in multiple cellular contexts, including cells with short (BIBR1532-treated) or long telomeres (POT1-ΔOB expressing), indicating that it is not dependent on the overall telomere length in the cells. We considered that the RAP1 IF signal may be influenced by the chromatinic state of the telomere: a more compacted chromatin of some telomeres could affect the antibody binding to the RAP1 protein, masking the epitope. For this reason, we operated to confirm these results using a system in which we visualized telomeres by overexpressing the TRF1-mCherry protein. By this approach, we could detect the telomeric signal without the use of the antibody. Interestingly, results from the two techniques converged indicating that the telomeric foci colocalizing with TERRA foci display significantly higher intensity that the telomeric signals not colocalizing with TERRA (data not shown). Longer telomeres are expected to contain a higher number of shelterin and TERRA-binding proteins TRF1 and TRF2, which may contribute to the preferential recruitment of TERRA to these chromosome ends. Furthermore, as telomeres are genomic loci difficult to be replicated due to their high repetitive sequence, longer telomeres may result in higher number of paused or stalled replication forks[186]. TERRA has been proposed to contribute to replication fork restart upon replicative stress at telomeres[187] which may suggest a possible biological function and the presence of an active recruitment mechanism of TERRA to longer telomeres. Nevertheless, it should be noted that at this point, while these results were very interesting to us, we cannot exclude that the brightest telomeric foci may represent clusters of telomeres instead of longer telomeres. Telomere clustering has been observed as common feature of ALT cancer cell, and it can also occur, although

much less pronounced than in ALT cells, in telomerase-positive cells[188]. We are currently trying to investigate this possibility by performing super resolution microscopy, both Stochastic Optical Reconstruction Microscopy (STORM) and Structured Illuminated Microscopy (SIM) to discriminate telomere clusters from single chromosome ends in fixed cells.

Evidence from our laboratory confirmed that TERRA molecules localize to chromosome ends mainly *in trans*, consistent with a scenario in which TERRA transcripts expressed from short telomeres relocate to the longer ones. Indeed, a previous master student in the lab, Elena Goretti, used the CRISPR/dCas9 reporter system to label the subtelomeric region of chromosome 15q in cells engineered to express endogenous telomere 15q TERRA transcripts tagged with the MS2-GFP system, also known as TERRA-MS2 clones which were previously generated in the AGS human stomach cancer cell line in our lab[164]. The use of the CRISPR/dCas9 system has been previously shown as a robust approach to detect repetitive sequences by live imaging[189,190]. In particular, co-expression of guide RNAs targeting repetitive genomic regions along with a BFP-fused dCas9 protein, enables the visualization of the targeted genomic locus in living cells by fluorescence microscopy. Live cell imaging of TERRA-MS2 clones upon expression of a guide RNA targeting a repetitive sequence within subtelomere 15q, allowed the detection of two discrete dCas9-BFP nuclear foci per cell co-localizing with TRF1-mCherry foci (Figure 33). These findings are in line with the presence of two copies of chromosome 15q in the AGS cell line.

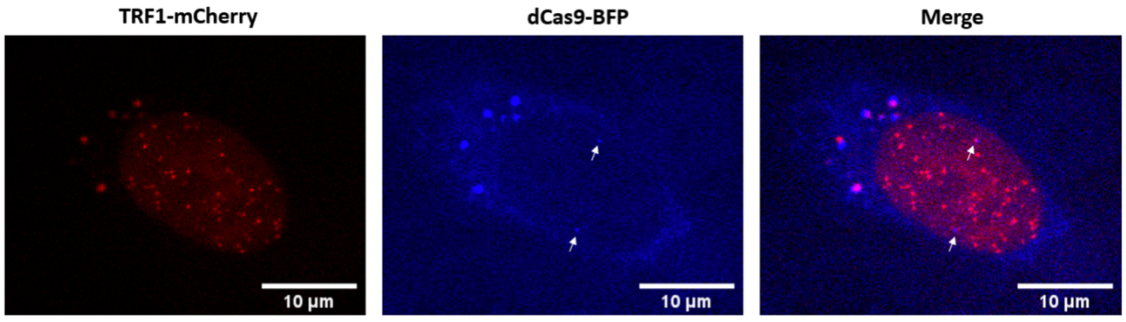

Figure 33: BFP-fused dCas9 allows the detection of telomere 15q in AGS MS2-15q-TERRA cells. Telomeres are detected by expression of TRF1 shelterin protein fused to mCherry fluorophore. Telomere 15q is detected through co-transfection of dCas9-BFP and a 15q-specific sgRNA. Examples of colocalization events between TRF1-mCherry and dCas9-BFP signals are highlighted by the white

arrows in the merge image. Scale bar: 10 μm. Live-cell imaging, images acquisition and analysis performed by Elena Goretti.

By this approach, it has been tested whether TERRA molecules localize to their telomere of origin, by performing live imaging of TERRA-MS2-GFP particles, corresponding to MS2-tagged TERRA transcripts expressed from telomere 15q, dCas9-BFP-tagged subtelomere 15q and TRF1-mCherry-tagged telomeres (Figure 34A). Quantification of TERRA-MS2-GFP foci colocalizing with subtelomere 15q or other telomeres revealed that only 7 out of 408 particles, corresponding to the 1.7% of the TERRA particles analyzed, colocalized with their telomere of origin (*in cis* localization), while 57 out of 408 particles (14% of the particles analyzed) were detected at other telomeres. 344 out of 408 did not localize at telomeres (84,3%) (Figure 34B). These findings are in line with my observations that TERRA transcripts which may be expressed from short telomeres quickly relocate to other chromosome ends. These live cell imaging studies were performed in collaboration with the laboratory of Dr. Pascal Chartrand at the University of Montreal.

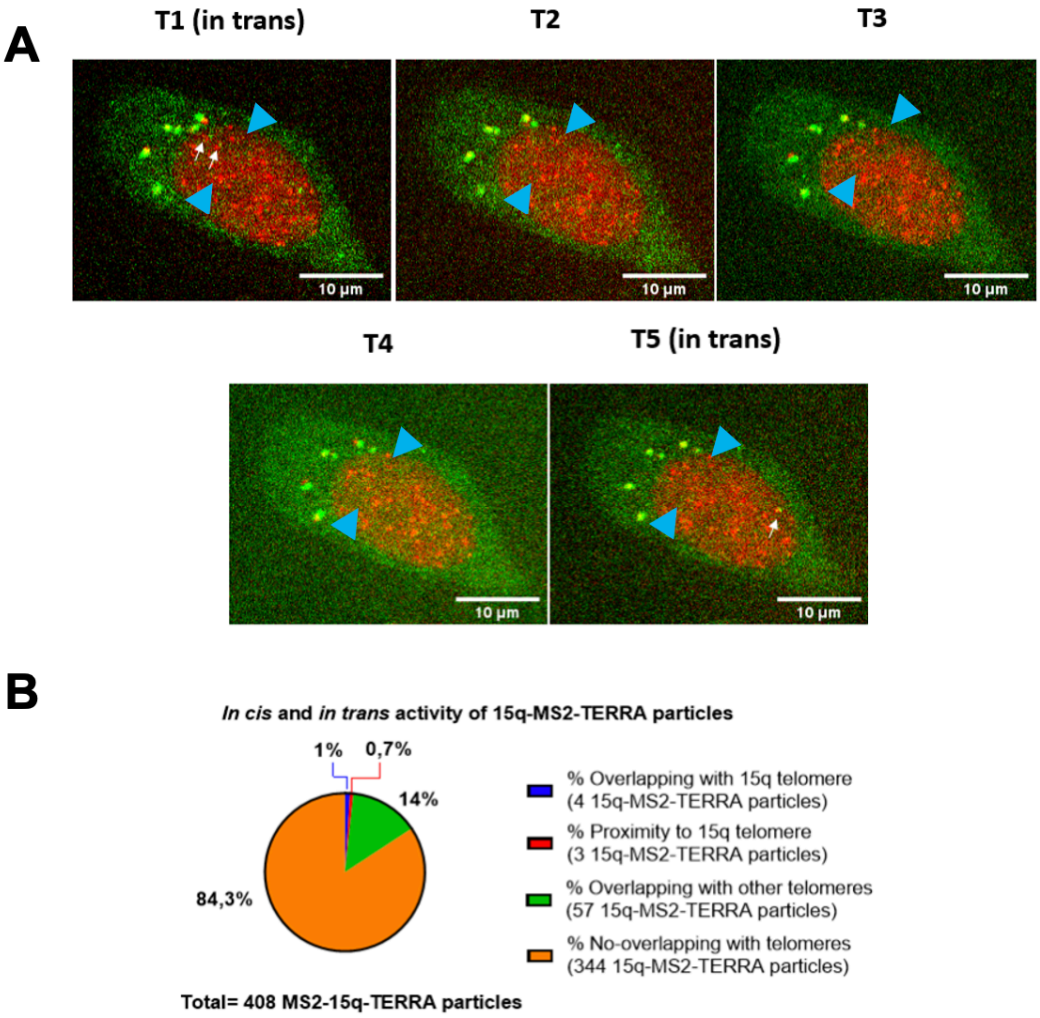

Figure 34: Telomere 15q-derived TERRA-MS2 does not predominantly localize to its telomere of origin. A) Time-lapse of 15q-derived TERRA-MS2-GFP molecules, TRF1-mCherry signal and dCas9-BFP co-transfected with 15q-specific sgRNA in AGS MS2-15q-TERRA clones. Examples of *in trans* localization of 15q-TERRA-MS2-GFP particles are shown in T1 and T5 frames, indicated by the white arrows pointing at TERRA-MS2_GFP foci colocalizing with TRF1-mCherry foci. Light blue arrows point to subtelomeres 15q. B) Quantification of 15q-TERRA-MS2-GFP particles localizing *in cis* or *in trans*. The pie-chart reports: the percentages of TERRA 15q-derived foci overlapping with or in proximity to the telomere 15q signal (*in cis*), the percentages of 15q-TERRA-MS2-GFP transcripts co-localizing or in proximity of other telomeres (*in trans*) and the percentage of TERRA-MS2 particles not colocalizing with telomeres. Scale bar: 10 µm. Live-cell imaging, images acquisition and analysis was performed by Elena Goretti.

Notably, an *in trans* localization of TERRA has been recently reported by the Lingner's lab[168]. In this study, expression of TERRA from extrachromosomal sites was achieved upon integration of a TERRA-expressing plasmid, using a CMV promoter, in HeLa cells. By these experiments, it was reported that TERRA molecules, even if expressed

from an extratelomeric site, relocate to chromosome ends, supporting an *in trans* localization of TERRA at telomeres.

In summary, from the results discussed in this thesis project, I propose a model in which TERRA acts as a negative regulator of telomere elongation by telomerase. In a steady state condition, TERRA localizes at telomeres and in the nucleoplasm, bound or unbound to telomerase. Telomeric TERRA is preferentially associated with the longer chromosome ends where it can act as a competitor of the single stranded telomeric DNA for the binding of the template region of h*TR* (Figure 35A and 35B). This mechanism could participate in tuning telomerase activity towards the shortest telomeres in the cell. Indeed, TERRA transcripts are displaced from short telomeres preventing interference with telomerase activity (Figure 35C). To confirm this model, we are currently leveraging an HeLa cell clone, in which TERRA expression can be repressed at a subset of telomeres through a TALE system (the cells were kindly provided by Dr. Claus Maria Azzalin laboratory). Using these cells, I will test whether telomere re-elongation is influenced by the repression of TERRA transcription.

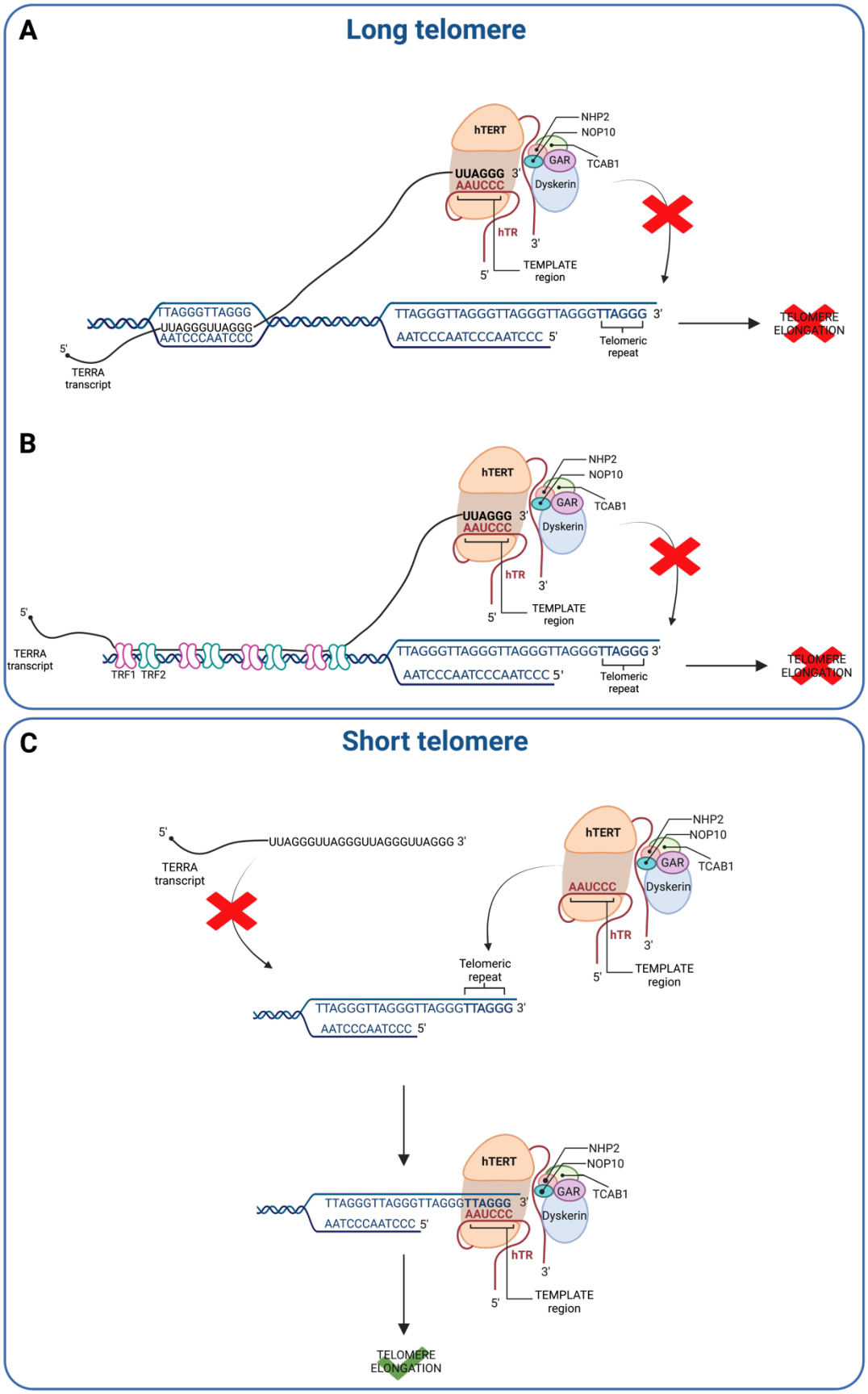

Figure 35: Proposed model for the regulation of telomerase activity by telomeric TERRA transcripts. A-B) At long telomeres TERRA forms an R-loop structures by base pairing with the

telomeric DNA C-rich strand (A) and/or binds telomere-binding proteins such as TRF1 and TRF2 (B). Recruitment and/or retainment of TERRA transcripts to these chromosome ends results in telomerase inhibition, competing with the single strand DNA 3' overhang for the base pairing of h*TR* template sequence, suppressing telomere elongation. C) TERRA transcripts are not recruited, or they are displaced from short chromosome ends. At these telomeres the base pairing of the template region of h*TR* to the telomeric 3' overhang is not inhibited by the presence of TERRA molecules and telomere elongation can proceed. Schematic created with Biorender.com

Importantly, in addition to the proposed telomeric function of TERRA in regulating telomerase activity, the results here presented suggest that TERRA transcripts may influence telomerase clustering. This function of TERRA may be exerted in the nucleoplasm, where most TERRA-h*TR* particles are detected, regulating telomerase holoenzyme formation or telomerase trafficking. Additional investigations on the subnuclear localization of TERRA transcripts and TERRA-h*TR* particles will help gain insights into this mechanism.

In this regard, we did not detect TERRA at Cajal bodies (data not shown), suggesting that TERRA transcripts are not involved in the regulation of h*TR* maturation steps that occur at these subnuclear compartments.

Since several functions have been proposed for TERRA at chromosome ends[118], we anticipate that not all TERRA molecules localizing at telomeres are involved in telomerase regulation. How the different roles of TERRA at telomeres are regulated remains to be defined. We expect that TERRA molecules would need to be recruited at the very end of the telomere to be able to regulate telomerase, as only in this position they would be able to compete with the single-stranded telomeric DNA for h*TR* binding. Future studies also involving mutant telomeric proteins binding TERRA will help understanding how the control of the telomeric localization of TERRA transcripts is achieved.

REFERENCES

1 O'Sullivan R., Karlseder J. Telomeres: protecting chromosomes against genome instability. Nat Rev Mol Cell Biol. 2010 11, 171–181. doi: 10.1038/nrm2848

2 Palm W., de Lange T. How shelterin protects mammalian telomeres. Annu Rev Genet. 2008 42:301–34. doi: 10.1146/annurev.genet.41.110306.130350

3 Blackburn E. H. Telomeres: No End in Sight. Cell. 1994 vol. 77. doi: 10.1016/0092-8674(94)90046-9

4 McElligott R., Wellinger R.J. The terminal DNA structure of mammalian chromosomes. The EMBO Journal. 1997 16: 3705-3714. doi: 10.1093/emboj/16.12.3705

5 Lejnine S., Makarov V.L., Langmore J.P. Conserved nucleoprotein structure at the ends of vertebrate and invertebrate chromosomes. Proc Natl Acad Sci U S A. 1995 Mar 14;92(6):2393-7. doi: 10.1073/pnas.92.6.2393.

6 Jain D., Cooper J. P. Telomeric strategies: Means to an end. Annual Review of Genetics. 2010 vol. 44 243–269. doi: 10.1146/annurev-genet-102108-134841

7 Wright W. E., Tesmer V. M., Huffman K. E., Levene S. D. and Shay J. W. Normal human chromosomes have long G-rich telomeric overhangs at one end. Genes Dev. 1997 Nov 1;11(21):2801-9. doi: 10.1101/gad.11.21.2801

8 Griffith J.D., Comeau L., Rosenfield S., Stansel R.M., Bianchi A., Moss H., de Lange T. Mammalian telomeres end in a large duplex loop. Cell. 1999 May 14;97(4):503-14. doi: 10.1016/s0092-8674(00)80760-6.

9 de Lange T. T-loops and the origin of telomeres. Nat Rev Mol Cell Biol 2004 5, 323–329. doi: 10.1038/nrm1359

10 Bryan T.M. G-Quadruplexes at Telomeres: Friend or Foe? Molecules 2020, 25, 3686. doi: 10.3390/molecules25163686

11 Wang Y., Patel DJ. Guanine residues in d(T2AG3) and d(T2G4) form parallel-stranded potassium cation stabilized G-quadruplexes with anti glycosidic torsion angles in solution. Biochemistry. 1992 Sep 8;31(35):8112-9. doi: 10.1021/bi00150a002.

12 Bochman M.L., Paeschke K., Zakian V.A. DNA secondary structures: stability and function of G-quadruplex structures. Nat Rev Genet. 2012 Nov;13(11):770-80. doi: 10.1038/nrg3296.

13 Paeschke K., Simonsson T., Postberg J., Rhodes D., Lipps H.J. Telomere end-binding proteins control the formation of G-quadruplex DNA structures in vivo. Nat Struct Mol Biol. 2005 Oct;12(10):847-54. doi: 10.1038/nsmb982.

14 Doksani Y., Wu J.Y., de Lange T., Zhuang X. Super-resolution fluorescence imaging of telomeres reveals TRF2-dependent T-loop formation. Cell. 2013 Oct 10;155(2):345-356. doi: 10.1016/j.cell.2013.09.048.

15 Srinivas N., Rachakonda S., Kumar R. Telomeres and Telomere Length: A General Overview. Cancers (Basel). 2020 Feb 28;12(3):558. doi: 10.3390/cancers12030558.

16 de Lange T. Shelterin: the protein complex that shapes and safeguards human telomeres. Genes Dev. 2005 Sep 15;19(18):2100-10. doi: 10.1101/gad.1346005.

17 de Lange T. Shelterin-Mediated Telomere Protection. Annu Rev Genet. 2018 Nov 23;52:223-247. doi: 10.1146/annurev-genet-032918-021921.

18 Court R., Chapman L., Fairall L., Rhodes D. How the human telomeric proteins TRF1 and TRF2 recognize telomeric DNA: a view from high-resolution crystal structures. EMBO Rep. 2005 Jan;6(1):39-45. doi: 10.1038/sj.embor.7400314. Erratum in: EMBO Rep. 2005 Feb;6(2):191

19 Broccoli D., Smogorzewska A., Chong L., de Lange T. Human telomeres contain two distinct Myb-related proteins, TRF1 and TRF2. Nat Genet. 1997 Oct;17(2):231-5. doi: 10.1038/ng1097-231.

20 Baumann P., Cech TR. Pot1, the putative telomere end-binding protein in fission yeast and humans. Science. 2001 May 11;292(5519):1171-5. doi: 10.1126/science.1060036. Erratum in: Science 2001 Jul 13;293(5528):214.

21 Ye J.Z., Hockemeyer D., Krutchinsky A.N., Loayza D., Hooper S.M., Chait B.T., de Lange T. POT1-interacting protein PIP1: a telomere length regulator that recruits POT1 to the TIN2/TRF1 complex. Genes Dev. 2004 Jul 15;18(14):1649-54. doi: 10.1101/gad.1215404.

22 Li B., Oestreich S., de Lange T. Identification of human RAP1: implications for telomere evolution. Cell. 2000 May 26;101(5):471-83. doi: 10.1016/s0092-8674(00)80858-2.

23 Janoušková E., Nečasová I., Pavloušková J., Zimmermann M., Hluchý M., Marini V., Nováková M., Hofr C. Human RAP1 modulates TRF2 attraction to telomeric DNA. Nucleic Acids Res. 2015 Mar 11;43(5):2691-700. doi: 10.1093/nar/gkv097.

24 Smith E.M., Pendlebury D.F., Nandakumar J. Structural biology of telomeres and telomerase. Cell Mol Life Sci. 2020 Jan;77(1):61-79. doi: 10.1007/s00018-019-03369-x.

25 Liu, D., O'Connor, M. S., Qin, J. & Songyang, Z. Telosome, a mammalian telomere-associated complex formed by multiple telomeric proteins. Journal of Biological Chemistry 279, 51338–51342 (2004).

26 Doksani Y., de Lange T. The role of double-strand break repair pathways at functional and dysfunctional telomeres. Cold Spring Harb Perspect Biol. 2014 Sep 16;6(12):a016576. doi: 10.1101/cshperspect.a016576.

27 Guo X., Deng Y., Lin Y., Cosme-Blanco W., Chan S., He H., Yuan G., Brown E.J., Chang S. Dysfunctional telomeres activate an ATM-ATR-dependent DNA damage response to suppress tumorigenesis. EMBO J. 2007 Nov 14;26(22):4709-19. doi: 10.1038/sj.emboj.7601893.

28 Flynn R.L., Centore R.C., O'Sullivan R.J., Rai R., Tse A., Songyang Z., Chang S., Karlseder J., Zou L. TERRA and hnRNPA1 orchestrate an RPA-to-POT1 switch on telomeric single-stranded DNA. Nature. 2011 Mar 24;471(7339):532-6. doi: 10.1038/nature09772.

29 de Lange T. How telomeres solve the end-protection problem. Science. 2009 Nov 13;326(5955):948-52. doi: 10.1126/science.1170633.

30 Schmutz I., Timashev L., Xie W., Patel D.J., de Lange T. TRF2 binds branched DNA to safeguard telomere integrity. Nat Struct Mol Biol. 2017 Sep;24(9):734-742. doi: 10.1038/nsmb.3451.

31 Hug N., Lingner J. Telomere length homeostasis. Chromosoma. 2006 Dec;115(6):413-25. doi: 10.1007/s00412-006-0067-3.

32 Verdun R.E., Karlseder J. Replication and protection of telomeres. Nature. 2007 Jun 21;447(7147):924-31. doi: 10.1038/nature05976.

33 Chow T.T., Zhao Y., Mak S.S., Shay J.W., Wright W.E. Early and late steps in telomere overhang processing in normal human cells: the position of the final RNA primer drives telomere shortening. Genes Dev. 2012 Jun 1;26(11):1167-78. doi: 10.1101/gad.187211.112

34 Shay J.W., Wright W.E. Senescence and immortalization: role of telomeres and telomerase. Carcinogenesis. 2005 May;26(5):867-74. doi: 10.1093/carcin/bgh296.

35 d'Adda di Fagagna F., Reaper P.M., Clay-Farrace L., Fiegler H., Carr P., Von Zglinicki T., Saretzki G., Carter N.P., Jackson S.P. A DNA damage checkpoint response in telomere-initiated senescence. Nature. 2003 Nov 13;426(6963):194-8. doi: 10.1038/nature02118.

36 Bodnar A.G., Ouellette M., Frolkis M., Holt S.E., Chiu C.P., Morin G.B., Harley C.B., Shay J.W., Lichtsteiner S., Wright W.E. Extension of life-span by introduction of telomerase into normal human cells. Science. 1998 Jan 16;279(5349):349-52. doi: 10.1126/science.279.5349.349.

37 Blasco M.A. Telomeres and human disease: ageing, cancer and beyond. Nat Rev Genet. 2005 Aug;6(8):611-22. doi: 10.1038/nrg1656.

38 Schmidt J.C., Cech T.R. Human telomerase: biogenesis, trafficking, recruitment, and activation. Genes Dev. 2015 Jun 1;29(11):1095-105. doi: 10.1101/gad.263863.115.

39 MacNeil D.E., Bensoussan H.J., Autexier C. Telomerase Regulation from Beginning to the End. Genes (Basel). 2016 Sep 14;7(9):64. doi: 10.3390/genes7090064.

40 Xi L., Cech T.R. Inventory of telomerase components in human cells reveals multiple subpopulations of hTR and hTERT. Nucleic Acids Res. 2014 Jul;42(13):8565-77. doi: 10.1093/nar/gku560.

41 Dunham M.A., Neumann A.A., Fasching C.L., Reddel R.R. Telomere maintenance by recombination in human cells. Nat Genet. 2000 Dec;26(4):447-50. doi: 10.1038/82586.

42 Greider C.W., Blackburn E.H. A telomeric sequence in the RNA of Tetrahymena telomerase required for telomere repeat synthesis. Nature. 1989 Jan 26;337(6205):331-7. doi: 10.1038/337331a0.

43 Wang Y., Sušac L., Feigon J. Structural Biology of Telomerase. Cold Spring Harb Perspect Biol. 2019 Dec 2;11(12):a032383. doi: 10.1101/cshperspect.a032383.

44 Shay J.W., Wright W.E. Telomeres and telomerase in normal and cancer stem cells. FEBS Lett. 2010 Sep 10;584(17):3819-25. doi: 10.1016/j.febslet.2010.05.026.

45 Townsley D.M., Dumitriu B., Young N.S. Bone marrow failure and the telomeropathies. Blood. 2014 Oct 30;124(18):2775-83. doi: 10.1182/blood-2014-05-526285.

46 Sarek G., Marzec P., Margalef P., Boulton S.J. Molecular basis of telomere dysfunction in human genetic diseases. Nat Struct Mol Biol. 2015 Nov;22(11):867-74. doi: 10.1038/nsmb.3093. Erratum in: Nat Struct Mol Biol. 2017 Jun 6;24(6):553.

47 Shay J.W. Role of Telomeres and Telomerase in Aging and Cancer. Cancer Discov. 2016 Jun;6(6):584-93. doi: 10.1158/2159-8290.CD-16-0062.

48 Marrone A., Walne A., Dokal I. Dyskeratosis congenita: telomerase, telomeres and anticipation. Curr Opin Genet Dev. 2005 Jun;15(3):249-57. doi: 10.1016/j.gde.2005.04.004.

49 Fujii H., Shao L., Colmegna I., Goronzy J.J., Weyand C.M. Telomerase insufficiency in rheumatoid arthritis. Proc Natl Acad Sci U S A. 2009 Mar 17;106(11):4360-5. doi: 10.1073/pnas.0811332106.

50 Artandi S.E., DePinho R.A. Telomeres and telomerase in cancer. Carcinogenesis. 2010 Jan;31(1):9-18. doi: 10.1093/carcin/bgp268.

51 Armanios M., Blackburn E.H. The telomere syndromes. Nat Rev Genet. 2012 Oct;13(10):693-704. doi: 10.1038/nrg3246. Epub 2012 Sep 11. Erratum in: Nat Rev Genet. 2013 Mar;14(3):235.

52 Bernardes de Jesus B., Blasco M.A. Telomerase at the intersection of cancer and aging. Trends Genet. 2013 Sep;29(9):513-20. doi: 10.1016/j.tig.2013.06.007.

53 Blackburn E.H., Greider C.W., Szostak J.W. Telomeres and telomerase: the path from maize, Tetrahymena and yeast to human cancer and aging. Nat Med. 2006 Oct;12(10):1133-8. doi: 10.1038/nm1006-1133.

54 Blackburn E.H., Collins K. Telomerase: an RNP enzyme synthesizes DNA. Cold Spring Harb Perspect Biol. 2011 May 1;3(5):a003558. doi: 10.1101/cshperspect.a003558.

55 Nguyen T.H.D, Tam J., Wu R.A., Greber B.J., Toso D., Nogales E., Collins K. Cryo-EM structure of substrate-bound human telomerase holoenzyme. Nature. 2018 May;557(7704):190-195. doi: 10.1038/s41586-018-0062-x.

56 Gomez D.E., Armando R.G., Farina H.G., Menna P.L., Cerrudo C.S., Ghiringhelli P.D., Alonso D.F. Telomere structure and telomerase in health and disease (review). Int J Oncol. 2012 Nov;41(5):1561-9. doi: 10.3892/ijo.2012.1611.

57 Ghanim G.E., Fountain A.J., van Roon A.M., Rangan R., Das R., Collins K., Nguyen T.H.D. Structure of human telomerase holoenzyme with bound telomeric DNA. Nature. 2021 May;593(7859):449-453. doi: 10.1038/s41586-021-03415-4.

58 Zhang Q., Kim N.K., Feigon J. Architecture of human telomerase RNA. Proc Natl Acad Sci U S A. 2011 Dec 20;108(51):20325-32. doi: 10.1073/pnas.1100279108.

59 Raghunandan M., Decottignies A. The multifaceted hTR telomerase RNA from a structural perspective: Distinct domains of hTR differentially interact with protein partners to orchestrate its telomerase-independent functions. Bioessays. 2021 Oct;43(10):e2100099. doi: 10.1002/bies.202100099.

60 Roake C.M., Artandi S.E. Regulation of human telomerase in homeostasis and disease. Nat Rev Mol Cell Biol. 2020 Jul;21(7):384-397. doi: 10.1038/s41580-020-0234-z.

61 Feng J., Funk W.D., Wang S.S., Weinrich S.L., Avilion A.A., Chiu C.P., Adams R.R., Chang E., Allsopp R.C., Yu J., et al. The RNA component of human telomerase. Science. 1995 Sep 1;269(5228):1236-41. doi: 10.1126/science.7544491

62 Blasco M.A., Funk W., Villeponteau B., Greider C.W. Functional characterization and developmental regulation of mouse telomerase RNA. Science. 1995 Sep 1;269(5228):1267-70. doi: 10.1126/science.7544492.

63 Tseng C.K., Wang H.F., Schroeder M.R., Baumann P. The H/ACA complex disrupts triplex in hTR precursor to permit processing by RRP6 and PARN. Nat Commun. 2018 Dec 21;9(1):5430. doi: 10.1038/s41467-018-07822-6.

64 Noël J.F., Larose S., Abou Elela S., Wellinger R.J. Budding yeast telomerase RNA transcription termination is dictated by the Nrd1/Nab3 non-coding RNA termination pathway. Nucleic Acids Res. 2012 Jul;40(12):5625-36. doi: 10.1093/nar/gks200.

65 Roake C.M., Chen L., Chakravarthy A.L., Ferrell J.E. Jr, Raffa G.D.., Artandi SE. Disruption of Telomerase RNA Maturation Kinetics Precipitates Disease. Mol Cell. 2019 May 16;74(4):688-700.e3. doi: 10.1016/j.molcel.2019.02.033.

66 Tseng C.K., Wang H.F., Burns A.M., Schroeder M.R., Gaspari M., Baumann P. Human Telomerase RNA Processing and Quality Control. Cell Rep. 2015 Dec 15;13(10):2232-43. doi: 10.1016/j.celrep.2015.10.075.

67 Shukla S., Schmidt J.C., Goldfarb K.C., Cech T.R., Parker R. Inhibition of telomerase RNA decay rescues telomerase deficiency caused by dyskerin or PARN defects. Nat Struct Mol Biol. 2016 Apr;23(4):286-92. doi: 10.1038/nsmb.3184.

68 Chen L., Roake C.M., Galati A., Bavasso F.., Micheli E, Saggio I., Schoeftner S., Cacchione S.., Gatti M, Artandi S.E., Raffa GD. Loss of Human TGS1 Hypermethylase Promotes Increased Telomerase RNA and Telomere Elongation. Cell Rep. 2020 Feb 4;30(5):1358-1372.e5. doi: 10.1016/j.celrep.2020.01.004.

69 Schnapp G., Rodi H.P., Rettig W.J., Schnapp A., Damm K. One-step affinity purification protocol for human telomerase. Nucleic Acids Res. 1998 Jul 1;26(13):3311-3. doi: 10.1093/nar/26.13.3311.

70 Xin H., Liu D., Wan M., Safari A., Kim H., Sun W., O'Connor M.S., Songyang Z. TPP1 is a homologue of ciliate TEBP-beta and interacts with POT1 to recruit telomerase. Nature. 2007 Feb 1;445(7127):559-62. doi: 10.1038/nature05469.

71 Egan E.D., Collins K. An enhanced H/ACA RNP assembly mechanism for human telomerase RNA. Mol Cell Biol. 2012 Jul;32(13):2428-39. doi: 10.1128/MCB.00286-12.

72 Egan E.D., Collins K. Biogenesis of telomerase ribonucleoproteins. RNA. 2012 Oct;18(10):1747-59. doi: 10.1261/rna.034629.112.

73 Darzacq X., Kittur N., Roy S., Shav-Tal Y., Singer R.H., Meier U.T. Stepwise RNP assembly at the site of H/ACA RNA transcription in human cells. J Cell Biol. 2006 Apr 24;173(2):207-18. doi: 10.1083/jcb.200601105.

74 Wang C., Meier U.T. Architecture and assembly of mammalian H/ACA small nucleolar and telomerase ribonucleoproteins. EMBO J. 2004 Apr 21;23(8):1857-67. doi: 10.1038/sj.emboj.7600181.

75 Hoareau-Aveilla C., Bonoli M., Caizergues-Ferrer M., Henry Y. hNaf1 is required for accumulation of human box H/ACA snoRNPs, scaRNPs, and telomerase. RNA. 2006 May;12(5):832-40. doi: 10.1261/rna.2344106.

76 Grozdanov P.N., Roy S., Kittur N., Meier U.T. SHQ1 is required prior to NAF1 for assembly of H/ACA small nucleolar and telomerase RNPs. RNA. 2009 Jun;15(6):1188-97. doi: 10.1261/rna.1532109.

77 Venteicher A.S., Meng Z., Mason P.J., Veenstra T.D., Artandi S.E. Identification of ATPases pontin and reptin as telomerase components essential for holoenzyme assembly. Cell. 2008 Mar 21;132(6):945-57. doi: 10.1016/j.cell.2008.01.019.

78 Holt S.E., Aisner D.L., Baur J., Tesmer V.M., Dy M., Ouellette M., Trager J.B., Morin G.B., Toft D.O., Shay J.W., Wright W.E., White M.A. Functional requirement of p23 and Hsp90 in telomerase complexes. Genes Dev. 1999 Apr 1;13(7):817-26. doi: 10.1101/gad.13.7.817.

79 Toogun O.A., Dezwaan D.C., Freeman B.C. The hsp90 molecular chaperone modulates multiple telomerase activities. Mol Cell Biol. 2008 Jan;28(1):457-67. doi: 10.1128/MCB.01417-07.

80 Keppler B.R., Grady A.T., Jarstfer M.B. The biochemical role of the heat shock protein 90 chaperone complex in establishing human telomerase activity. J Biol Chem. 2006 Jul 21;281(29):19840-8. doi: 10.1074/jbc.M511067200.

81 Freund A., Zhong F.L., Venteicher A.S., Meng Z., Veenstra T.D., Frydman J., Artandi S.E. Proteostatic control of telomerase function through TRiC-mediated folding of TCAB1. Cell. 2014 Dec 4;159(6):1389-403. doi: 10.1016/j.cell.2014.10.059.

82 Laprade H., Querido E., Smith M.J., Guérit D., Crimmins H., Conomos D., Pourret E., Chartrand P., Sfeir A. Single-Molecule Imaging of Telomerase RNA Reveals a Recruitment-Retention Model for Telomere Elongation. Mol Cell. 2020 Jul 2;79(1):115-126.e6. doi: 10.1016/j.molcel.2020.05.005.

83 Schmidt J.C., Zaug A.J., Kufer R., Cech T.R. Dynamics of human telomerase recruitment depend on template-telomere base pairing. Mol Biol Cell. 2018 Apr 1;29(7):869-880. doi: 10.1091/mbc.E17-11-0637.

84 Zhao Y., Sfeir A.J., Zou Y., Buseman C.M., Chow T.T., Shay J.W., Wright W.E. Telomere extension occurs at most chromosome ends and is uncoupled from fill-in in human cancer cells. Cell. 2009 Aug 7;138(3):463-75. doi: 10.1016/j.cell.2009.05.026.

85 Wu R.A., Tam J., Collins K. DNA-binding determinants and cellular thresholds for human telomerase repeat addition processivity. EMBO J. 2017 Jul 3;36(13):1908-1927. doi: 10.15252/embj.201796887.

86 Mozdy A.D., Cech T.R. Low abundance of telomerase in yeast: implications for telomerase haploinsufficiency. RNA. 2006 Sep;12(9):1721-37. doi: 10.1261/rna.134706.

87 Xi L., Cech T.R. Inventory of telomerase components in human cells reveals multiple subpopulations of hTR and hTERT. Nucleic Acids Res. 2014 Jul;42(13):8565-77. doi: 10.1093/nar/gku560.

88 Chong L., van Steensel B., Broccoli D., Erdjument-Bromage H., Hanish J., Tempst P., de Lange T. A human telomeric protein. Science. 1995 Dec 8;270(5242):1663-7. doi: 10.1126/science.270.5242.1663.

89 Wang F., Podell E.R., Zaug A.J., Yang Y., Baciu P., Cech T.R., Lei M. The POT1-TPP1 telomere complex is a telomerase processivity factor. Nature. 2007 Feb 1;445(7127):506-10. doi: 10.1038/nature05454.

90 Abreu E., Aritonovska E., Reichenbach P., Cristofari G., Culp B., Terns R.M., Lingner J., Terns M.P. TIN2-tethered TPP1 recruits human telomerase to telomeres in vivo. Mol Cell Biol. 2010 Jun;30(12):2971-82. doi: 10.1128/MCB.00240-10.

91 Nandakumar J., Cech T.R. DNA-induced dimerization of the single-stranded DNA binding telomeric protein Pot1 from Schizosaccharomyces pombe. Nucleic Acids Res. 2012 Jan;40(1):235-44. doi: 10.1093/nar/gkr721.

92 Sexton A.N., Youmans D.T., Collins K. Specificity requirements for human telomere protein interaction with telomerase holoenzyme. J Biol Chem. 2012 Oct 5;287(41):34455-64. doi: 10.1074/jbc.M112.394767.

93 Zhong F.L., Batista L.F., Freund A., Pech M.F., Venteicher A.S., Artandi S.E. TPP1 OB-fold domain controls telomere maintenance by recruiting telomerase to chromosome ends. Cell. 2012 Aug 3;150(3):481-94. doi: 10.1016/j.cell.2012.07.012.

94 Schmidt J.C., Dalby A.B., Cech T.R. Identification of human TERT elements necessary for telomerase recruitment to telomeres. Elife. 2014 Oct 1;3:e03563. doi: 10.7554/eLife.03563.

95 Kocak H., Ballew B.J., Bisht K., Eggebeen R., Hicks B.D., Suman S., O'Neil A., Giri N.; NCI DCEG Cancer Genomics Research Laboratory; NCI DCEG Cancer Sequencing Working Group; Maillard I., Alter B.P., Keegan C.E., Nandakumar J., Savage S.A. Hoyeraal-Hreidarsson syndrome caused by a germline mutation in the TEL patch of the telomere protein TPP1. Genes Dev. 2014 Oct 1;28(19):2090-102. doi: 10.1101/gad.248567.114.

96 Schmidt J.C., Zaug A.J., Cech T.R. Live Cell Imaging Reveals the Dynamics of Telomerase Recruitment to Telomeres. Cell. 2016 Aug 25;166(5):1188-1197.e9. doi: 10.1016/j.cell.2016.07.033.

97 Schmidt J.C., Zaug A.J., Kufer R., Cech T.R. Dynamics of human telomerase recruitment depend on template-telomere base pairing. Mol Biol Cell. 2018 Apr 1;29(7):869-880. doi: 10.1091/mbc.E17-11-0637.

98 Jády B.E., Richard P., Bertrand E., Kiss T. Cell cycle-dependent recruitment of telomerase RNA and Cajal bodies to human telomeres. Mol Biol Cell. 2006 Feb;17(2):944-54. doi: 10.1091/mbc.e05-09-0904.

99 Miyake Y., Nakamura M., Nabetani A., Shimamura S., Tamura M., Yonehara S., Saito M., Ishikawa F. RPA-like mammalian Ctc1-Stn1-Ten1 complex binds to single-stranded DNA and protects telomeres independently of the Pot1 pathway. Mol Cell. 2009 Oct 23;36(2):193-206. doi: 10.1016/j.molcel.2009.08.009.

100 Surovtseva Y.V., Churikov D., Boltz K.A., Song X., Lamb J.C., Warrington R., Leehy K., Heacock M., Price C.M., Shippen D.E. Conserved telomere maintenance component 1 interacts with STN1 and maintains chromosome ends in higher eukaryotes. Mol Cell. 2009 Oct 23;36(2):207-18. doi: 10.1016/j.molcel.2009.09.017.

101 Casteel D.E., Zhuang S., Zeng Y., Perrino F.W., Boss G.R., Goulian M., Pilz R.B. A DNA polymerase- α·primase cofactor with homology to replication protein A-32

regulates DNA replication in mammalian cells. J Biol Chem. 2009 Feb 27;284(9):5807-18. doi: 10.1074/jbc.M807593200.

102 Chen L.Y., Redon S., Lingner J. The human CST complex is a terminator of telomerase activity. Nature. 2012 Aug 23;488(7412):540-4. doi: 10.1038/nature11269.

103 Tardat M., Déjardin J. Telomere chromatin establishment and its maintenance during mammalian development. Chromosoma. 2018 Mar;127(1):3-18. doi: 10.1007/s00412-017-0656-3.

104 Blasco M.A. The epigenetic regulation of mammalian telomeres. Nat Rev Genet. 2007 Apr;8(4):299-309. doi: 10.1038/nrg2047.

105 Benetti R., Gonzalo S., Jaco I., Schotta G., Klatt P., Jenuwein T., Blasco M.A. Suv4-20h deficiency results in telomere elongation and derepression of telomere recombination. J Cell Biol. 2007 Sep 10;178(6):925-36. doi: 10.1083/jcb.200703081.

106 Baur J.A., Zou Y., Shay J.W., Wright W.E. Telomere position effect in human cells. Science. 2001 Jun 15;292(5524):2075-7. doi: 10.1126/science.1062329.

107 Rudenko G., Van der Ploeg L.H. Transcription of telomere repeats in protozoa. EMBO J. 1989 Sep;8(9):2633-8. doi: 10.1002/j.1460-2075.1989.tb08403.x.

108 Azzalin C.M., Reichenbach P., Khoriauli L., Giulotto E., Lingner J. Telomeric repeat containing RNA and RNA surveillance factors at mammalian chromosome ends. Science. 2007 Nov 2;318(5851):798-801. doi: 10.1126/science.1147182.

109 Schoeftner S., Blasco M.A. Developmentally regulated transcription of mammalian telomeres by DNA-dependent RNA polymerase II. Nat Cell Biol. 2008 Feb;10(2):228-36.

110 Cusanelli E., Chartrand P. Telomeric repeat-containing RNA TERRA: a noncoding RNA connecting telomere biology to genome integrity. Front Genet. 2015 Apr 14;6:143. doi: 10.3389/fgene.2015.00143.

111 Luke B., Panza A., Redon S., Iglesias N., Li Z., Lingner J. The Rat1p 5' to 3' exonuclease degrades telomeric repeat-containing RNA and promotes telomere elongation in Saccharomyces cerevisiae. Mol Cell. 2008 Nov 21;32(4):465-77. doi: 10.1016/j.molcel.2008.10.019.

112 Vrbsky J., Akimcheva S., Watson J.M., Turner T.L., Daxinger L., Vyskot B., Aufsatz W., Riha K. siRNA-mediated methylation of Arabidopsis telomeres. PLoS Genet. 2010 Jun 10;6(6):e1000986. doi: 10.1371/journal.pgen.1000986.

113 Porro A., Feuerhahn S., Reichenbach P., Lingner J.. Molecular dissection of telomeric repeat-containing RNA biogenesis unveils the presence of distinct and multiple regulatory pathways. Mol Cell Biol. 2010 Oct;30(20):4808-17. doi: 10.1128/MCB.00460-10.

114 Nergadze S.G., Farnung B.O., Wischnewski H., Khoriauli L., Vitelli V., Chawla R., Giulotto E., Azzalin C.M. CpG-island promoters drive transcription of human telomeres. RNA. 2009 Dec;15(12):2186-94. doi: 10.1261/rna.1748309.

115 Porro A., Feuerhahn S., Delafontaine J., Riethman H., Rougemont J., Lingner J. Functional characterization of the TERRA transcriptome at damaged telomeres. Nat Commun. 2014 Oct 31;5:5379. doi: 10.1038/ncomms6379.

116 Azzalin C.M., Lingner J. Telomere functions grounding on TERRA firma. Trends Cell Biol. 2015 Jan;25(1):29-36. doi: 10.1016/j.tcb.2014.08.007.

117 Azzalin C.M., Lingner J. Telomeres: the silence is broken. Cell Cycle. 2008 May 1;7(9):1161-5. doi: 10.4161/cc.7.9.5836.

118 Bettin N., Oss Pegorar C., Cusanelli E. The Emerging Roles of TERRA in Telomere Maintenance and Genome Stability. Cells. 2019 Mar 15;8(3):246. doi: 10.3390/cells8030246.

119 Porro A., Feuerhahn S., Delafontaine J., Riethman H., Rougemont J., Lingner J. Functional characterization of the TERRA transcriptome at damaged telomeres. Nat Commun. 2014 Oct 31;5:5379. doi: 10.1038/ncomms6379.

120 Deng Z., Wang Z., Stong N., Plasschaert R., Moczan A., Chen H.S., Hu S., Wikramasinghe P., Davuluri R.V., Bartolomei M.S., Riethman H., Lieberman P.M. A role for CTCF and cohesin in subtelomere chromatin organization, TERRA transcription, and telomere end protection. EMBO J. 2012 Nov 5;31(21):4165-78. doi: 10.1038/emboj.2012.266.

121 Arnoult N., Van Beneden A., Decottignies A. Telomere length regulates TERRA levels through increased trimethylation of telomeric H3K9 and HP1α. Nat Struct Mol

Biol. 2012 Sep;19(9):948-56. doi: 10.1038/nsmb.2364. Erratum in: Nat Struct Mol Biol. 2013 Feb;20(2):244.

122 Marion R.M., Strati K., Li H., Tejera A., Schoeftner S., Ortega S., Serrano M., Blasco M.A. Telomeres acquire embryonic stem cell characteristics in induced pluripotent stem cells. Cell Stem Cell. 2009 Feb 6;4(2):141-54. doi: 10.1016/j.stem.2008.12.010.

123 Caslini C., Connelly J.A., Serna A., Broccoli D., Hess J.L. MLL associates with telomeres and regulates telomeric repeat-containing RNA transcription. Mol Cell Biol. 2009 Aug;29(16):4519-26. doi: 10.1128/MCB.00195-09. Erratum in: Mol Cell Biol. 2021 Jan 25;41(2):

124 Tutton S., Azzam G.A., Stong N., Vladimirova O., Wiedmer A., Monteith J.A., Beishline K., Wang Z., Deng Z., Riethman H., McMahon S.B., Murphy M., Lieberman P.M. Subtelomeric p53 binding prevents accumulation of DNA damage at human telomeres. EMBO J. 2016 Jan 18;35(2):193-207. doi: 10.15252/embj.201490880.

125 Gonzalez-Vasconcellos I., Schneider R., Anastasov N., Alonso-Rodriguez S., Sanli-Bonazzi B., Fernández J.L., Atkinson M.J. The Rb1 tumour suppressor gene modifies telomeric chromatin architecture by regulating TERRA expression. Sci Rep. 2017 Feb 7;7:42056. doi: 10.1038/srep42056.

126 Koskas S., Decottignies A., Dufour S., Pezet M., Verdel A., Vourc'h C., Faure V. Heat shock factor 1 promotes TERRA transcription and telomere protection upon heat stress. Nucleic Acids Res. 2017 Jun 20;45(11):6321-6333. doi: 10.1093/nar/gkx208.

127 Graf M., Bonetti D., Lockhart A., Serhal K., Kellner V., Maicher A., Jolivet P., Teixeira M.T., Luke B. Telomere Length Determines TERRA and R-Loop Regulation through the Cell Cycle. Cell. 2017 Jun 29;170(1):72-85.e14. doi: 10.1016/j.cell.2017.06.006.

128 Maicher A., Lockhart A., Luke B. Breaking new ground: digging into TERRA function. Biochim Biophys Acta. 2014 May;1839(5):387-94. doi: 10.1016/j.bbagrm.2014.03.012.

129 Perez-Romero C.A., Lalonde M., Chartrand P., Cusanelli E. Induction and relocalization of telomeric repeat-containing RNAs during diauxic shift in budding yeast. Curr Genet. 2018 Oct;64(5):1117-1127. doi: 10.1007/s00294-018-0829-5.

130 Wang Z., Deng Z., Dahmane N., Tsai K., Wang P., Williams D.R., Kossenkov A.V., Showe L.C., Zhang R., Huang Q., Conejo-Garcia J.R., Lieberman P.M. Telomeric repeat-containing RNA (TERRA) constitutes a nucleoprotein component of extracellular inflammatory exosomes. Proc Natl Acad Sci U S A. 2015 Nov 17;112(46):E6293-300. doi: 10.1073/pnas.1505962112.

131 Wang Z., Lieberman P.M. The crosstalk of telomere dysfunction and inflammation through cell-free TERRA containing exosomes. RNA Biol. 2016 Aug 2;13(8):690-5. doi: 10.1080/15476286.2016.1203503.

132 Lee Y.W., Arora R., Wischnewski H., Azzalin C.M. TRF1 participates in chromosome end protection by averting TRF2-dependent telomeric R loops. Nat Struct Mol Biol. 2018 Feb;25(2):147-153. doi: 10.1038/s41594-017-0021-5.

133 Toubiana S., Selig S. DNA:RNA hybrids at telomeres - when it is better to be out of the (R) loop. FEBS J. 2018 Jul;285(14):2552-2566. doi: 10.1111/febs.14464.

134 Vohhodina J., Goehring L.J., Liu B., Kong Q., Botchkarev V.V. Jr, Huynh M., Liu Z., Abderazzaq F.O., Clark A.P., Ficarro S.B., Marto J.A., Hatchi E., Livingston D.M. BRCA1 binds TERRA RNA and suppresses R-Loop-based telomeric DNA damage. Nat Commun. 2021 Jun 10;12(1):3542. doi: 10.1038/s41467-021-23716-6.

135 Arora R., Lee Y., Wischnewski H., Brun C.M., Schwarz T., Azzalin CM. RNaseH1 regulates TERRA-telomeric DNA hybrids and telomere maintenance in ALT tumour cells. Nat Commun. 2014 Oct 21;5:5220. doi: 10.1038/ncomms6220.

136 Skourti-Stathaki K., Kamieniarz-Gdula K., Proudfoot N.J. R-loops induce repressive chromatin marks over mammalian gene terminators. Nature. 2014 Dec 18;516(7531):436-9. doi: 10.1038/nature13787.

137 Rippe K., Luke B. TERRA and the state of the telomere. Nat Struct Mol Biol. 2015 Nov;22(11):853-8. doi: 10.1038/nsmb.3078.

138 Petti E., Buemi V., Zappone A., Schillaci O., Broccia P.V., Dinami R., Matteoni S., Benetti R., Schoeftner S. SFPQ and NONO suppress RNA:DNA-hybrid-related telomere instability. Nat Commun. 2019 Mar 1;10(1):1001. doi: 10.1038/s41467-019-08863-1.

139 Pan X., Chen Y., Biju B., Ahmed N., Kong J., Goldenberg M., Huang J., Mohan N., Klosek S., Parsa K., Guh C.Y., Lu R., Pickett H.A., Chu H.P., Zhang D. FANCM

suppresses DNA replication stress at ALT telomeres by disrupting TERRA R-loops. Sci Rep. 2019 Dec 13;9(1):19110. doi: 10.1038/s41598-019-55537-5.

140 Balk B., Maicher A., Dees M., Klermund J., Luke-Glaser S., Bender K., Luke B. Telomeric RNA-DNA hybrids affect telomere-length dynamics and senescence. Nat Struct Mol Biol. 2013 Oct;20(10):1199-205. doi: 10.1038/nsmb.2662.

141 Sagie S., Toubiana S., Hartono S.R., Katzir H., Tzur-Gilat A., Havazelet S., Francastel C., Velasco G., Chédin F., Selig S. Telomeres in ICF syndrome cells are vulnerable to DNA damage due to elevated DNA:RNA hybrids. Nat Commun. 2017 Jan 24;8:14015. doi: 10.1038/ncomms14015.

142 Postepska-Igielska A., Krunic D., Schmitt N., Greulich-Bode K.M., Boukamp P., Grummt I. The chromatin remodelling complex NoRC safeguards genome stability by heterochromatin formation at telomeres and centromeres. EMBO Rep. 2013 Aug;14(8):704-10. doi: 10.1038/embor.2013.87. Erratum in: EMBO Rep. 2013 Sep;14(9):845.

143 Scheibe M., Arnoult N., Kappei D., Buchholz F., Decottignies A., Butter F., Mann M. Quantitative interaction screen of telomeric repeat-containing RNA reveals novel TERRA regulators. Genome Res. 2013 Dec;23(12):2149-57. doi: 10.1101/gr.151878.112.

144 Deng Z., Norseen J., Wiedmer A., Riethman H., Lieberman P.M. TERRA RNA binding to TRF2 facilitates heterochromatin formation and ORC recruitment at telomeres. Mol Cell. 2009 Aug 28;35(4):403-13. doi: 10.1016/j.molcel.2009.06.025.

145 Montero J.J., López-Silanes I., Megías D., F Fraga M., Castells-García Á., Blasco M.A. TERRA recruitment of polycomb to telomeres is essential for histone trymethylation marks at telomeric heterochromatin. Nat Commun. 2018 Apr 18;9(1):1548. doi: 10.1038/s41467-018-03916-3.

146 Takahama K., Takada A., Tada S., Shimizu M., Sayama K., Kurokawa R., Oyoshi T. Regulation of telomere length by G-quadruplex telomere DNA- and TERRA-binding protein TLS/FUS. Chem Biol. 2013 Mar 21;20(3):341-50. doi: 10.1016/j.chembiol.2013.02.013.

147 Biffi G., Tannahill D., Balasubramanian S. An intramolecular G-quadruplex structure is required for binding of telomeric repeat-containing RNA to the telomeric

protein TRF2. J Am Chem Soc. 2012 Jul 25;134(29):11974-6. doi: 10.1021/ja305734x.

148 Chu H.P., Cifuentes-Rojas C., Kesner B., Aeby E., Lee H.G., Wei C., Oh H.J., Boukhali M., Haas W., Lee J.T. TERRA RNA Antagonizes ATRX and Protects Telomeres. Cell. 2017 Jun 29;170(1):86-101.e16. doi: 10.1016/j.cell.2017.06.017.

149 Beishline K., Vladimirova O., Tutton S., Wang Z., Deng Z., Lieberman P.M. CTCF driven TERRA transcription facilitates completion of telomere DNA replication. Nat Commun. 2017 Dec 13;8(1):2114. doi: 10.1038/s41467-017-02212-w.

150 Porro A., Feuerhahn S., Lingner J. TERRA-reinforced association of LSD1 with MRE11 promotes processing of uncapped telomeres. Cell Rep. 2014 Feb 27;6(4):765-76. doi: 10.1016/j.celrep.2014.01.022.

151 López de Silanes I., Stagno d'Alcontres M., Blasco M.A. TERRA transcripts are bound by a complex array of RNA-binding proteins. Nat Commun. 2010 Jun 29;1:33. doi: 10.1038/ncomms1032.

152 Flynn R.L., Cox K.E., Jeitany M., Wakimoto H., Bryll A.R., Ganem N.J., Bersani F., Pineda J.R., Suvà M.L., Benes C.H., Haber D.A., Boussin F.D., Zou L. Alternative lengthening of telomeres renders cancer cells hypersensitive to ATR inhibitors. Science. 2015 Jan 16;347(6219):273-7. doi: 10.1126/science.1257216.

153 Domingues-Silva B., Silva B., Azzalin C.M. ALTernative Functions for Human FANCM at Telomeres. Front Mol Biosci. 2019 Sep 6;6:84. doi: 10.3389/fmolb.2019.00084.

154 Ohle C., Tesorero R., Schermann G., Dobrev N., Sinning I., Fischer T. Transient RNA-DNA Hybrids Are Required for Efficient Double-Strand Break Repair. Cell. 2016 Nov 3;167(4):1001-1013.e7. doi: 10.1016/j.cell.2016.10.001.

155 Lalonde M., Chartrand P. TERRA, a Multifaceted Regulator of Telomerase Activity at Telomeres. J Mol Biol. 2020 Jul 10;432(15):4232-4243. doi: 10.1016/j.jmb.2020.02.004.

156 Redon S., Reichenbach P., Lingner J. The non-coding RNA TERRA is a natural ligand and direct inhibitor of human telomerase. Nucleic Acids Res. 2010 Sep;38(17):5797-806. doi: 10.1093/nar/gkq296.

157 Farnung B.O., Brun C.M., Arora R., Lorenzi L.E., Azzalin C.M. Telomerase efficiently elongates highly transcribing telomeres in human cancer cells. PLoS One. 2012;7(4):e35714. doi: 10.1371/journal.pone.0035714.

158 Kreilmeier T., Mejri D., Hauck M., Kleiter M., Holzmann K. Telomere Transcripts Target Telomerase in Human Cancer Cells. Genes (Basel). 2016 Aug 16;7(8):46. doi: 10.3390/genes7080046

159 Feretzaki M., Renck Nunes P., Lingner J. Expression and differential regulation of human TERRA at several chromosome ends. RNA. 2019 Nov;25(11):1470-1480. doi: 10.1261/rna.072322.119.

160 Yehezkel S., Segev Y., Viegas-Péquignot E., Skorecki K., Selig S. Hypomethylation of subtelomeric regions in ICF syndrome is associated with abnormally short telomeres and enhanced transcription from telomeric regions. Hum Mol Genet. 2008 Sep 15;17(18):2776-89. doi: 10.1093/hmg/ddn177.

161 Cusanelli E., Romero C.A., Chartrand P. Telomeric noncoding RNA TERRA is induced by telomere shortening to nucleate telomerase molecules at short telomeres. Mol Cell. 2013 Sep 26;51(6):780-91. doi: 10.1016/j.molcel.2013.08.029.

162 Moravec M., Wischnewski H., Bah A., Hu Y., Liu N., Lafranchi L., King M.C., Azzalin C.M. TERRA promotes telomerase-mediated telomere elongation in Schizosaccharomyces pombe. EMBO Rep. 2016 Jul;17(7):999-1012. doi: 10.15252/embr.201541708.

163 Querido E., Sfeir A., Chartrand P. Imaging of Telomerase RNA by Single-Molecule Inexpensive FISH Combined with Immunofluorescence. STAR Protoc. 2020 Sep 10;1(2):100104. doi: 10.1016/j.xpro.2020.100104.

164 Avogaro L., Querido E., Dalachi M., Jantsch M.F., Chartrand P., Cusanelli E. Live-cell imaging reveals the dynamics and function of single-telomere TERRA molecules in cancer cells. RNA Biol. 2018;15(6):787-796. doi: 10.1080/15476286.2018.1456300.

165 Vogan J.M., Zhang X., Youmans D.T., Regalado S.G., Johnson J.Z., Hockemeyer D., Collins K. Minimized human telomerase maintains telomeres and resolves endogenous roles of H/ACA proteins, TCAB1, and Cajal bodies. Elife. 2016 Aug 15;5:e18221. doi: 10.7554/eLife.18221.

166 Pascolo E., Wenz C., Lingner J., Hauel N., Priepke H., Kauffmann I, Garin-Chesa P., Rettig W.J., Damm K., Schnapp A. Mechanism of human telomerase inhibition by BIBR1532, a synthetic, non-nucleosidic drug candidate. J Biol Chem. 2002 May 3;277(18):15566-72. doi: 10.1074/jbc.M201266200.

167 Bryan C., Rice C., Hoffman H., Harkisheimer M., Sweeney M., Skordalakes E. Structural Basis of Telomerase Inhibition by the Highly Specific BIBR1532. Structure. 2015 Oct 6;23(10):1934-1942. doi: 10.1016/j.str.2015.08.006.

168 Feretzaki M., Pospisilova M., Valador Fernandes R., Lunardi T., Krejci L., Lingner J. RAD51-dependent recruitment of TERRA lncRNA to telomeres through R-loops. Nature. 2020 Nov;587(7833):303-308. doi: 10.1038/s41586-020-2815-6.

169 Tsai R.X., Fang K.C., Yang P.C., Hsieh Y.H., Chiang I.T., Chen Y., Lee H.G., Lee J.T., Chu HC. TERRA regulates DNA G-quadruplex formation and ATRX recruitment to chromatin. Nucleic Acids Res. 2022 Nov 28;50(21):12217-12234. doi: 10.1093/nar/gkac1114.

170 Lansdorp P.M., Verwoerd N.P., van de Rijke F.M., Dragowska V., Little M.T., Dirks R.W., Raap A.K., Tanke H.J. Heterogeneity in telomere length of human chromosomes. Hum Mol Genet. 1996 May;5(5):685-91. doi: 10.1093/hmg/5.5.685.

171 Henderson S., Allsopp R., Spector D., Wang S.S., Harley C. In situ analysis of changes in telomere size during replicative aging and cell transformation. J Cell Biol. 1996 Jul;134(1):1-12. doi: 10.1083/jcb.134.1.1.

172 Kroupa M., Tomasova K., Kavec M., Skrobanek P., Buchler T., Kumar R., Vodickova L., Vodicka P. TElomeric repeat-containing RNA (TERRA): Physiological functions and relevance in cancer. Front Oncol. 2022 Aug 2;12:913314. doi: 10.3389/fonc.2022.913314.

173 Ulaner G.A., Hu J.F., Vu T.H., Giudice L.C., Hoffman A.R. Telomerase activity in human development is regulated by human telomerase reverse transcriptase (hTERT) transcription and by alternate splicing of hTERT transcripts. Cancer Res. 1998 Sep 15;58(18):4168-72.

174 Zaug A.J., Lim C.J., Olson C.L., Carilli M.T.., Goodrich K.J., Wuttke D.S., Cech T.R. CST does not evict elongating telomerase but prevents initiation by ssDNA binding. Nucleic Acids Res. 2021 Nov 18;49(20):11653-11665. doi: 10.1093/nar/gkab942.

175 Savoca V., Rivosecchi J., Gaiatto A., Rossi A., Mosca R., Gialdini I., Zubovic L., Tebaldi T., Macchi P., Cusanelli E. TERRA stability is regulated by RALY and polyadenylation in a telomere-specific manner. Cell Reports. 2023, in press

176 Chen L., Zhang C., Ma W., Huang J., Zhao Y., Liu H. METTL3-mediated m6A modification stabilizes TERRA and maintains telomere stability. Nucleic Acids Res. 2022 Nov 11;50(20):11619-11634. doi: 10.1093/nar/gkac1027.

177 de Lange Lab. Retrovirus Production and Infection. https://delangelab.org/protocols

178 Rossiello F., Fumagalli M., d'Adda di Fagagna F. ImmunoFISH for adherent cultured mammalian cells. Bio-protocol 2013 3(24):e999. doi: 10.21769/BioProtoc.999.

179 Avogaro L., Oss Pegorar C., Bettin N., Cusanelli E. Generation of Cancer Cell Clones to Visualize Telomeric Repeat-containing RNA TERRA Expressed from a Single Telomere in Living Cells. J Vis Exp. 2019 Jan 17;(143). doi: 10.3791/58790.

180 Loayza D., De Lange T. POT1 as a terminal transducer of TRF1 telomere length control. Nature. 2003 Jun 26;423(6943):1013-8. doi: 10.1038/nature01688.

181 Tsanov N., Samacoits A., Chouaib R,. Traboulsi A.M., Gostan T., Weber C., Zimmer C., Zibara K., Walter T., Peter M., Bertrand E., Mueller F. smiFISH and FISH-quant - a flexible single RNA detection approach with super-resolution capability. Nucleic Acids Res. 2016 Dec 15;44(22):e165. doi: 10.1093/nar/gkw784.

182 Ollion J., Cochennec J., Loll F., Escudé C., Boudier T. TANGO: a generic tool for high-throughput 3D image analysis for studying nuclear organization. Bioinformatics. 2013 Jul 15;29(14):1840-1. doi: 10.1093/bioinformatics/btt276.

183 Gilles J.F., Dos Santos M., Boudier T., Bolte S., Heck N. DiAna, an ImageJ tool for object-based 3D co-localization and distance analysis. Methods. 2017 Feb 15;115:55-64. doi: 10.1016/j.ymeth.2016.11.016.

184 Venteicher A.S., Abreu E.B.., Meng Z, McCann K.E., Terns R.M., Veenstra T.D., Terns M.P., Artandi S.E. A human telomerase holoenzyme protein required for Cajal body localization and telomere synthesis. Science. 2009 Jan 30;323(5914):644-8. doi: 10.1126/science.1165357.

185 Zhong F., Savage S.A., Shkreli M., Giri N., Jessop L., Myers T., Chen R., Alter B.P., Artandi S.E. Disruption of telomerase trafficking by TCAB1 mutation causes dyskeratosis congenita. Genes Dev. 2011 Jan 1;25(1):11-6. doi: 10.1101/gad.2006411.

186 Fouché N., Ozgür S., Roy D., Griffith J.D. Replication fork regression in repetitive DNAs. Nucleic Acids Res. 2006;34(20):6044-50. doi: 10.1093/nar/gkl757.

187 Silva B., Arora R., Bione S., Azzalin C.M. TERRA transcription destabilizes telomere integrity to initiate break-induced replication in human ALT cells. Nat Commun. 2021 Jun 18;12(1):3760. doi: 10.1038/s41467-021-24097-6.

188 Crabbe L., Cesare A.J., Kasuboski J.M., Fitzpatrick J.A., Karlseder J. Human telomeres are tethered to the nuclear envelope during postmitotic nuclear assembly. Cell Rep. 2012 Dec 27;2(6):1521-9. doi: 10.1016/j.celrep.2012.11.019.

189 Chen B., Gilbert L.A., Cimini B.A., Schnitzbauer J., Zhang W., Li G.W., Park J., Blackburn E.H., Weissman J.S., Qi L.S., Huang B. Dynamic imaging of genomic loci in living human cells by an optimized CRISPR/Cas system. Cell. 2013 Dec 19;155(7):1479-91. doi: 10.1016/j.cell.2013.12.001. Erratum in: Cell. 2014 Jan 16;156(1-2):373.

190 Qin P., Parlak M., Kuscu C., Bandaria J., Mir M., Szlachta K., Singh R., Darzacq X., Yildiz A., Adli M. Live cell imaging of low- and non-repetitive chromosome loci using CRISPR-Cas9. Nat Commun. 2017 Mar 14;8:14725. doi: 10.1038/ncomms14725.

191 Yadav T., Zhang J.M., Ouyang J., Leung W., Simoneau A., Zou L. TERRA and RAD51AP1 promote alternative lengthening of telomeres through an R- to D-loop switch. Mol Cell. 2022 Nov 3;82(21):3985-4000.e4. doi: 10.1016/j.molcel.2022.09.026. Epub 2022 Oct 19.

SUPPLEMENTARY MATERIAL

To validate the use of RAP1 IF signal integrated density quantification as a proxy for telomere length determination in fixed cells, telomeric DNA FISH and RAP1 IF (Figure S1A) were performed by Marta Andolfato, previous master student in the lab. By performing telomeric DNA FISH/IF the average integrated density of telomeres per cell was quantified and then the distance in the integrated density of each telomeric focus from the average telomere integrated density of the cell was determined using both techniques. These analyses revealed a strong positive correlation between RAP1 IF and telomeric DNA FISH signals (Spearman's correlation coefficient = 0.7, n = 342, $p < 0.0001$) (Figure S1B and S1C), indicating that quantification of RAP1 IF foci integrated density can be used to discriminate long versus short telomeres compared to the average telomere length of the cell.

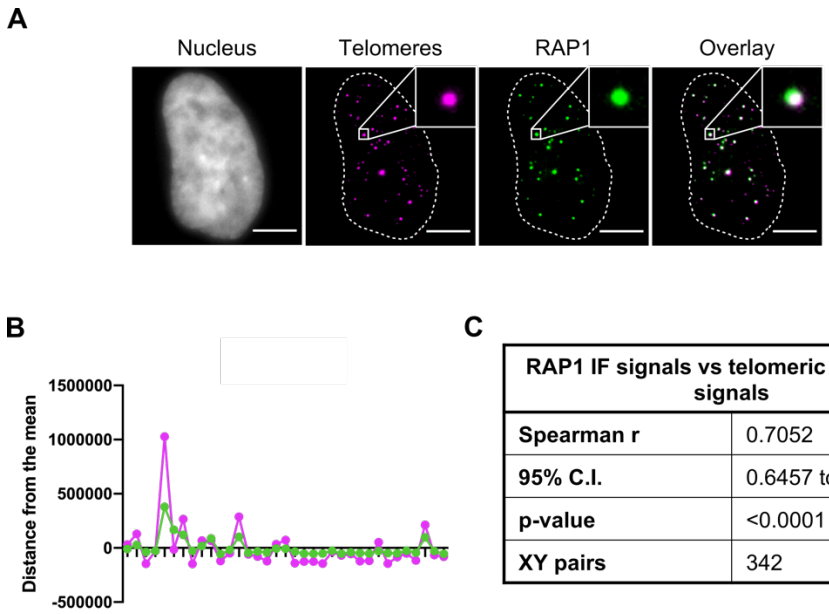

C

RAP1 IF signals vs telomeric DNA-FISH signals	
Spearman r	0.7052
95% C.I.	0.6457 to 0.7561
p-value	<0.0001
XY pairs	342

Supplementary Figure S1: RAP1 immunofluorescence is a reliable approach to assess telomere length. A) Detection of telomeres either through DNA-FISH or RAP1 IF in HeLa cells. The two signals overlap completely, the slight shift is due to microscope resolution. Overlapping example can be observed in figure insert at higher magnification. B) An example of the trend observed for RAP1 and telomeric probe signals in one nucleus. Distance from the average integrated density is shown. Each dot represents a single telomere focus (RAP1 in green and TeloC probe in magenta). C) Table reporting the positive correlation between RAP1 IF and telomeric DNA-FISH signals assessed on 342 foci with Spearman's rank correlation coefficient which resulted equal to 0.7 (strong positive correlation). Scale bar: 5 μm. Experiment performed, and images acquired and analyzed by Marta Andolfato.

ACKNOWLEDGMENTS

Grazie **Emilio** che poco più di cinque anni fa mi hai accolta nel tuo laboratorio come tirocinante magistrale dandomi la possibilità di scoprire che la ricerca è la mia vera passione. Grazie per aver creduto in me e nelle mie capacità quando ancora nessuno le aveva intraviste. Grazie per avermi affidato un progetto di dottorato tanto interessante quanto sfidante e per avermi sempre spronata ad andare avanti. Ho passato degli anni bellissimi con te e tutti i membri ed ex membri del laboratorio Cusanelli, anni che mi hanno profondamente resa felice ma che al contempo sono stati duri da affrontare in qualche occasione. Grazie per avermi dato la possibilità di seguire diversi studenti nel corso negli anni, grazie a queste esperienze ho imparato molto e questo percorso di dottorato senza tutti loro non sarebbe stato lo stesso. Grazie per avermi sostenuta sempre, per avermi ascoltata ogni qualvolta sentissi il bisogno di parlare…sei stato un porto sicuro durante tutto il percorso! Lavorare con te è stato per me un onore e non lo dimenticherò.

Vorrei anche ringraziare i professori **Luca Fava** ed **Alessio Zippo** che fin dal primo anno di dottorato hanno ascoltato con piacere gli avanzamenti del progetto dando riscontri utili ed input costruttivi.

I wish to thank also Dr. **Miguel Godinho Ferreira** and prof. **Grazia Daniela Raffa** for reading this work, giving useful and constructive feedbacks and for their participation as members of my thesis committee.

Ringrazio il Dr. **Claus Maria Azzalin** per avermi ospitata nel suo laboratorio per un paio di mesi in una meravigliosa (anche se molto piovosa) Lisbona facendomi sentire subito parte del suo gruppo. Un grazie anche a tutti i membri del laboratorio Azzalin per avermi accolta subito con piacere nel gruppo.

Grazie a tutti gli studenti che ho tutorato in questi anni, senza di voi questo percorso sarebbe stato totalmente diverso. **Irene**, quando sei arrivata nel gruppo ero una neolaureata che aveva ancora molto da imparare e poco da insegnarti. Quante avventure abbiamo passato insieme…non le dimenticherò mai! **Marta**, il tuo arrivo è stato fatale per me…hai vissuto sulla tua pelle il mio primo anno di dottorato con una me ancora molto inesperta, che non sapeva gestire le emozioni, si abbatteva per ogni cosa, e che non sapeva essere una tutor. Come se tutto questo non bastasse, in

quell'anno è arrivato il COVID-19 e tutto ha preso una piega ancora più complicata. Sei stata una certezza durante quell'anno e lo sei tutt'ora. Grazie Marta per avermi fatto capire quanto avessi da dare al mondo ma che avrei dovuto cambiare approccio verso il mondo stesso. Lavorare con te è stato un vero e proprio piacere e poterlo rifare a Lisbona è stato molto emozionante. Thank you **Eslam** for teaching me how to deal with a different culture and perspective. We learned how to communicate and synergically work together and it has been amazing. **Alessandra** ed **Irene**, le triennali che non volevo seguire ma che ho adorato. Lavorare con voi è stato molto stimolante. Grazie a tutti voi, questo traguardo è anche merito vostro!

Grazie ai miei **colleghi** di laboratorio e del CIBIO, la vostra stima ed il vostro supporto sono stati fondamentali in questi anni. Siete troppi da nominare (il che significa che sono qui davvero da tanto tempo!) e ho paura di dimenticare qualcuno ma posso dire con certezza che senza tutti voi nulla sarebbe stato lo stesso!

Claudio, in questi cinque anni sei stato un amico oltre che un collega, una persona su cui ho sempre potuto fare affidamento e ti ringrazio per questo. **Caterina**, punto fermo per me all'interno del lab ma anche nella vita, con te ho affrontato temi importanti di vita e discusso molto anche di esperimenti. Grazie per la tua amicizia! **Julieta**, un vortice di energia che mi ha contagiata e mi ha sempre sostenuta. Parlare con te, discutere di scienza ma anche di vita è sempre molto stimolante. Sei un esempio per me, ti stimo molto e sono grata di aver avuto l'opportunità di lavorare con te!

Un ringraziamento speciale va fatto a te **Matteo** che sei stato e sei tutt'ora il mio angelo custode, insostituibile presenza nella mia vita! Da te ho imparato tanto a livello tecnico/sperimentale ma ho soprattutto imparato che esistono al mondo persone che ti vogliono bene per ciò che sei! Grazie mille di tutto, il raggiungimento di questo traguardo è anche merito tuo! Nulla sarebbe lo stesso senza di te amico mio!

Stefania e **Giovanna**, trovarvi è stata una fatalità, conoscervi un piacere e avervi come amiche un onore. Grazie per avermi ascoltata e supportata sempre, ognuna a modo suo. Siete anime speciali con le quali condivido gioie e dolori, felicità e tristezza. Senza di voi sarebbe tutto diverso! Grazie per esserci sempre.

Grazie alle amiche sparse nel mondo che, nonostante la distanza, i fusi orari e la vita che scorre diversamente, ci sono sempre state. In particolare, grazie ad **Elisabetta**, **Alice, Chiara** ed **Elena** perché mi sono sempre state vicine.

Alan, la tua presenza ed il tuo supporto in questi ultimi dieci mesi sono stati essenziali, fondamentali, unici. Un solo grazie non potrà mai bastare per eguagliare tutto il bene che mi hai fatto e continui a farmi ogni giorno. Sei davvero tanto speciale e sono fortunata di poter condividere la vita con te.

Mamma Sabina e **papà Giorgio**, senza di voi non sarei la persona che sono. Grazie per avermi sempre supportata e spinta a seguire i miei interessi e le mie passioni. Grazie per avermi sopportata, per esservi fatti carico dei miei periodi bui, per avermi sempre ascoltata e motivata ad andare avanti. Oggi siamo in tre a prendere il dottorato perché senza di voi non sarei mai arrivata fin qui. Spero sarete sempre fieri di me.

Infine, GRAZIE a tutte le persone che ho incontrato nella mia vita, mi avete tutti quanti aiutato ad essere la persona che sono: **Nicole Bettin, PhD.**